PAM68:
A New Component of the
PSII Biogenesis Machinery

Dissertation
zur Erlangung des Doktorgrades
der Fakultät für Biologie
der Ludwig-Maximilians-Universität München

Vorgelegt von
Jessica Zühlke
aus München

München
November 2009

Erstgutachter: Prof. Dr. Dario Leister
Zweitgutachter: Prof. Dr. Jörg Nickelsen
Tag der mündlichen Prüfung: 02.12.2009

Contents

Abbreviations

°C	Degree celsius
Å	Angstrom; 1 x 10^{-10} m
ACA	Aminocaproic acid
APS	Ammoniumpersulfate
ATP	Adenine triphosphate
Auto	Autofluorescence
ß-Car	ß-carotene
ß-DM	ß-dodecylmaltoside
BN gel	Blue native gel
BSA	*Bovine serum albumin*
C-terminus	Carboxy terminus
Ci	Curie
cDNA	Complementary deoxyribonucleic acid
CES	Control by epistasy of synthesis
Chl	Chlorophyll
Co-IP	Co-immunoprecipitation
Col-0	*Arabidopsis* ecotype Columbia
CP43	Chlorophyll binding protein 43
CP47	Chlorophyll binding protein 47
cpSRP	Chloroplast signal recognition particle
CtpA	Carboxyl-terminal processing protease A
CYP	Cyclophilin
cyt	Cytochrome
D	Dark
Da	Dalton
DCMU	3-(3,4-dichlorophenyl)-1,1-dimethylurea
DNA	Deoxyribonucleic acid
DTT	Dithiothreitol
ECL	*Enhanced chemiluminescent substrate*
EDTA	Ethylene diamin tetraacetic acid
EGTA	Ethylene glycol tetraacetic acid
ETR	Electron transport rate
F_0	Minimal fluorescence
F_m	Maximal fluorescence
F_V	Variable fluorescence
Fd	Ferredoxin
FNR	Ferredoxin NADPH dehydrogenase
g	Gram
g	Times the force of gravity
h	Hour
HCF	High chlorophyll fluorescence
HEPES	4-(2-hydroxyethyl)-1-piperazineethanesulfonic acid
HL	High light
HPLC	High performance liquid chromatography
IgG	Immunoglobulin G
k	Kilo
LB	Left T-DNA border
LEF	Linear electron flow
L*er*	*Arabidopsis* ecotype Landsberg *erecta*

LHC	Light harvesting complex
LL	Low light
LMW	Low molecular weight
LPA	Low PSII accumulation
µ	Micro
m	Meter
M	Mole(s) per litre
MES	2-(N-morpholino)ethanesulfonic acid
min	Minute(s)
mol	Mole
MOPS	3-N-morpholinopropanesulfonic acid
MS	Mass spectrometry
N-terminus	Amino terminus
NAD(P)	Nicotinamide adenine dinucleotide (phosphate)
NDH	NAD(P)H dehydrogenase complex
NPQ	Non-photochemical quenching
OEC	Oxygen evolving complex
P680	Reaction center of PSII
P700	Reaction center of PSI
PAGE	Polyacrylamide gel electrophorese
PAM	Pulse amplitude modulation
PAM68	Photosynthesis affected mutant 68
PAR	Photosynthetic active radiation
PEG	Polyethyleneglycol
PCR	Polymerase chain reaction
PSI	Photosystem I
PSII	Photosystem II
PQ	Plastoquinone
PQH_2	Plastohydroquinone
PVDF	Polyvinylidene difluoride
Q_A	Primary electron acceptor plastoquinone
qP	Photochemical quenching
RB	Right T-DNA border
RC	Reaction centre
RFP	Red fluorescent protein
RNA	Ribonucleic acid
ROS	Reactive oxygen species
rpm	Rounds per minute
Rubisco	Ribulose biphosphate carboxylase/ oxygenase
r.u.	Relative units
s	Second(s)
SD	Standard deviation
SDS	Sodium dodecyl sulphate
TLP	Thylakoid lumen protein
TMD	Transmembrane domain
U	enzyme unit
v/v	Volume per volume
w/v	Weight per volume
WT	Wild-type

Summary

Photosynthetic light reactions rely on the proper function of multisubunit protein complexes that reside in the thylakoid membrane. In plants, the biogenesis of these complexes needs the stoichiometric synthesis and sequential integration of chloroplast- and nucleus-encoded proteins into the thylakoid membrane of the chloroplast. Thus, the assembly processes require additional auxiliary and regulatory factors to assist this complex, multistep process. Due to the limited coding capacity of the chloroplast genome, the biogenesis and assembly is mainly regulated by nucleus-encoded proteins. Several of them have already been identified in recent years, but there is still a repertoire of assembly and maintenance factors that has to be determined. Here we show that a novel transmembrane protein, named PAM68, which is located in thylakoids of photoautotrophic organisms, plays a critical role in the biogenesis of photosystem II (PSII) in *Arabidopsis*. Mutant plants with the *PAM68* gene interrupted by T-DNA insertion show stunted growth and pale green leaves. Analyses of leaf chlorophyll fluorescence, pigment composition and amounts of photosynthetic proteins suggest that *pam68* mutant plants have a defect in PSII biogenesis. Protein labelling assays indicate a decrease in the synthesis rate of the PSII core protein D1 resulting in reduced amounts of assembled complexes. These results, together with the analysis of polysome association with *psbA* mRNA, provide evidence that PAM68 is necessary either for the stability of the D1 nascent chain or for its co-translational integration into the thylakoid membrane. In flowering plants a homologue of PAM68 exists, PAM68HL, which is crucial for the activity of the NAD(P)H-dehydrogenase (NDH) complex. Interruption of the *PAM68HL* gene does not result in any visible phenotype. However, biochemical analyses reveal defects in the NDH complex, as the PSI/NDH supercomplex is absent. This deficiency is confirmed by spectroscopic measurements. A double mutation of *PAM68* and its homologue does not lead to an additive phenotype. Taken together, these results exclude that PAM68 and PAM68HL have redundant functions.

Zusammenfassung

Die Elektronentransportkette der Photosynthese setzt sich aus verschiedenen Proteinkomplexen, welche sich in der Thylakoidmembran der Chloroplasten befinden, zusammen. Deren einwandfreie Funktionsweise ist abhängig von einer akkuraten Assemblierung der einzelnen Untereinheiten, die zum einen Teil in den Chloroplasten und zum anderen Teil im Zellkern kodiert werden. Die Biogenese der Proteinkomplexe ist komplex und vielschichtig und erfordert daher zusätzliche Hilfs- und Regulationsfaktoren. Aufgrund der begrenzten Kodierungskapazität des Chloroplastengenoms werden die Biogenese und Assemblierung vor allem durch kernkodierte Proteine reguliert. Einige davon wurden bereits in den letzten Jahren entdeckt, aber es existiert immer noch eine Vielzahl an Faktoren für die Assemblierung und Aufrechterhaltung, die identifiziert werden müssen. Hier stellen wir ein neues Transmembranprotein vor, PAM68 genannt, das in den Thylakoiden von photoautotrophen Organismen lokalisiert ist und eine entscheidende Rolle bei der Biogenese von Photosystem II (PSII) in *Arabidopsis* spielt. Mutierte Pflanzen mit einer T-DNA Insertion im *PAM68*-Gen sind im Wachstum gehemmt und besitzen blass-grüne Blätter. Messungen der Chlorophyll-Fluoreszenz, Pigmentzusammensetzung und der Expression photosynthetischer Proteine in der *pam68*-Mutante deuten auf einen Defekt in der PSII-Biogenese hin. Versuche mit markierten Proteinen zeigen eine verminderte Syntheserate des PSII-Kernproteins D1, was zu einer Reduktion der assemblierten Komplexe führt. Diese Ergebnisse liefern den Hinweis, dass PAM68 entweder an der Stabilisierung des naszierenden D1-Proteins oder an dessen ko-translationeller Integration in die Thylakoidmembran beteiligt ist. Darauf deutet auch die untersuchte Assoziation von der *psbA*-mRNA mit Polysomen hin. In Blütenpflanzen existiert ein homologes Protein, PAM68HL, welches wichtig für die Aktivität des NAD(P)H-Dehydrogenase-Komplexes ist. Ein Ausschalten des *PAM68HL* Gens resultiert nicht in einem sichtbaren Phänotyp. Allerdings deuten biochemische Untersuchungen auf einen Defekt im NDH-Komplex hin, da der PSI/NDH-Superkomplex nicht vorhanden ist. Spektroskopische Analysen bestätigen diese Defizienz. Da eine Doppelmutation von *PAM68* und dem Homolog nicht zu einem verstärkten Phänotypen führt, kann eine redundante Funktion von PAM68 und PAM68HL ausgeschlossen werden.

1) Introduction

1.1) Photosynthesis in Flowering Plants

Photosynthesis is the most important energy source for life on earth. Oxygenic photosynthesis occurs in plants, algae, and cyanobacteria. In plants and green algae the photosynthetic apparatus is located in the chloroplast (Fig. 1.1) This complex double-membrane organelle has evolved from a cyanobacterial ancestor that was taken up by a primitive eukaryotic cell through endosymbiosis (Margulis, 1971). During evolution, the vast majority of the chloroplast genes were

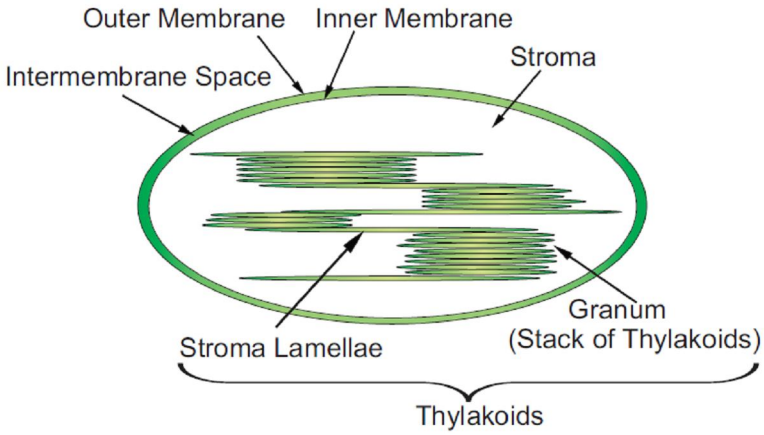

Fig. 1.1: Schematic picture of the chloroplast of flowering plants.

transferred to the nucleus of the host cell (Kleine *et al.*, 2009). Therefore, these proteins have to be imported into the chloroplast as they are encoded in the nuclear genome. For proteins that are localised to the thylakoid membrane, further internal transport pathways are required (for review see Soll and Schleiff, 2004; Schünemann, 2007).

The thylakoid membrane is composed of three structurally distinct domains: the planar appressed membranes of the grana, the non-appressed stroma lamellae, and the highly curved, non-appressed margins of the grana (Dekker and Boekema, 2005; Anderson, 2006). This heterogeneity has an important impact on the localisation of proteins needed for the light-dependent reactions of photosynthesis. The photosynthetic apparatus consists of four multisubunit-complexes (Fig. 1.2): the two photosystems (PSII and PSI), the cytochrome b_6f-complex and the ATP-synthase. PSII and its associated light-harvesting complex are preferentially located in the stacked grana regions, while the cytochrome b_6f-

complex, PSI and the ATP-synthase are found in the margins of the grana as well as in stroma thylakoids (Mullineaux, 2005). These complexes are required for the electron transfer chain, which drives photosynthesis. Light excitation of PSII leads to the release of electrons from P_{680}, the primary donor of PSII, which are

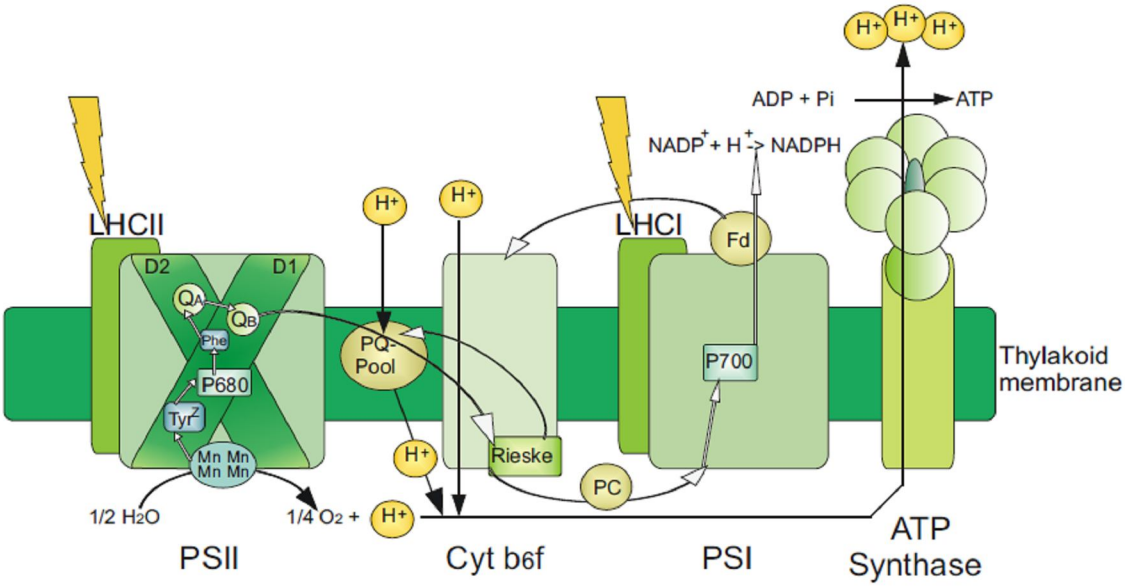

Fig. 1.2: The thylakoid membrane of the chloroplast.

The four multi-subunit complexes of the photosynthetic apparatus: Photosystem II (PSII), cytochrome *b*$_6$*f*-complex, photosystem I and the ATP synthase. Electron transfer: electrons (white arrows), H+ (black arrows).

captured by the first electron acceptor Q_A. Electrons are then transferred to the cytochrome *b*$_6$*f*-complex via the plastoquinone pool (PQ-pool) and further on to PSI via plastocyanin (PC). In the PSI complex a second light excitation takes place, and the electrons are transferred with the help of several components to the electron carrier protein ferredoxin (Fd), which is used to reduce NADP. In total this process leads to the oxidation of water to molecular oxygen and the reduction of $NADP^+$ to NADPH. The electron flow through this transport chain additionally leads to the translocation of protons into the thylakoid lumen. The energy stored in the resulting proton gradient is converted by the ATP-synthase to ATP.

1.2) Photosystem II: Biogenesis and Assembly

Photosystem II (PSII) is a pigment-protein complex embedded in the thylakoid membrane of cyanobacteria and chloroplasts that drives the electron transfer from water to plastoquinone. In flowering plants, PSII consists of more than 20

subunits (Nelson and Yocum, 2006). The reaction centre core of this photosystem, consisting of the D1 and D2 protein, the α– and β–subunit of cytochrome *b*559 and the PsbI and PsbW proteins, performs the primary charge separation. Oxygen-evolving PSII complexes additionally contain the intrinsic chlorophyll *a* (Chl *a*) binding proteins CP47 and CP43, as well as the extrinsic, lumenal proteins of the oxygen-evolving complex (OEC; PsbO, PsbP, PsbQ) that bind the manganese cluster (Mn cluster), and some additional low molecular weight subunits (Shi and Schröder, 2004). The D1 and D2 heterodimer binds all the intermediate redox components of PSII required for the electron transfer from the Mn cluster to the plastoquinone pool (Chl *a* P_{680}, pheophytin, non-heme Fe^{2+}, quinones; Nanba and Satoh, 1987). The molecular mechanism underlying the biogenesis and assembly of PSII is not fully understood, although our knowledge of the structure and function of PSII has greatly advanced in recent years. It has been demonstrated that at least three different processes can be distinguished in the formation of PSII complexes, depending on the developmental stage of the plastid (Baena-González and Aro, 2002): i) early biogenesis of thylakoid membranes during the transition from etioplasts to chloroplasts, ii) *de novo* biogenesis of PSII centres in light, iii) repair of light-induced damage to PSII. During each of these PSII formation processes, the sequential synthesis of PSII proteins and a stepwise assembly is indispensable. Hence, these procedures probably share common regulatory steps, although they clearly differ from each other in many aspects.

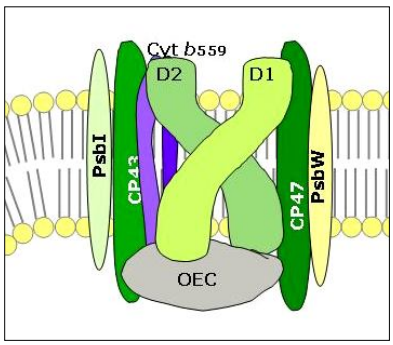

Fig. 1.3: PSII reaction centre.

1.2.1) Early Biogenesis of PSII

The early biogenesis starts already in etiolated seedlings in the dark. In the precursor of the chloroplast, the etioplast, several PSII subunits are already synthesised and assembled into pre-thylakoid membranes. This is the case for cyt *b*559 (Ohashi *et al.,* 1992; Müller and Eichacker, 1999), PsbH (Hird *et al.,* 1991), the OEC proteins (Gamble and Mullet, 1989) and D2 (Müller and Eichacker, 1999). These proteins can be synthesised independently of light,

whereas other components require the recruitment of cofactors like chlorophyll for proper folding and insertion into the membrane. Only upon illumination, the Chl precursor protochlorophyllide is converted into Chl *a* (von Wettstein *et al.,* 1995), and the synthesis of such chlorophyll-binding proteins (CP43, CP47 and D1) can take place (Eichacker *et al.,* 1990; Kim *et al.,* 1994). As every step in the early biogenesis of PSII is strictly regulated, also these Chl-binding proteins accumulate in a coordinated manner (Jensen *et al.*, 1986; de Vitry *et al.*, 1989; Yu and Vermaas, 1990). First, CP47 is inserted into the pre-complex consisting of D2 and cyt *b*559. Afterwards, or probably concomitantly with CP47, D1 is cotranslationally assembled and processed at its C-terminus. This step precedes the assembly of the CP43 protein (Zhang *et al.*, 2000). Afterwards, the Mn cluster can be ligated followed by a subsequent photo-activation of the OEC (Bowyer *et al.,* 1992). For the low molecular weight proteins (LMW) that are stoichiometric components of PSII, such strict formation steps have not been found to-date. They are supposed to be integrated at different stages of the PSII assembly process (Hager *et al.,* 2002; Suorsa *et al.,* 2004; Rokka *et al*., 2005). The final establishment of a functional PSII requires then dimerisation of PSII monomers and the association of LHCII trimers.

Beside the order of synthesis, also the integration of photosynthetic proteins into the thylakoid membrane is strictly coordinated, although not all proteins use the same mechanism of insertion. D1 is cotranslationally translocated to the membrane with the cpSRP54 particle (chloroplast signal recognition particle; Schünemann *et al.*, 1998; Nilsson and van Wijk, 2002). Several chloroplast-encoded thylakoid membrane proteins probably use the same pathway. cpSRP54 is also involved in the cpSRP targeting pathway of nucleus-encoded proteins, which seems to be limited to the integration of light harvesting Chl *a*/*b* binding proteins into the thylakoid membrane (LHCPs; Schünemann, 2004; Tzvetkova-Chevolleau *et al.*, 2007). For this, it has to form a complex with cpSRP43. Additionally to the cpSRP-pathway, three other routes for nucleus-encoded subunits have been described until now (cpTat, cpSec, and the spontaneous integration pathway; Schünemann, 2007). The latter is the only process that functions without the assistance of other proteins or energy (Jarvis and Robinson, 2004).

1.2.2) *De Novo* Biogenesis of PSII in Light

The process of *de novo* biogenesis of PSII is difficult to tackle directly, and often for the studies on biogenesis of PSII complexes in light various PSII mutants have been utilised. Depletion of main PSII core subunits in cyanobacteria or plants resulted in a disruption of the whole complex and in the disappearance of other central subunits (Baena-González and Aro, 2002). This is the case for the reaction centre components cyt *b*559, D1, D2, and CP47 (Pakrasi *et al.*, 1990, Suorsa *et al*., 2001; Erickson *et al.,* 1986; Vermaas, 1988; de Vitry *et al*., 1989; Jensen *et al.,* 1986; Nilsson *et al.,* 1990). The following depletion of additional PSII core proteins after mutating one RC-component has different reasons. In cyanobacteria, the amount of close assembly partners is regulated proteolytically leading to an accelerated degradation (Yu and Vermaas, 1990). Chloroplasts of green algae and plants exhibit another control of protein synthesis, namely a tight control of translation. This phenomenon, called CES ("control by epistasy of synthesis") is well-characterised for the cyt b_6f-complex, where the synthesis of cytochrome *f* is repressed in the absence of other subunits of the cyt b_6f-complex in *Chlamydomonas* (Wollman *et al.*, 1999; Choquet *et al.*, 1998). Studies with PSII mutants on the other hand showed that D2 is indispensable for synthesis of D1 (de Vitry *et al.*, 1999) and the absence of cyt *b*559 leads to repression of D1, D2, CP47, and CP43 (Morais *et al.*, 1998). This dependence of synthesis is reinforced by the presence of the PSII-subunits cyt *b*559 and D2 already at early phases of chloroplast development as mentioned above. Also in the *de novo* synthesis of PSII proteins in leaves of mature plants, these two subunits seem to be the first ones integrated into the thylakoid membrane. An observed interaction of D2 with D1 translation intermediates (Zhang *et al.*, 1999) gives further support to this stepwise synthesis of proteins.

The order of the next assembly steps seems to be the same as for the early biogenesis of PSII. After insertion of the reaction centre D1, and the processing of its C-terminus (Oelmüller *et al.*, 1996), CP43 can be integrated into the complex. This step is assisted by the "LOW PSII ACCUMULATION 2" (LPA2) protein, which was suggested to form a complex with Albino3 (Alb3), a component of the integration machinery of thylakoid proteins (Ma *et al.*, 2007). After that, the Mn cluster (Bowyer *et al.,* 1992) and other cofactors can attach, followed by the association of the OEC proteins and LMW-proteins, dimerisation of the whole

complex and binding of the light-harvesting apparatus. However, the difference between early and *de novo* biogenesis lies in the regulation of the PSII subunits when one of them is missing. Although mature chloroplasts of *Chlamydomonas* D1-less mutants failed to accumulate D2 or cyt *b*559 (Morais *et al.*, 1998), both proteins were synthesised in etioplasts before the onset of illumination. Thus, early chloroplast development is regulated by both the developmental step and light information (Gamble and Mullet, 1989).

1.2.3) Repair-Cycle of PSII

As a result of the strong oxidative chemistry of water splitting, organisms that perform oxygenic photosynthesis are subject to the production of reactive oxygen species (ROS) or other radicals, which are destructive to proteins and pigments (Barber and Andersson, 1992; Niyogi, 1998; Nishiyama *et al.*, 2006). This photodamage occurs under all light intensities (Krause and Weis, 1991; Prasil *et al*., 1992; Aro *et al.,* 1993). Under normal light conditions, photosynthetic organisms are able to overcome photodamage by a rapid and efficient repair of the damaged proteins. The main target of this light-induced photoinhibition is the PSII-complex and specifically the D1 protein (Mattoo *et al.*, 1984; Prasil *et al.,* 1992; Aro *et al.,* 1993). As a consequence, the PSII core is subjected to a multi-step repair cycle, thereby maintaining the function of the photosynthetic light reactions (Baeno-Gonzalez and Aro, 2002; Aro *et al.,* 1993). According to current knowledge, PSII is the most dynamically regulated part of the light reactions in the thylakoid membrane (Tikkanen *et al.*, 2008). However, after light-induced damage of PSII core proteins, the corresponding complex must exit the grana stacks and migrate to the stroma lamellae, where the ribosomes have access. In the stroma thylakoids the PSII complex has to be partially disassembled,

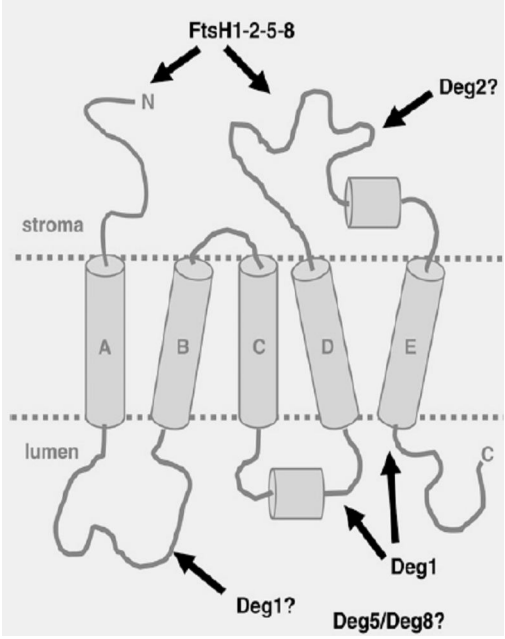

Fig. 1.4: Model for degradation of D1 during repair from photoinhibition.

The transmembrane helices of D1 are marked A to E. Adapted from Kapri-Pardes *et al.*, 2007.

depending on the extent of damage. After migration of the damaged PSII proteins, degradation takes place. This process must be tightly coordinated with the synthesis of new subunits and their incorporation into the PSII complex. There has been much effort to identify the proteases involved in D1 protein degradation. It has been demonstrated that the primary cleavage of the damaged D1 protein occurs on the stromal loop connecting the membrane-spanning helices D and E (Greenberg *et al.*, 1987) by the Deg2 protease (Haußühl *et al.*, 2001; Fig. 1.4). Simultaneously, a newly synthesised functional copy replaces the damaged D1 protein. Further degradation of D1 is conducted by an integral membrane metalloendopeptidase, FtsH (Lindahl *et al*., 2000). Both proteases are also involved in the degradation of the damaged D2 and PsbH proteins. Another protease has been identified, the Deg1 protease, which is located in the thylakoid lumen (Kapri-Pardes *et al.*, 2007). It was suggested that Deg1 cleaves the D1 protein in the lumenal loop connecting the transmembrane helices C and D. The lumenal immunophilin TLP18.3 (thylakoid lumen protein of 18.3 kDa) is not directly involved in the degradation of damaged D1 but seems to facilitate this process (Sirpiö *et al.*, 2007).

After a new D1 copy has been inserted a reconstitution of the PSII-complex takes place (binding of cofactors, integration of disassembled subunits) and the complex re-migrates to the grana stacks of the thylakoid membrane (Tikkanen *et al.*, 2008).

1.3) Synthesis and Integration of the PSII Reaction Centre Protein D1

The mature D1 protein has five transmembrane domains (see also Fig. 1.4) with its N-terminus on the stromal side of the thylakoids. The D1 protein is encoded by the plastid *psbA* gene and translated on thylakoid membrane-bound ribosomes (Zhang and Aro, 2002). The *psbA* transcript is remarkably stable in chloroplasts with a half-life between 10 and 40 hours (Mullet and Klein, 1987). In chloroplasts of flowering plants, the main regulatory step for the regulation of the amount of D1 protein is the translation initiation of *psbA* mRNAs leading to only minor fluctuations in *psbA* transcripts. In cyanobacteria, on the other hand, the regulation occurs at the level of transcription initiation (Golden *et al.*, 1986;

Mohamed and Jansson, 1989). However, a light-induced increase in the ATP/ADP ratio and the generation of reducing compounds were proposed to induce the association of ribosomes with the *psbA* mRNA and a subsequent initiation of translation in flowering plants. The HCF173 (high chlorophyll fluorescence 173) protein is essential for this initiation. In an *Arabidopsis* mutant lacking this protein, the synthesis of D1 was drastically decreased (Schult *et al.*, 2007). This nucleus-encoded factor is thought to be either involved in basic aspects of D1 synthesis or to be part of the regulatory apparatus adjusting *psbA* mRNA translation.

Like initiation of translation, the elongation of D1 is also dependent on light, as no full length D1 was found in etioplasts in the dark (Klein and Mullet, 1987; Klein *et al.*, 1988). Only upon illumination and concomitantly with pigment biosynthesis, accumulation of the full length D1 starts, without considerable increase of *psbA* mRNA in polysomes (Mullet *et al.*, 1990; Kim *et al.*, 1994). During the elongation of the D1 protein, ribosomes pause at specific sites (Kim *et al.*, 1991; Zhang *et al.*, 1999). This distinct pausing in mature chloroplasts is thought to be important for the binding of Chl *a* to D1 intermediates, thereby allowing the stabilisation of full length D1 directly upon release from ribosomes (Kim *et al.*, 1994). A nucleus-encoded auxiliary factor that is essential for the binding of Chl *a* to the D1 protein was described (HCF136; Meurer *et al.*, 1998; Plücken *et al.*, 2002). In the absence of HCF136, precursor-D1 (pD1) is synthesised but the assembly of stable PSII RC complexes is blocked and the D1 is degraded (Plücken *et al.*, 2002). Mutant seedlings were unable to grow on soil and were not able to produce any flowers when grown on sucrose-complemented medium (Meurer *et al.*, 1998). Besides stabilisation mechanisms, the elongation of *psbA* mRNA is also dependent on optimal photosynthetic electron transport, particularly on the production of reducing compounds by PSI (probably thioredoxin but this is still under debate; Kuroda *et al.*, 1996; Zhang *et al.*, 2000), and on the maintenance of a proton gradient across the thylakoid membrane (Mühlbauer and Eichacker, 1998). Additionally, the availability of assembly partners in the thylakoid membrane is essential for the translation of D1 (CES process) as already described above.

However, the synthesised D1 protein has to be inserted into the thylakoid membrane. It was shown that the new D1 protein is assembled cotranslationally

into the existing PSII complex composed of at least D2 and cyt *b*559 (α- and ß-subunit; Zhang *et al.*, 1999). The chloroplast signal recognition particle cpSRP54

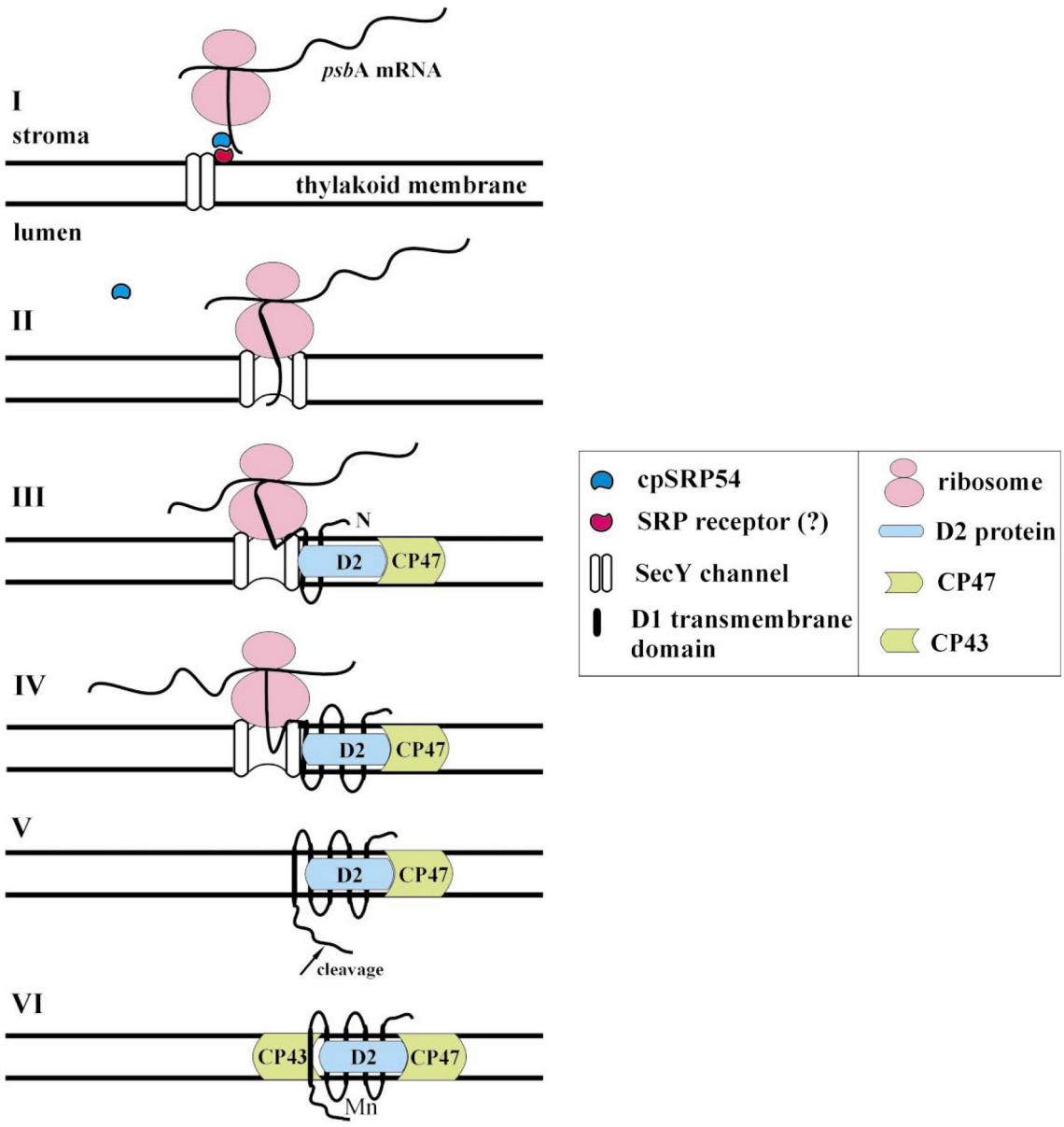

Fig. 1.5: Co- and posttranslational steps of D1 synthesis (Zhang and Aro, 2002).

I) Targeting of nascent D1 by cpSRP54; II) Insertion into cpSecY channel; III) and IV) Lateral exit of nascent D1 from cpSecY and interaction with other proteins; V) Termination and C-terminal processing; VI) Posttranslational association of CP43 into PSII.

(Nilsson *et al.*, 1999) is the first interactor of the ribosome nascent D1 chain complex and targets it to the thylakoid membrane (Fig. 1.5; depicted from Zhang and Aro, 2002). Afterwards, the D1 protein elongation and membrane insertion occur concomitantly. The insertion of the elongating D1 protein into the thylakoid membrane is likely to involve a cpSecY/E translocon channel, as shown by cross-linking and immunoprecipitation experiments (Zhang *et al.*, 2001). Additionally,

the integration process is supposed to require also the Alb3 protein, because the homologue in *Chlamydomonas*, Alb3.1, has been found to interact with D1 and to assist its assembly into PSII (Ossenbühl *et al.*, 2004). Pasch and co-workers (2005) could confirm this interaction with the *Arabidopsis* homologue using the yeast split-ubiquitin system. In those protein-protein interaction studies, Alb3 was also able to bind D2, CP43, and the PSI reaction centre protein PsaA. Another protein involved in the assembly of D1 into the PSII complex is the "LOW PSII ACCUMULATION 1" (LPA1; Peng *et al.*, 2006). The protein interacts specifically with D1 as shown in split-ubiquitin studies and is required for efficient PSII assembly, probably through direct interaction with D1. During integration into the thylakoid membrane, the proper folding of D1 is important for subsequent assembly of other subunits. This folding process is guided by the lumenal immunophilin CYP38 (Sirpiö *et al.*, 2008).

After proper insertion of D1 into the thylakoid membrane, C-terminal processing of the pD1 protein by the lumenal CtpA protease is essential for the formation of functional PSII complexes (Bowyer *et al.*, 1992; Oelmüller *et al.*, 1996). This process probably precedes the assembly of the CP43 protein (Zhang *et al.*, 2000), although it was also assumed that association of CP43 may accelerate the C-terminal processing of D1 (Zhang and Aro, 2002). However, only after both steps the ligation of the Mn cluster and the oxygen evolving complex to the lumenal side of PSII is possible.

1.4) Pulse Amplitude Modulation (PAM)

Besides the auxiliary proteins like LPA1 or HCF136, there are many more nucleus-encoded proteins with a possible role in the biogenesis, assembly or repair of photosystem II. Moreover, each stage of PSII assembly appears to be assisted by one or more proteins. Thus, there are several other components, which still have to be described to resolve the whole complexity of PSII assembly.

One instrument for the detection of additional auxiliary proteins that might be involved in PSII assembly is the Pulse Amplitude Modulation fluorometer (PAM; Schreiber *et al.*, 1986). It has been designed to quantify fluorescence and can thus been used to identify mutants with defects in photosynthesis. The functional state of PSII can easily be monitored by this non-invasive chlorophyll fluorescence measurement (Krause and Weis, 1991). The underlying principle is

quite simple. Light energy absorbed by photosynthetic pigments is used for photochemistry (charge separation fuelling electron transport), re-emitted by chlorophyll as fluorescence, or released as a consequence of thermal dissipation. In more detail, each quantum yield of light absorbed by a chlorophyll molecule raises an electron from the ground state to an excited state (Fracheboud, Y.; www.zealquest.com/upload/article/Using Chlorophyll Fluorescence to Study Photosynthesis.pdf). Upon de-excitation from a Chl *a* molecule from excited state 1 to ground state, a small proportion (3-5% *in vivo*) of excitation energy is dissipated as red fluorescence. This chlorophyll fluorescence is complementary to photochemistry and heat dissipation, which are alternative pathways of de-excitation in photosynthetic organisms. In general, when heat dissipation and photochemistry are low, the fluorescence yield is high. Therefore, changes in the fluorescence yield are a good indicator for changes in photochemical efficiency and heat dissipation.

Maximum fluorescence can be measured under conditions, when heat dissipation is negligible. For this, a very strong saturation light pulse (8000 µmol m^{-2} s^{-1}; 1 sec) is applied on dark-adapted plants and fluorescence raises from the ground state value (F_0) to its maximum value, F_m. Under this condition, the first electron acceptor of PSII (Q_A) is fully reduced and the maximum quantum efficiency of PSII primary photochemistry can be calculated ($F_V/F_m = (F_m-F_0)/F_m$). In healthy leaves, this value is always close to 0.8, independently of the plant species studied. If this value is reduced, parts of PSII reaction centres are probably damaged (= process of photoinhibition), which is often observed in plants under stress conditions, or with reductions in the amount of PSII. For the calculation of light induced changes in photochemistry and heat dissipation, a second saturating light pulse must be applied.

1.5) Aims of Thesis

During the past few years considerable progress has been made in resolving the three-dimensional structures of the thylakoid-embedded protein complexes (PSII, cyt b_6f, PSI, ATP-synthase). Currently, resolutions at 2-4 Å are possible (Zouni *et al.*, 2001; Kamiya and Shen, 2003; Stroebel *et al.*, 2003; Loll *et al.*, 2005; Amunts *et al.*, 2007). Besides structural studies, an emphasis has been put also on the identification of molecular chaperones and other auxiliary proteins involved in the

biogenesis and sustenance of the photosynthetic complexes (for review see Mulo *et al.*, 2008). Auxiliary proteins are challenging targets for research as most of them are low in abundance or expressed only transiently, e.g. under certain growth conditions or in a particular growth phase (Klimmek *et al.*, 2006; Nowaczyk *et al.*, 2006). Due to the limited coding capacity of the chloroplast genome, these factors are mainly nucleus-encoded proteins (Goldschmidt-Clermont, 1998; Barkan and Goldschmidt-Clermont, 2000; Rochaix, 2001; Leister, 2003). With the help of the PAM system, an extensive screen for additional auxiliary factors was realised (Varotto *et al.*, 2000). It was used for the detection of mutated plants that showed a reduced photosynthetic performance. In this screen, a promising candidate for a PSII-mutant was identified, the *pam68*-mutant (*photosynthesis affected mutant*).

2) Materials and Methods

2.1) Materials

2.1.1) Chemicals

All chemicals were purchased from Sigma-Aldrich (Munich, Germany), Roth (Karlsruhe, Germany), Applichem (Darmstadt, Germany), Merck (Darmstadt, Germany), Serva (Heidelberg, Germany) and Duchefa (Haarlem, Netherlands), except where stated otherwise. All chemicals were analytical grade.

2.1.2) Antibiotics

Antibiotics were provided by Roth (Karlsruhe, Germany), Duchefa (Haarlem, Netherlands) and by Sigma-Aldrich (Munich, Germany).

	E. coli	Agrobacterium	Plant
Ampicillin	100 µg/ml	100 µg/ml	-
Carbenicillin	50 µg/ml	50 µg/ml	-
Rifampicin	-	100 µg/ml	-
Gentamycin	-	25 µg/ml	-
Hygromycin	-	-	15 µg/ml

Table 2.1: Antibiotics used for selection experiments in different organisms.

2.1.3) Kits and Enzymes

Enzymes used for cloning were obtained from New England Biolabs (Frankfurt, Germany), Roche (Penzberg, Germany), Fermentas (St. Leon-Rot, Germany) and Qiagen (Hildesheim, Germany). Those enzymes employed for the synthesis of cDNA were purchased from Invitrogen (Karlsruhe, Germany). For DNA purifications kits from Qiagen (Hildesheim, Germany) were used. Western-detection was carried out with the Enhanced Chemiluminescence Kit (ECL; Pierce, Rockford, USA).

2.1.3.1) Kits

NucleoBond Xtra Midi	Macherey-Nagel GmbH & Co. KG, Düren
NucleoSpin Plasmid	Macherey-Nagel GmbH & Co. KG, Düren
QIAquick PCR Purification Kit	Qiagen, Hilden
pGEM®-T and pGEM®-T Easy Vector Systems	Promega Corporation, Madison (USA)
Pierce ECL Western Blotting Substrate	Perbio Science Deutschland GmbH, Bonn

Table 2.2: Kits used for DNA-isolation/purification, cloning, and western detection.

2.1.3.2) Enzymes

Taq DNA Polymerase	Qiagen, Hildesheim
Phusion™ High-Fidelity DNA Polymerase	New England Biolabs GmbH, Frankfurt am Main
Antarctic Phosphatase	New England Biolabs GmbH, Frankfurt am Main
SuperScript® III Reverse Transcriptase	Invitrogen, Karlsruhe
DNA Polymerase I, Large (Klenow) Fragment	New England Biolabs GmbH, Frankfurt am Main

Table 2.3: Enzymes used for cloning, cDNA synthesis, and production of probes for Northern analyses.

2.1.4) Membranes

Nitrocellulose and PVDF membranes used for Western Blot analyses were acquired from Millipore (Eschborn, Germany) and positively charged Nylon membranes used for Northern Blot analyses from Roche (Penzberg, Germany).

2.1.5) Antibodies

Peptide synthesis, generation of antibodies in rabbits and their monospecific purification was performed by Biogenes (Berlin, Germany) for the PAM68 (CSDEDDDDEDEDD-amide) and PAM68HL-Protein (CSRTSEDPGRPD-amide). The used peptides are localised upstream of the first transmembrane domain of both proteins and downstream of the predicted cTP after utilisation of a hydrophobicity plot (for details see Chapter 3.3.5). Commercially available primary antibodies against photosynthetic polypeptides were purchased from Agrisera.

Protein	Immunogen	Supplier
D1	Whole protein	Prof. Dr. J. Soll (Department of Botany, LMU, Munich)
D2	C-terminal	Agrisera (Vänas, Sweden)
CP47	n.d.	Agrisera (Vänas, Sweden)
CP43	aa 257-450 of *A. thaliana*	Agrisera (Vänas, Sweden)
PsbE	KLH-conjugated synthetic peptide of *A. thaliana*	Agrisera (Vänas, Sweden)
PsbO	N-terminal peptide from *A. thaliana* PsbO1	Agrisera (Vänas, Sweden)
LHCII (Lhcb2)	BSA-conjugated synthetic peptide from angiosperms and gymnosperms	Agrisera (Vänas, Sweden)
PsaF	n.d.	Prof. Dr. H.V. Scheller (Department of Plant Biology and Biotechnology, Copenhagen, Denmark)
PsaH	n.d.	Prof. Dr. H.V. Scheller (Department of Plant Biology and Biotechnology, Copenhagen, Denmark)
PsaL	KLH-conjugated synthetic peptide from *A. thaliana*	Agrisera (Vänas, Sweden)
Lhca3	Synthetic peptide from *A. thaliana*	Agrisera (Vänas, Sweden)
Cyt f	GST fusion to cyt f from *Chlamydomonas reinhardtii*	Agrisera (Vänas, Sweden)
CF_1-α/ß	n.d.	Prof. Dr. A. Barkan (Institute of Molecular Biology, Wisconsin, USA)
CF_1-δ	n.d.	PD Dr. J. Meurer (Department of Botany, LMU, Munich)
FNR	n.d.	Prof. Dr. H.V. Scheller (Department of Plant Biology and Biotechnology, Copenhagen, Denmark)
Actin	Purified *A. thaliana* actin protein	Dianova (Hamburg, Germany)
Rabbit	Horseradish peroxidase-conjugated donkey antibody to rabbit	GE-Healthcare (Munich, Germany)
Chicken	Peroxidase antibody produced in rabbit	Sigma-Aldrich (Munich, Germany)
Mouse	Horseradish peroxidase-conjugated donkey antibody to mouse	GE-Healthcare (Munich, Germany)

Table 2.4: Antibodies used for immunoblot-analyses.

2.2) Methods

2.2.1) Plant Material and Growth Conditions

Arabidopsis thaliana (*Arabidopsis*) seeds were stratified for 2 days at 2-5°C in the dark to break dormancy and then sown out on potting soil (Stender AG, A210). Plants were grown in a growth chamber illuminated with a 16 h-light (20°C) / 8 h-dark (15°C) cycle with a PFD of 120 µmol photons $m^{-2}s^{-1}$ (GL, growing light) or under controlled greenhouse conditions (PFD 70-90 µmol photons $m^{-2}s^{-1}$, 16 h light / 8 h dark cycles). The fertilizer Wuxal Super (8% N, 8% P_2O_5, 6% K_2O; MANNA, Deutschland) was used according to the manufacturer's instructions.

The insertion mutant lines carried either T-DNA or *Dissociation* (*Ds*) element insertions and were identified by searching the insertion flanking database SIGNAL (http://signal.salk.edu/cgi-bin/tdna express). The *pam68-1* mutant (GABI_152D07) derives from the GABI-KAT collection (Li *et al.*, 2003), the *pam68-2* (SALK_044323) and *pam68hl* (SALK_143426) from the SALK T-DNA collection (http://signal.salk.edu/; Alonso *et al*., 2003) with all three of them in the Columbia-0 (Col-0) background. The *lpa1* mutant (CSHL_ET6851) originates from the Cold Spring Harbor Laboratory and carries a *Dissociation* (*Ds*) element insertion in the Landsberg *erecta* (Ler) background (Martienssen, 1998). Unless stated elsewhere, full-grown rosette leaves of 4 weeks old plants were used for all biochemical and physiological measurements.

2.2.2) Nucleic Acid Analyses

2.2.2.1) DNA Analysis

Arabidopsis DNA was isolated by disruption of leaf material frozen in liquid nitrogen with metal beads and addition of isolation buffer (200 mM Tris/HCl (pH 7.5), 250 mM NaCl, 25 mM EDTA, 0.5% SDS). DNA in the supernatant was precipitated by addition of 0.8 volumes of isopropanol and centrifugation at 16,000 x *g* at room temperature (RT) for 20 min. For PCR amplifications of DNA templates 0.5 mM oligonucleotide primers, 0.2 mM dNTPs and 2.5 U Taq polymerase were used. The polymerase used was either Qiagen Taq polymerase for mutant screenings or Phusion® High-Fidelity DNA-polymerase for cloning. The insertion flanking sites were identified by sequencing after PCR-amplifications using a combination of gene- and insertion-specific primers. T-DNA primer specific for the T-DNA transformation vector pROK2 (SALK-collection; Fig.

6.1) was LBa1; for the vector pAC161 (GABI-KAT collection; Fig. 6.2) LBgk1; for the enhancer trap (ET) transposable Ds element (CSHL collection) Ds3-4 (Table 2.5). Primers specific for confirmation of the knock-out alleles *pam68-1* and *pam68-2* were At4g19100-503F, At4g19100-1386R and At4g19100-1598R, for *pam68hl* At5g52780-6F and At5g52780-579R, for *lpa1* At1g02910-654F and At1g02910-1521R.

Oligonucleotides	Sequence 5´->3´
At4g19100-503F (P1)	GGCTTCTGTACCATGTTCCTT
At4g19100-478s (P2)	TCCTCCTAAGAAAACCAAGAAG
At4g19100-901R (P5)	TCTCTAAGCGGTTAATGCAAGT
At4g19100-1261R (P6)	ACACCAGCTAAAGCCGTACC
At4g19100-1386R (P7)	CTATCTCTTGTCTGAGGAATTC
At4g19100-1598R (P9)	GCGTGTGTGAAATTTGGTTTGC
At5g52780-6F (P1)	CATTAGAAGAAGAAATAGAAATGAG
At5g52780-101F (P2)	CACAATCCAAAAACCCTATATCC
At5g52780-463R (P4)	GAGTCCAAAAAGAGAGTTAGTC
At5g52780-579R (P6)	AGCCAGCTTAAAAGTTTTTATGAG
At1g02910-654F	GTGAAAGATGCTCTTGTTCAGT
At1g02910-1521R	GCTGCACAAGTTCAACAACGC
LBa1 (P10)	TGGTTCACGTAGTGGGCCATCG
LbGK1 (P11)	CCCATTTGGACGTGAATGTAGACAC
Ds3-4	CCGTCCCGCAAGTTAAATATG
PAM68-TKTL-c1F (including the sequence of the T7 promoter)	ACCTAGTAATACGACTCACTATAGGGCG AGCCGCCATGGCTTCTGTACCATGTTCC
PAM68-TKTL-c624R	TTGACTCTATCTCTTGTCTGAGGAATTC
PAM68-RFP-F	CGCCATGGCTTCTGTACCATGTTCC
PAM68-RFP-R	CGCCATGGCACCTCCTCTCTTGTCTGAGG AATTCCA

Table 2.5: Oligonucleotides employed for identification of gene insertion lines and cloning.

2.2.2.2) RNA Analysis

For RNA analysis, total leaf RNA was extracted from fresh tissue using the phenol-containing TRIzol reagent (Invitrogen, Karlsruhe) and chloroform. RNA was precipitated from the aqueous phase with isopropanol and 0.8 M sodium citrate/1.2 M NaCl and centrifugation at 12,000 x *g* at 4°C. Reverse transcriptase-mediated PCRs (RT-PCR) were carried out by synthesising first-strand cDNA

using the SuperScript™ Reverse Transcriptase and dT oligomers, followed by PCR with specific primers for PAM68 (*pam68-1*: P1/P6 -> upstream of insertion, *pam68-2*: P1/P5 -> upstream of insertion; P1/P7 across both insertions; for sequences see Table 2.5). *ACTIN1* served as a control (see Table 2.6).

Northern analyses were performed under stringent conditions, according to Sambrook *et al*. (1989). Normally, 10 µg of total cellular RNA was used. RNA was denatured through incubation with formaldehyde, electrophoretically separated in 2% agarose gels in MEN buffer (20 mM MOPS, 5 mM Na-acetate, 1 mM EDTA) and transferred onto a positively charged nylon membrane (Roche, Penzberg) in 20x SSC buffer (3M NaCl, 0.3 M Na-citrate (pH 7)). RNA was fixed to the membrane by UV radiation.

Probes complementary to nuclear and chloroplast genes were used for the hybridisations. Table 2.6 lists the genes analysed and the primers used to amplify the probes. Primers specific for *PAM68* (P1 and P6) are listed in Table 2.5. All probes were cDNA fragments labelled with ^{33}P-dCTP. Hybridisations were performed overnight in hybridisation buffer (0.25 M NaH_2PO_4/Na_2HPO_4 (pH 7), 7% SDS, 100 µg/ml herring sperm ssDNA) at 65°C. Prehybridisations were carried out in the same buffer for at least four hours. After hybridisation, filters were washed twice with washing buffer 1 (0.1% SDS, 0.3 M NaCl, 20 mM NaH_2PO_4/Na_2HPO_4 (pH 7), 2 mM EDTA) at 65°C and once with washing buffer 2 (5 mM NaH_2PO_4, 1 mM EDTA, 0.2% SDS) at room temperature. For exposure, filters were sealed in plastic bags. Signals were analysed and quantified by using a phosphoimager (Typhoon TRIO Variable Mode Imager; Amersham Biosiences) and the program IMAGE QUANT (version 5.2).

Genes	Forward primer (5´->3´)	Reverse primer (5´->3´)
ACTIN1	TGCGACAATGGAACTGGAATG	GGATAGCATGTGGAAGTGCATACC
psbA	TCCGGTGCCATTATTCCTAC	CTTCTTCTTGCCCGAATCTG
psbB	CGGGTCTTTGGAGTTACGAA	TCCAGCAACAACAAAAGCTG
psbD	CCGCTGCAGTTTCTACTCCT	CGGCTTGAGTTGGGTTAAAA
LHCB3	GACAGAGTGAAGTACTTAGGA	AGCCAAACATCGAGAACATAGC
ATPD	GCAGCATCAAGCTACGCGAT	CCAAGTTCAAGCTGAGAAGCA
rbcL	CGTTGGAGAGACCGTTTCTT	CAAAGCCCAAAGTTGACTCC

Table 2.6: Oligonucleotides employed for Northern probe generation.

2.2.2.3) Analysis of mRNAs Associated With Polysomes

Polysomes were isolated as described by Barkan (1988) with some modifications. Frozen leaf tissue (200 mg) was ground with mortar and pestle in liquid nitrogen and thawed in polysome extraction buffer (Jackson and Larkins, 1976) supplemented with 100 mM 2-mercaptoethanol, 2% Triton X-100, 100 µg/ml chloramphenicol, 25 µg/ml cycloheximide, and 0.5 mg/ml heparin. Subsequently, the microsomal membranes were filtered through a syringe supplemented with glass wool, and the flow-through was solubilised with 1% Triton X-100 and 0.5% sodium deoxycholate. The solubilised material was layered onto 15% to 55% continuous sucrose gradients and centrifuged in a Beckman LE-80K ultracentrifuge (SW 60 Ti rotor) at 243,000 x *g* for 65 min at 4°C. The sucrose gradient was fractionated into 11 fractions and 20 mM EDTA and 0.5% SDS were added. The mRNA associated with polysomes was then extracted with phenol/chloroform/isoamyl alcohol (25:24:1) followed by precipitation at room temperature with 95% ethanol. All samples were then subjected to Northern analyses.

2.2.3) Transformation of Bacteria and Plants (*Arabidopsis thaliana*)

2.2.3.1) Bacterial Strains

The *E. coli* strain used was DH5α (Bethesda Res. Lab., 1986; Taylor *et al.*, 1993). The bacteria were propagated in LB medium or on LB-agar plates at 37°C as desribed in Sambrook *et al.* (1989). The Agrobacterium strain used was *Agrobacterium tumefaciens* GV3101, which carries a gentamycin resistance on the Ti plasmid (pMP90RK; Koncz *et al*., 1990). Agrobacteria were grown at 28°C in YEB medium supplemented with 100 µg/ml rifampicin and 25 µg/ml gentamycin.

2.2.3.2) Agrobacterium Binary Vectors

For complementation of the *pam68-2* mutant, plants were transformed with 35S::PAM68/pH2GW7 (for vector map of pH2GW7 see Fig. 6.3; Karimi *et al.,* 2002), which carries the complete *PAM68* coding region downstream of a 35S promoter. For selection of transfected plants, the vector carries a hygromycin resistance gene (HygR).

2.2.3.3) *Agrobacterium*-Mediated Transformation of *A. thaliana*

Arabidopsis mutant plants were transformed by dipping developing floral tissues as reported (Clough and Bent, 1998). Budding plants were dipped for 10 s in an *Agrobacterium tumefaciens* suspension containing 2.5% sucrose and the surfactant Silwet L-77 (0.02%). Sucrose and surfactant are critical to the success of the floral dip method. After dipping, plants were covered with clear plastic for two days to sustain high humidity levels, which facilitates transformation. Subsequently, the plants were transferred to the greenhouse and grown to full maturity until seeds could be harvested. For selection of positive transformants, seed were sterilised with 15% Na-hypochlorite supplemented with 2% HCl and sown out on sterile media containing 15 µg/ml hygromycin.

2.2.4) Biochemical Analyses

2.2.4.1) Antibody Production

Antibodies against epitopes of PAM68 and PAM68HL were produced in rabbits. Epitope synthesis, injection into rabbits, collection of serum and subsequent monospecific purification of IgGs was carried out by Biogenes (Berlin, Germany). The epitopes ranging in size from 10 to 11 amino acids were designed in such way that they were specific for the respective proteins (fasta search: www.arabidopsis.org/cgi-bin/fasta/nph-TAIRfasta.pl) and covered a hydrophilic stretch of amino acids with high antigenicity. For analysis of hydrophility the hydrophobicity plot of Marc N. Offman was employed (http://www.bmm.icnet.uk/~offman01/hydro.html). The amino acid sequences of the epitopes in one letter code were DEDDDDEDEDD for PAM68 and RTSEKPGRPD for PAM68HL.

2.2.4.2) SDS-PAGE

Identical amounts of proteins equivalent to 2-5 µg of chlorophylls calculated as described in Porra *et al.* (2002) were solubilised in SDS loading buffer (50 mM Tris/HCl (pH 6.8), 4% w/v SDS, 12% v/v glycerol, 50 mM DTT, 0.01% bromophenol blue), loaded and separated by SDS-PAGE (12%-16% acrylamide) as described by Schägger and von Jagow (1987). After an overnight run at 30 mA per gel (150 mm x 180 mm x 15 mm separating gel; anode buffer: 0.2 M Tris/HCl (pH 8.9), cathode buffer: 0.1 M Tris, 0.1 M Tricine, 0.1% SDS), gels were

either stained with silver or Coomassie Brilliant Blue to visualise proteins according to standard protocols. Alternatively, specific proteins were detected using the method of immunoblot analysis.

2.2.4.3) Immunoblot Analysis

Proteins separated by native or SDS-PAGE were transferred to polyvinylidene difluoride (PVDF) membranes according to Towbin *et al.* (1979) by a semi-dry blotting system using a current corresponding to 1 mA cm^{-2} in transfer buffer (96 mM glycine, 10 mM Tris, 10% (v/v) methanol). Filters were blocked in TTBS buffer (10 mM Tris/HCl (pH 8), 150 mM NaCl, 0.1% Tween-20) with 5% milk powder. Hybridisation with antibodies was performed in TTBS with 3% milk powder. Primary antibodies were incubated for 2 h at RT or overnight at 4°C, secondary antibodies for 1 h at RT. Washing steps after antibody-incubation were performed in TTBS. Signals were detected using the Enhanced Chemiluminescence Western Blotting Kit (Pierce, Rockford, USA).

2.2.4.4) Total Protein Isolation

Leaves were disrupted in the presence of liquid nitrogen and total proteins were isolated by adding extraction buffer (100 mM Tris/HCl (pH 8.0), 50 mM EDTA (pH 8.0), 0.25 M NaCl, and 1 mM DTT, 0.7% (w/v) SDS) and incubation at 65°C for 10 min. After centrifugation at 10,000 x *g* for 10 min, the chlorophyll concentration of the supernatant was determined as described in Porra *et al.* (2002) and total proteins according to 5 µg of chlorophyll were precipitated with 100% acetone, resuspended in protein loading dye (0.5 M urea, 2% SDS, 7% glycerol, 55 mM Tris/HCl (pH 6.8), 4% 2-mercaptoethanol) and loaded onto a SDS gel.

2.2.4.5) Preparation of Thylakoid Membranes

Leaves from 4-week-old plants were harvested in the middle of the light period. Leaf material was homogenised in ice-cold buffer containing 0.5% milk powder, 0.4 M sorbitol and 0.1 M Tricine/KOH (pH 7.8), the resulting homogenate was filtered through nylon mesh and centrifuged at 4°C, 6000 x *g* for 5 min. Subsequently, chloroplasts were broken in 25 mM HEPES/KOH (pH 7.8), 10 mM EDTA (pH 8.0) and thylakoids were collected by centrifugation at 10,000 x *g* for 10 min and either resuspended in a buffer containing 50% glycerol, 10 mM

HEPES/KOH (pH 7.5), 1 mM EDTA (pH 8.0) for longer storage or directly resuspended in protein loading dye.

2.2.4.6) Blue Native and Second Dimension Gels

Leaves from 4- to 5-week-old plants were harvested and thylakoids were prepared as already described (Bassi *et al.*, 1985). For the native PAGE analysis, protein amounts equivalent to 60 µg of chlorophyll for WT and 30 µg for *pam68-2* were washed twice with 20 mM HEPES/KOH (pH 7.8), 10 mM EDTA (pH 8.0), and subsequently solubilised in 750 mM ε-aminocaproic acid, 50 mM Bis-Tris/HCl (pH 7.0), 5 mM EDTA (pH 7.0), 50 mM NaCl for 20 min with 1.25% (w/v) n-dodecyl-ß-D-maltoside (ß-DM) on ice. Solubilised protein complexes were separated from unsolubilised by centrifugation for 20 min at 16,000 x *g*, 4°C. The supernatant was supplemented with 5% (w/v) Coomassie Brilliant Blue G250 in 750 mM aminocaproic acid, and loaded onto gradient-polyacrylamide gels (4-12% acrylamide). One–dimensional BN-PAGE and two-dimensional BN/SDS-PAGE were carried out as described by Schägger and von Jagow (1991).

2.2.4.7) *In vitro* Import in Pea Chloroplasts

The coding region for *PAM68* was amplified by PCR (using the primers PAM68-TKTL-c1F and PAM68-TKTL-c624R; for sequences see Table 2.5). The constructs were verified by DNA sequencing (http://www.genetik.biologie.uni-muenchen.de/sequencing). mRNA was obtained by transcription with T7-RNA polymerase according to manufacturer's instructions (Fermentas, St. Leon-Rot, Germany) and used for translation in wheat germ (Wheat Germ Extract System, Promega, Madison, USA) in the presence of [^{35}S]methionine at 30°C for 1 h. The translation mixture was centrifuged at 50,000 x g for 1 h at 4°C prior to import experiments.

Intact chloroplasts were isolated from 10-day-old pea leaves (*Pisum sativum*, var. Golf) and purified through Percoll density gradients as described (Waegemann and Soll, 1991). Import assays were performed with chloroplasts equivalent to 20 µg of chlorophyll in 100 µl of import buffer (10 mM methionine, 10 mM cysteine, 20 mM potassium gluconate, 10 mM $NaHCO_3$, 330 mM sorbitol, 50 mM HEPES/KOH (pH 7.6), 5 mM $MgCl_2$; Nada and Soll, 2004). The amount of translation product never exceeded 10% of the total reaction volume. The import

was carried out at 25°C for 30 min. Chloroplasts were subsequently re-purified over a 40% Percoll cushion in import buffer. The chloroplasts were washed twice (30 mM sorbitol, 50 mM HEPES (pH 7.6), 0.5 mM $CaCl_2$) and subjected to SDS-PAGE. For thermolysin treatment, chloroplasts were washed in 330 mM sorbitol, 50 mM HEPES (pH 7.6), 0.5 mM $CaCl_2$ and incubated with 20 µg/ml thermolysin (Calbiochem, Darmstadt, Germany) for 20 min on ice. The reaction was stopped by addition of EDTA (pH 8) to a final concentration of 5 mM and chloroplasts were washed once again.

To obtain the membrane fraction, chloroplasts were hypotonically lysed in 50 mM HEPES/KOH (pH 7.6) and membranes were collected after centrifugation at 10,000 g for 10 min at 4°C. Treatment with 6 M urea was carried out in 50 mM HEPES/KOH (pH 7.6) for 15 min at 25°C (Nada and Soll, 2004). Solubilised proteins were separated from the insoluble fraction after centrifugation at 10,000 x g for 10 min at 4°C. Radiolabelled proteins were separated by SDS-PAGE and detected with the Typhoon phosphoimager.

2.2.4.8) *In vivo* Labelling With 35S-Methionine

For the radioactive labelling of chloroplast proteins according to Pesaresi *et al.* (2001), leaves of 4-week-old Arabidopsis plants grown in the climate chamber (16 h/8 h light/dark cycle with a PFD of 120 µmol photons $m^{-2}s^{-1}$) were preincubated with 20 µg/ml cycloheximide (in a buffer containing 1 mM KH_2PO_4 (pH 6.3), 0.1% Tween-20) to block the synthesis of nuclear-encoded proteins followed by a vacuum-infiltration in a syringe containing 1 mCi of [^{35}S] L-methionine/cysteine in 5 ml of 1 mM KH_2PO_4 (pH 6.3), 0.1% Tween-20 and illuminated with 20 µmol photons $m^{-2}s^{-1}$.

Afterwards, thylakoid membranes were isolated according to chapter 2.2.4.5. Thylakoids were loaded onto a SDS-PAGE gel, which was either dried or subjected to a semi-dry blotting transfer according to Towbin *et al.* (1979). Signals were quantified by using the Typhoon phosphoimager and the program IMAGE QUANT (version 5.2).

2.2.4.9) Lincomycin-Treatment With Intact Leaves

Intact *Arabidopsis* leaves of 4-week-old plants were incubated in 1 mM KH_2PO_4 (pH 6.3) and 0.1% Tween-20 containing 100 µg/ml lincomycin, to block synthesis of chloroplast-encoded proteins, and illuminated for various times under growth light conditions (120 µmol photons $m^{-2}s^{-1}$). After this treatment, the thylakoid membranes were isolated (see section 2.2.4.5), and the contents of proteins were determined through immunoblot analysis.

2.2.5) Pigment Analysis

Pigment content was analysed by reverse-phase HPLC as described previously by Färber *et al.* (1997). For pigment extraction, leaf discs were weighted, frozen in liquid nitrogen and pestled in microcentrifuge tubes in the presence of acetone. After a short centrifugation, pigment extracts were either used directly for HPLC analysis or stored for up to 2 days at -20°C (the pigment analysis was performed in collaboration with Prof. Peter Jahns, Düsseldorf, Germany).

2.2.6) *In silico* Analyses

For the analysis of gene models and their coverage by full-length mRNAs or ESTs, the NCBI (www.ncbi.nlm.nih.gov), MIPS (http://mips.gsf.de/proj/thal/db/index.html), and TAIR (www.arabidopsis.org) databases were used. To identify orthologues, the protein sequences were blasted against the translated nucleotide database using NCBI tblastn (www.ncbi.nlm.nih.gov/blast/Blast.cgi). For the confirmation of *Chlamydomonas reinhardtii,* cyanobacterial and poplar homologues, the JGI Chlamy v2.0.58 Blast (http://genome.jgi-psf.org/Chlre4/Chlre4.home.html), the Cyanobase similarity search (http://genome.kazusa.or.jp/cyanobase) and the JGI Populus trichocarpa v2.0.58 (http://genome.jgi-psf.org/Poptr1_1/Poptr1_1.home.html) online programs were applied.

Digital Northerns were performed by using the Genevestigator site (www.genevestigator.com; Zimmermann *et al.*, 2004). Amino acid sequences were aligned using the CLUSTAL-W program (www.ebi.ac.uk/clustalw/; Chenna *et al.*, 2003) and alignments were shaded according to sequence similarity using the Boxshade server 3.21 (www.ch.embnet.org/software/BOX_form.html). Sequence identities and similarities were calculated using NCBI Blast 2

sequences (Tatusova and Madden, 1999). A phylogram was built using the programs PHYLIP version 3.67, Protmlk (*PHYL*ogeny *I*nference *P*ackage; http://evolution.genetics.washington.edu/phylip.html) and PhyloDraw version 0.8 (http://pearl.cs.pusan.ac.kr/phylodraw/).

Co-regulated gene relationships in *Arabidopsis* were estimated by using the ATTED-II program (version 5.2; Obayashi *et al.*, 2009; www.atted.jp/).

Predictions of chloroplast targeting were performed with the following algorithms: TargetP (version 1.1; http://www.cbs.dtu.dk/services/TargetP/; Emanuelsson *et al.*, 2000), ChloroP (version 1.1; http://www.cbs.dtu.dk/services/ChloroP/; Emanuelsson *et al.*, 1999), MitoProt (http://ihg2.helmholtz-muenchen.de/ihg/mitoprot.html; Claros and Vincens, 1996), Predotar (http://urgi.versailles.inra.fr/predotar/predotar.html; Small *et al.*, 2004), PSORT (http://psort.ims.u-tokyo.ac.jp/form.html), iPSORT (http://hc.ims.u-tokyo.ac.jp/iPSORT/; Bannai *et al.,* 2002), WolfPSORT (http://wolfpsort.org/ ; Horton *et al.*, 2007), BaCelLo (http://gpcr.biocomp.unibo.it/bacello/; Pierleoni *et al.*, 2006), and PCLR v. 0.9 (http://www.andrewschein.com/pclr/ ; Schein *et al.*, 2001). Protein molecular weights were calculated using Protparam (http://www.expasy.org/ tools/protparam.html) and transmembrane domains were predicted using the TMHMM Server v. 2.0 (www.cbs.dtu.dk/services/ TMHMM-2.0).

2.2.7) Intracellular Localisation of dsRED Fusions

The red fluorescent protein from the reef coral *Discosoma* (dsRED) (Jach *et al.*, 2001) was used as a reporter to determine the intracellular localisation of PAM68 in transient gene expression assays. The coding regions of the *PAM68* gene were amplified using primers PAM68-RFP-F/PAM68-RFP-R (see Table 2.5), and cloned upstream of the dsRed sequence using the *Nco*I restriction enzyme. Sterile cotyledons of 2 week-old plants (ecotype ColGl-1) were cut into small pieces and incubated for 16 h at 24°C in the dark in a protoplasting solution (10 mM MES, 20 mM $CaCl_2$, 0.5 M mannitol (pH 5.8), 0.1 g/ml macerozyme (Duchefa), 0.1 g/ml cellulase (Duchefa) followed by the isolation of protoplasts as described in Dovzhenko *et al.* (2003). Plasmid DNA (40 µg) was introduced into protoplasts by PEG transfection as previously described (Koop *et al.*, 1996). Microscopy analysis (with Fluorescence Axio Imager microscope in ApoTome mode (Zeiss)) was conducted after 16 h of incubation at 23°C in the dark.

Fluorescence was excited with the X-Cite Series 120 fluorescence lamp (EXFO) and images were collected in the 565–620 nm (dsRED fluorescence) and 670–750 nm (chlorophyll autofluorescence) ranges.

2.2.8) Determination of Photosynthetic Parameters Using the PAM Fluorometer

In vivo Chl *a* fluorescence of single leaves was measured using either the Pulse Amplitude Modulation 101/103 (PAM 101/103) as already described in Varotto *et al.* (2000) or the Dual-PAM-100 Fluorometer (Walz, Effeltrich, Germany). Plants were dark adapted for 20 min and minimal fluorescence (F_0) was measured. Then pulses (0.8 s) of white light (5000 µmol photons $m^{-2}s^{-1}$) were used to determine the maximum fluorescence (F_m) and the ratio $(F_m – F_0) / F_m = F_v / F_m$ (maximum quantum yield of PSII) was calculated. A 10 min illumination with actinic light of varying intensities was supplied to drive electron transport between PSII and PSI. Then firstly steady state fluorescence (F_m) and then by a further saturation pulse (0.8 s, 5000 µmol photons m^{-2} s^{-1}) F_m' were determined and the effective quantum yield of PSII (Yield) was calculated as $(F_m'- F_s) / F_m'$. Additionally the photosynthetic parameters qP (photo-chemical quenching $(F_m' – F_s) / (F_m' – F_0)$) and NPQ (non-photochemical quenching $(F_m - F_m')/ F_m'$) were determined.

2.2.9) Split-Ubiquitin Assay

For split ubiquitin assay, the coding sequence of the mature PAM68 and PAM68HL protein (without predicted cTP) were cloned in pAMBV4 (Fig. 6.4) encoding the Cub fragment and used as bait in interaction studies. The reporter in this plasmid consists of the LexA-DNA-binding domain and the VP16-activation domain. The prey proteins were generated by cloning the coding sequences of mature proteins into pADSL-Nx (Fig. 6.4), which encodes the Nub fragment. This vector also encodes a hemagglutinin-epitope tag. The full-length genes of LPA1, LPA2, HCF136 and PsbB were obtained by polymerase chain reaction (PCR) amplification from total cDNA (for a list of primers, refer to Table 2.7). Both vectors originally derived from Dualsystems Biotech AG (Zürich, Switzerland).

Interaction studies were performed in the lab of Prof. Danja Schünemann (Fakultät für Biologie und Biotechnologie, Ruhr-Universität Bochum; Pasch *et al.*, 2005).

Construct	**Forward Primer**	**Reverse Primer**
PAM68-Cub	CGTCTAGACAAAAATGGATAAAACGAAGATCAAG	CGCCATGGATTCTCTTGTCTGAGGAATTCCA
PAM68HL-Cub	CGCCATGGAAAAATGACCTCTGAAAAACCCG	CGCCATGGATTTGGTCCTCTTTCCACATCTC
Nub-LPA1	ATGGATCCGATGCTCTTGTTCAGTTTGA	GCGAATTCGCTCATCTTTCTAACTTGCTGAGA
Nub-LPA2	CGCCCGGGTATCAAAGAATTCAAGCTCTTCC	ATCTCGAGTCACTCTTGACCCTTCATTTTC
Nub-HCF136	ATCCCGGGTAGATGAACAGTTATCCGAATG	ATCTCGAGTCAGCCAACATATCGGAGCAA
Nub-PsbB	ATCCCGGGTAGGTTTGCCTTGGTATCGTGT	ATCTCGAGTCAGACTGCTTGTCGTTTTGTA

Table 2.7: Primer list for split-ubiquitin.

List of primers (5´ -> 3´ orientation) used for cloning bait (*PAM68, PAM68HL*) and prey (*LPA1, LPA2, HCF136, psbB*) sequences for the split-ubiquitin assay. Restriction sites are underlined.

3) Results

3.1) Characterisation of PAM68

The following work is based on a screen for photosynthetic affected mutants (PAM-mutants). The screen was carried out via Chl *a* fluorescence measurements (Maxwell and Johnson, 2000). This non-invasive tool was used to identify T-DNA insertion lines that showed an altered yield of fluorescence, a good indicator for diminished photosynthetic capacity. The plants used for the experiment derived from the GABI-Kat collection (German plant genomics research program; (Li *et al.*, 2003)). The aim of the GABI-Kat project was to build a large T-DNA mutagenised *Arabidopsis thaliana* (*Arabidopsis*) population with sequence-indexed insertion sites. The positions of these sites were located with the help of flanking sequence tags as described in Li *et al.* (2003).
A mutation in the *Arabidopsis* gene encoding the PAM68 protein (Photosynthesis Affected Mutant 68, At4g19100) led to a remarkable reduction in the F_V/F_M ratio (0.37 in the mutant vs 0.84 in the wild-type), which represents the maximum efficiency of PSII photochemistry. Hence, the *pam68-1* mutant was classified as a putative PSII-mutant and characterised in this work. Additionally, the homologue of PAM68 in *Arabidopsis*, PAM68HL (At5g52780), is part of this work.

3.2) Confirmation of Knock-Out Lines

3.2.1) Deletion of *PAM68* Results in Stunted Growth

The gene structure and the resulting protein structure of *PAM68* (*AT4G19100*) are illustrated in Figure 3.1A. The gene of 907 bp consists of two exons (57 and 588 bp) and one intron (262 bp). The protein has a predicted chloroplastid transit peptide (cTP; for detail see chapter 3.3) and two transmembrane domains (TMD; TMHMM Server v. 2.0). For *PAM68* two knockout alleles were used, *pam68-1* and *pam68-2*. Both of them carry the insertion in the second exon of the gene (*pam68-1* 848 bp, *pam68-2* 499 bp downstream of the ATG). The SALK line was found by searching T-DNA insertion flanking databases. To verify T-DNA insertions primer combinations specific for *PAM68* and the relative T-DNA border (LB, left border) were used (for detailed primer list see chapter 2.2.2.1). PCR-analysis of genomic DNA demonstrated that the gene is disrupted by the T-DNA

in both lines (Fig. 3.1B). The T-DNA insertion of *pam68-1* carries two left borders, one at each end of the T-DNA. For *pam68-2* only one left border exists downstream of the T-DNA. In the latter one no transcript was detectable in an RT-PCR experiment indicating that the T-DNA insertion has disrupted the expression of the *PAM68* gene (Fig. 3.1C). In *pam68-1*, a truncated version of

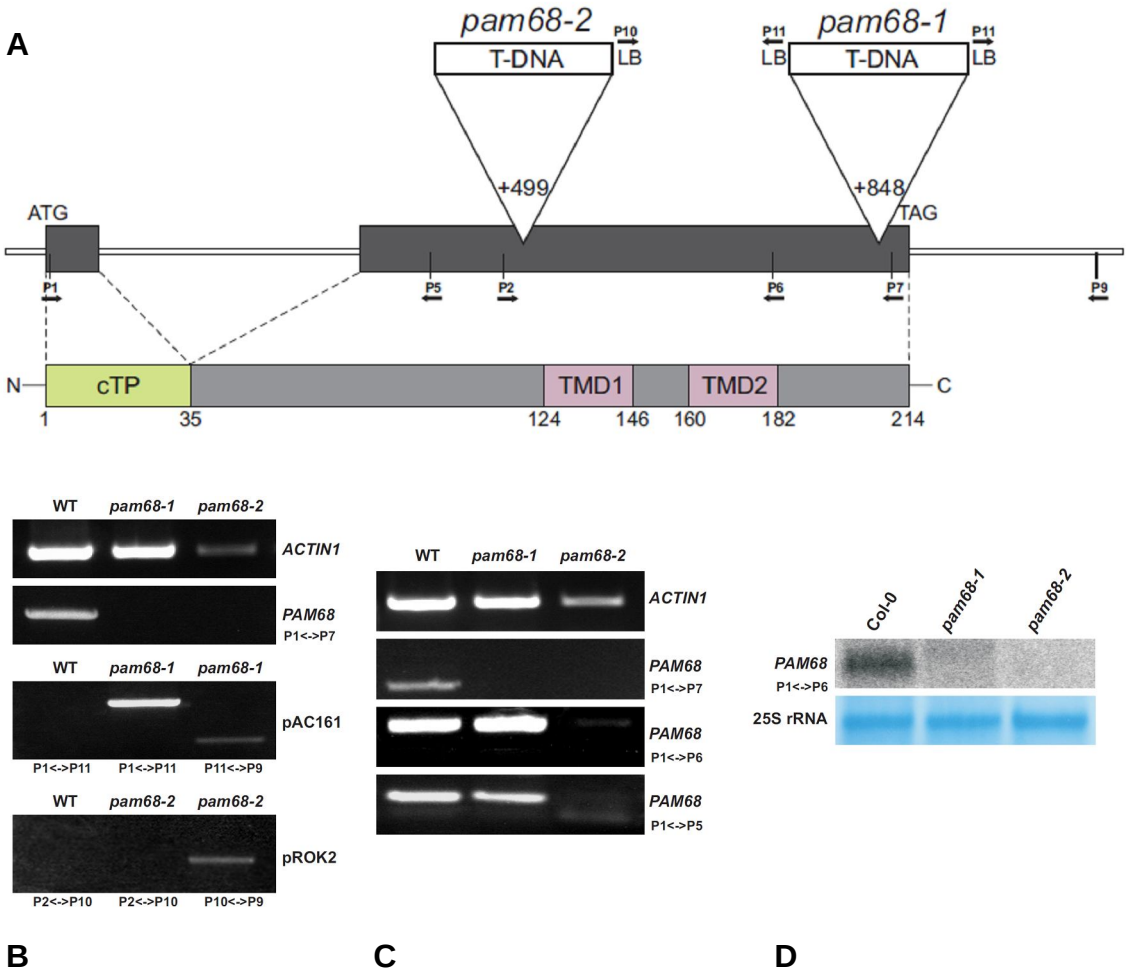

Fig. 3.1: Genetic characterisation of *PAM68* mutants.

A) Schematic diagram of *PAM68* gene and the corresponding protein. **Gene:** Exons (grey boxes) and introns (white line) are indicated. The positions of the T-DNA insertions corresponding to *pam68-1* and *pam68-2* are shown. ATG = start codon, TAG = stop codon, LB = left border of T-DNA. **Protein:** Chloroplast targeting sequence (cTP) and transmembrane domains (TMD) are indicated. N = N-terminus, C = C-terminus. **B)** Verification of T-DNA insertions. Positions of primers used are depicted in A). pAC161 = vector used for mutagenesis of *pam68-1* (GABI-KAT line); pROK2 = vector used for mutagenesis of *pam68-2* (SALK line). **C)** RT-PCR analysis of *PAM68* gene expression. **D)** Northern analysis of *Pam68* transcript.

PAM68 is expressed (part upstream of the T-DNA insertion). Nevertheless, for both lines no transcript was detectable in Northern analyses Fig. 3.1D). Both mutant alleles showed the same stunted growth phenotype with pale green

leaves (Fig. 3.2A). For comparison of the development, growth kinetics was carried out. The leaf area of wild-type and mutant plants was measured over a time period of 25 days starting with the day of germination (Fig. 3.2B). 4 weeks

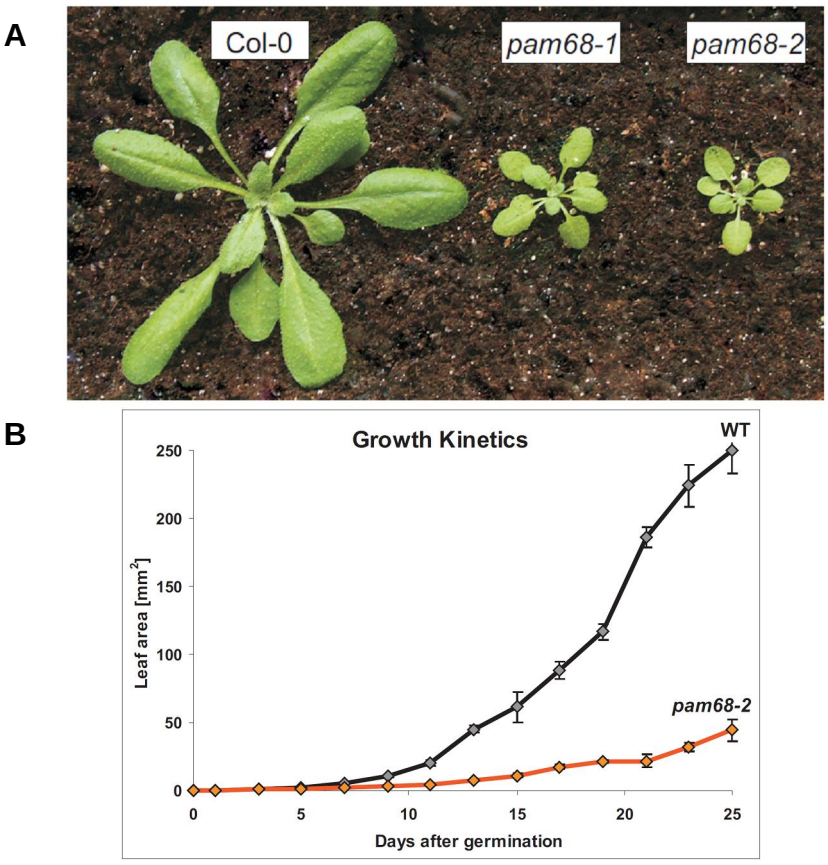

Fig. 3.2: Growing phenotypes of WT, *pam68-1* and *pam68-2*.

A) 4-week-old plants grown in the growth chamber under a 16 h/ 8 h dark/light regime and a PFD of 120 µmol photons $m^{-2}s^{-1}$ (GL). **B)** Growth kinetics of WT (Columbia-0, Col-0) and *pam68-2*. Values are averages ± SE of five replicate experiments.

after germination the size of the mutant plant leaves was about 20% of wild-type. Anyway, the mutants can germinate and perform the whole life cycle on soil, also in the greenhouse, and are able to produce fertile seeds.

To confirm the knock-out also on protein level, total proteins and thylakoid proteins of *pam68-2* mutant and WT plants were isolated and subjected to Western analysis using monospecific epitope antibodies raised against PAM68 (see chapter 3.2.5). The protein could be detected in thylakoid fractions from WT at the predicted size of ~20 kDa, but not in the mutant (see diploma thesis of Renate Kreller).

3.2.2) *pam68hl* Exhibits No Growth Phenotype

The homologue of PAM68 exhibits only one exon (507 bp). The gene structure and the resulting protein structure are shown in Figure 3.3A. The corresponding protein has also two TMDs (TMHMM Server v. 2.0) and a cTP. PCR analyses of genomic DNA from wild-type and mutant plants suggested a disruption of the *PAM68HL* gene by the T-DNA (Fig. 3.3B). Sequencing of the mutant allele showed that the T-DNA insertion led to the generation of a new stop codon resulting in a truncated gene of 469 bp instead of 507 bp. This truncated version was expressed at wild-type level as shown in Figure 3.3C. Immunoblot analyses of total proteins and thylakoid proteins of *pam68hl* mutant and WT plants using monospecific epitope antibodies raised against PAM68HL confirmed the full knock-out of PAM68 on protein level (see diploma thesis of Renate Kreller). In

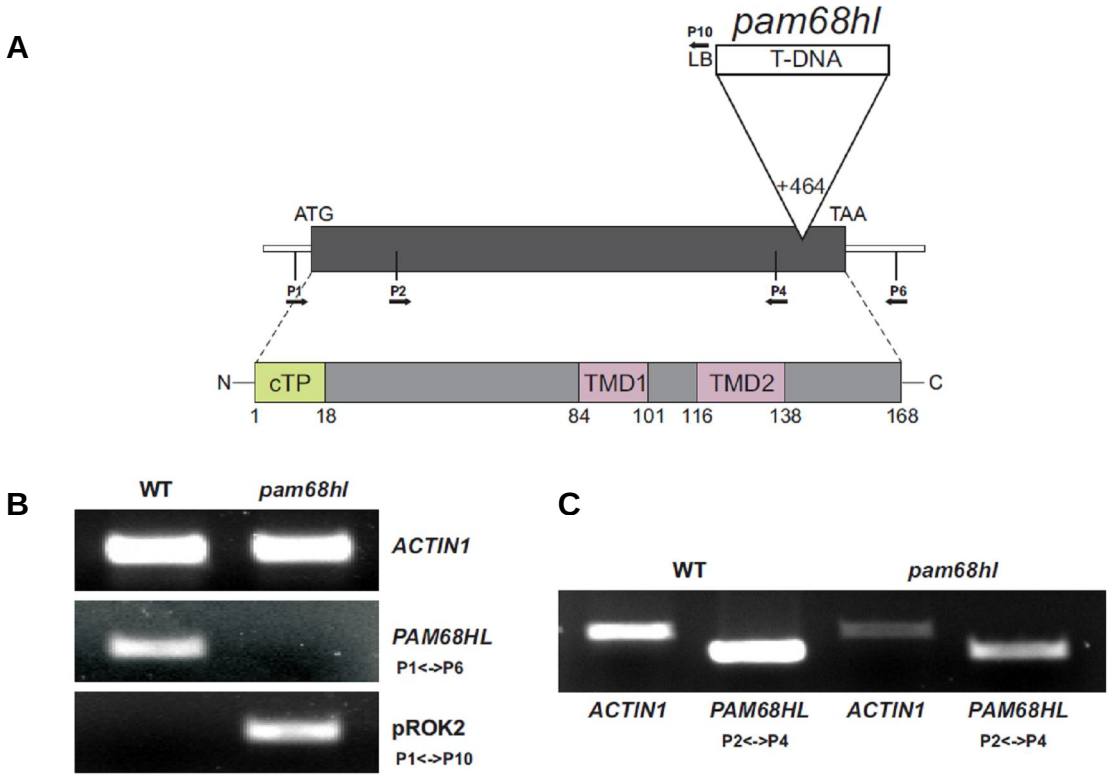

Fig. 3.3: Genetic characterisation of *PAM68HL* mutant.

A) Schematic diagram of *PAM68HL* gene and corresponding protein. **Gene:** Exon (grey box) is indicated. The position of the T-DNA insertion corresponding to *pam68hl* is shown. ATG = start codon, TAG = stop codon, LB = left border of T-DNA. **Protein:** Chloroplast targeting sequence (cTP) and transmembrane domains (TMD) are indicated. N = N-terminus, C = C-terminus. **B)** Verification of T-DNA insertion. Positions of primers used are shown in A). pROK2 = vector used for mutagenesis of *pam68hl* (SALK line). **C)** RT-PCR analysis of *PAM68HL* gene expression upstream of the T-DNA insertion.

wild-type preparations the protein showed the predicted size of ~17 kDa, and was also detectable in the thylakoid fraction, suggesting a thylakoid membrane localisation. The mutant plants displayed no phenotype compared to wild-type (see section 3.2.4).

3.2.3) Complementation of *pam68-2* Rescues the Growth Phenotype

To demonstrate that the phenotype of *pam68-2* was attributable to the mutation of the *PAM68* gene, we conducted complementation experiments with the *pam68-2* mutant as background, using the 645 bp full-length coding sequence driven by a single Cauliflower Mosaic Virus 35S promoter. Positive transformants were selected by hygromycin resistance (*35S::PAM68*; Fig. 3.4A) and successful complementation was confirmed by PCR, immunoblot-analyses (see Fig. 3.14D) and PAM-measurements (see Fig. 3.12). In the PCR-analysis of complemented plants with primers covering the whole *PAM68* gene two bands came up (Fig. 3.4B). The lower band reflected the introduced coding sequence without intron (645 bp), the upper one represented the gene including the intron (907 bp).

Fig. 3.4: Complementation of *pam68-2*.

A) 4-week-old plants growing under GL conditions in the climate chamber. The coding sequence of *PAM68* was ligated into the plant expression vector pH2GW7 (Invitrogen) under the control of a single Cauliflower Mosaic Virus 35S promoter (*35S::PAM68*) and the construct was used to transform flowers of *pam68-2* mutant plants by the floral dip method (Clough and Bent, 1998). **B)** PCR-analysis with genomic DNA of wild-type and complemented plants. Position of primers is depicted in Fig. 3.4A.

The transformed plants displayed wild-type-like growth, thus confirming that growth defects in *pam68-2* resulted from mutation of the *PAM68* gene. Immunoblot-analyses with the peptide-antibody against PAM68 demonstrated

that the *35S::PAM68* line is an overexpressor of PAM68 protein (see diploma thesis of Renate Kreller).

3.2.4) Double Mutation Does Not Result in an Additional Phenotype

The double mutant *pam68-2*/*pam68hl* was created crossing homozygous *pam68-2* and *pam68hl* plants with *pam68-2* as female plant. The F2 generation was then screened by PCR for homozygous double mutants. The double mutant exhibited exactly the same growing phenotype as *pam68-2* (Fig. 3.5).

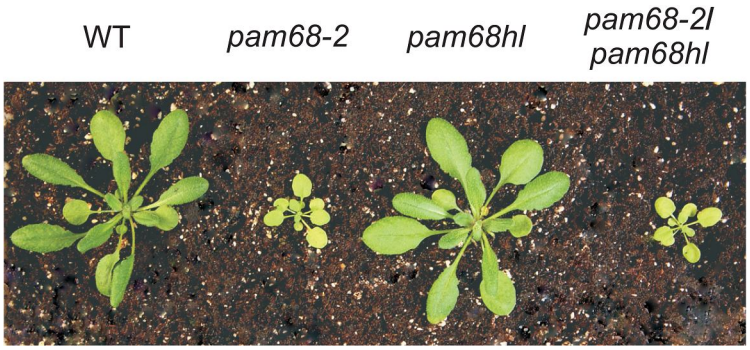

Fig. 3.5: Phenotypes of WT, *pam68-2*, *pam68hl*, and *pam68-2/pam68hl* plants.

4-week-old plants growing under GL conditions in the climate chamber. *pam68hl* was crossed in the background of *pam68-2*.

3.2.5) Production of Peptide Antibodies

As mentioned above, PAM68 and PAM68HL are predicted to have to transmembrane domains. Therefore peptide antibodies against epitopes of the proteins should be created for hydrophilic parts. For analysis of hydrophility the hydrophobicity plot of Marc N. Offman was employed (Fig. 3.6). The protein sequences were applied without predicted cTPs. For both proteins, the longest hydrophilic stretches were localised upstream of the first TMD. The amino acid sequences of the epitopes used for antibody production were DEDDDDEDEDD for PAM68 and RTSEKPGRPD for PAM68HL in one letter code. Both antibodies were used for the verification of the knock-out lines of *PAM68* and *PAM68HL* (see diploma thesis of Renate Kreller).

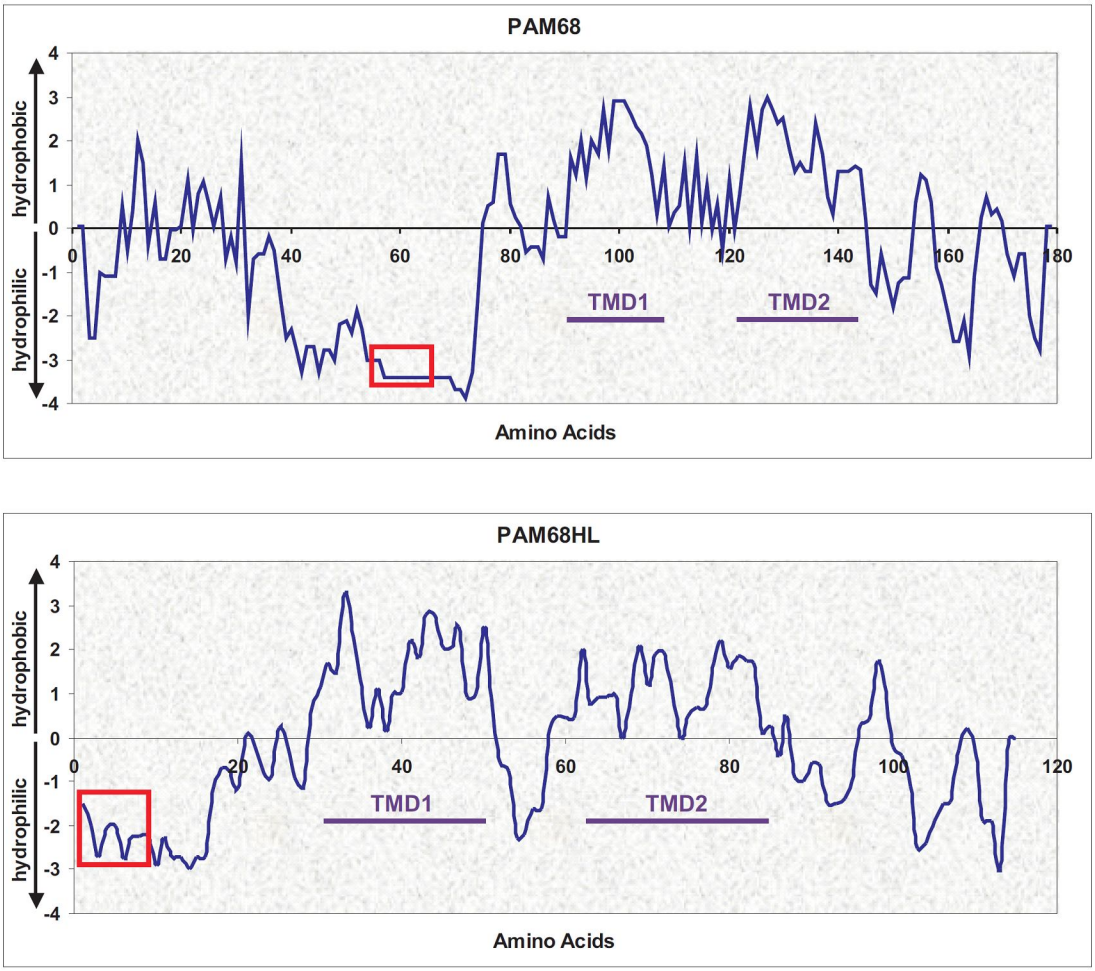

Fig. 3.6: Hydrophobicity plot 1.0 by Marc Offman

The chosen hydrophilic stretch for the peptide synthesis is marked in red rectangles; TMD = transmembrane domain. http://www.bmm.icnet.uk/~offman01/.

3.3) *PAM68* Encodes a Thylakoid Membrane Protein of Cyanobacterial Origin

Even though database searches failed to detect any sequence motives or domains that could shed some light on the function of PAM68, a blast of PAM68 protein against the translated nucleotide database of NCBI (tblastn; Chapter 2.2.6) showed a strong conservation in the proteome of all photosynthetic organisms (Fig. 3.7), especially in the C-terminus. For detailed analysis of the identity and similarity between PAM68 and its orthologues, protein sequences were aligned using Blast2sequences (NCBI; Chapter 2.2.6). Thereby, the sequences of *Arabidopsis, Ricinus, Populus, Vitis* and *Maize* were aligned without predicted cTP. The highest homology to PAM68 was found in *Ricinus*,

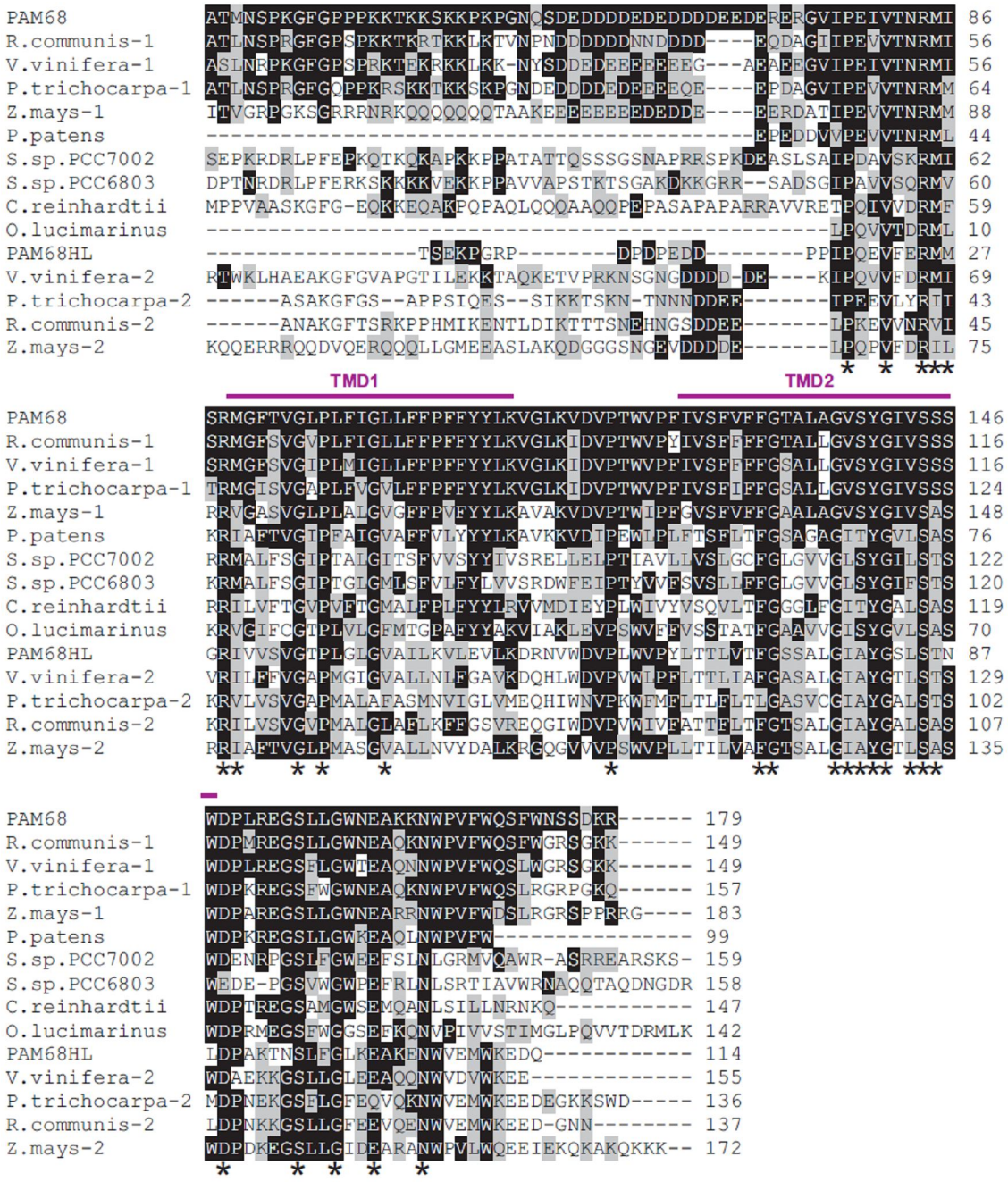

Fig. 3.7: Protein sequence alignment of PAM68.

The protein sequence of PAM68 was compared with related sequences from *Arabidopsis thaliana* (At5g52780), *Ricinus communis* (R.communis-1: GI:255557684, R.communis-2: GI:255545165), *Vitis vinifera* (V.vinifera-1: GI:225466098, V.vinifera-2: GI:225464603), *Populus trichocarpa* (P.trichocarpa-1: GI:224138363, P.trichocarpa-2: GI:224079761), *Zea mays* (Z.mays-1: GI:226491093, Z.mays-2: GI:226491403), *Physcomitrella patens* subsp. patens (GI:168061716), *Chlamydomonas reinhardtii* (GI:159464826), *Ostreococcus lucimarinus* (GI:144576265), *Synechocystis* sp. PCC 6803 (sll0933), *Synechococcus* sp. PCC 7002 (SYNPCC7002_A1824). These sequences were aligned using ClustalW and BoxShade. The sequences for flowering plants were analysed without predicted cTPs (*Arabidopsis, Ricinus, Vitis, Populus,* maize). Conserved amino acids are highlighted by black boxes, whereas grey ones indicate closely related amino acids. The two predicted transmembrane domains of PAM68 are marked by purple bars; conserved amino acids are marked by

wine and poplar. The homologue in *Arabidopsis* (PAM68HL) exhibited 38% identity and 58% similarity to PAM68. In all analysed flowering plants, two homologues could be found (in *Populus trichocarpa*, *Vitis vinifera*, *Zea mays*, and *Ricinus communis*). One of them showed always much more homology to either PAM68 (Ricinus-1: 75%/90%, Vitis-1: 71%/83%, Populus-1: 70%/86%, Maize-1: 71%/80 identity/similarity) or PAM68HL (Ricinus-2: 52%/75, Vitis-2: 58%/83%, Populus-2: 41%/68%, Maize-2: 49%/66% identity/similarity). This suggests a duplication event during evolution probably after endosymbiosis. The

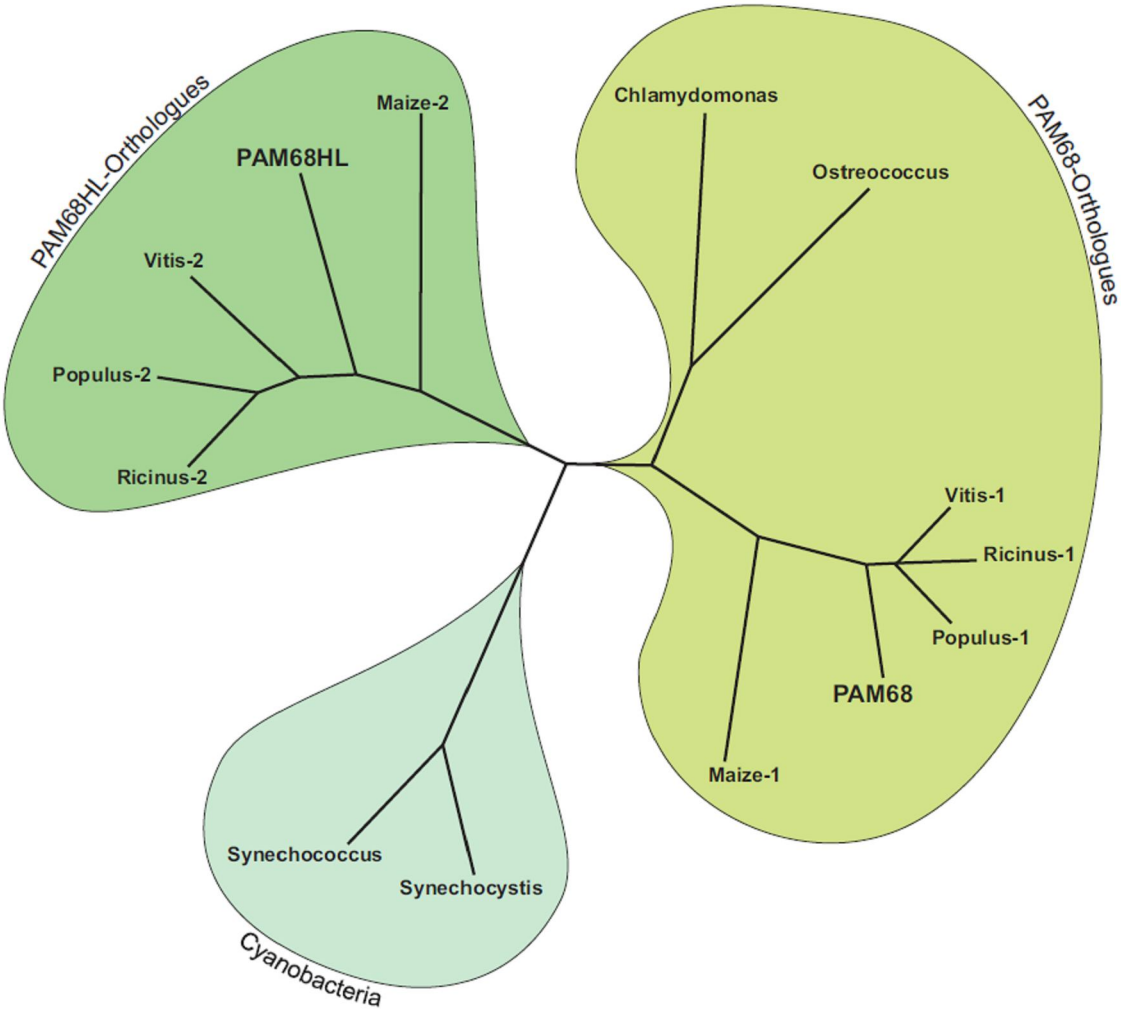

Fig. 3.8: Unrooted phylogram of PAM68 and its orthologues.

The phylogram was built out of the sequences of PAM68 and its orthologues using the programs PHYLIP version 3.67 and PhyloDraw version 0.8 (see section 2.2.6). The presumable duplication event is marked by a blue circle.

orthologue in *Physcomitrella* showed more similarity to PAM68 than to PAM68HL (77% and 59%, respectively). An unrooted phylogram, created from all sequences (flowering plants without cTP), except *Physcomitrella*, is shown in

Figure 3.8. The orthologues of the green algae *Chlamydomonas reinhardtii* and *Ostreococcus lucimarinus* are also more closely related to PAM68 (41% and 48% identity, respectively) than to PAM68HL (36% and 37% identity, respectively), assuming a duplication event during evolution.

Bioinformatic analyses predicted a chloroplast targeting peptide (cTP) of 35 amino acids for PAM68 resulting in a mature protein with a calculated molecular

	ChloroP	iPSORT	PCLR	Predotar	TargetP	MitoProt	WoLF PSORT	PSORT	BaCelLo
PAM68	cTP	mTP or cTP	cTP	cTP	cTP	mTP	cTP	cTP	cTP
PAM68HL	cTP	mTP or cTP	cTP	mTP	mTP	mTP	cTP	PM or cTP	cTP

Table 3.1: Prediction of chloroplast targeting peptides.

A combination of programs predicting N-terminal chloroplast or mitochondrial transit peptides (see chapter 2.2.6) was used to predict targeting of PAM68 and PAM68HL.

weight of ~20 kDa (Table 3.1). For PAM68HL some algorithms predicted a cTP with a length of 54 amino acids leading to a mature protein of ~17 kDa. The localisation for PAM68 was determined by two *in vitro* import experiments. First, the whole coding sequence of *PAM68* was fused to the red-fluorescent protein (RFP; Jach *et al.*, 2001) and transfected into *Arabidopsis* protoplasts. Comparison of the position of signals from the RFP fusion and from chlorophyll autofluorescence confirmed the chloroplast localisation of PAM68 (Fig. 3.9A). Second, radiolabelled PAM68 protein could be imported into pea chloroplasts (Fig. 3.9B). The translation product of PAM68 (TL), which represented the precursor of PAM68, appeared at the predicted size of about 24 kDa. After import into the chloroplast, the cTP was cleaved off and the mature protein ran at a height of ~20 kDa. Treatment with thermolysin led to the degradation of the precursor but not of the mature protein. As thermolysin is only able to destroy polypeptides that reside outside or on the surface of the chloroplast, this analysis demonstrates that PAM68 is effectively transported into the chloroplast. The appearance of two bands after import may be due to posttranslational modifications of the protein once it has been imported into the chloroplast.

Further bioinformatics analyses of PAM68 and PAM68HL indicated two transmembrane domains in the C-terminal part of both proteins (depicted in Fig. 3.1 and 3.3; TMHMM Server v. 2.0). Recent proteomics approaches gave also a hint for the localisation of PAM68 and PAM68HL as both were found in thylakoid

membrane preparations (Zybailov *et al.*, 2008; PAM68HL also Peltier *et al.*, 2004).

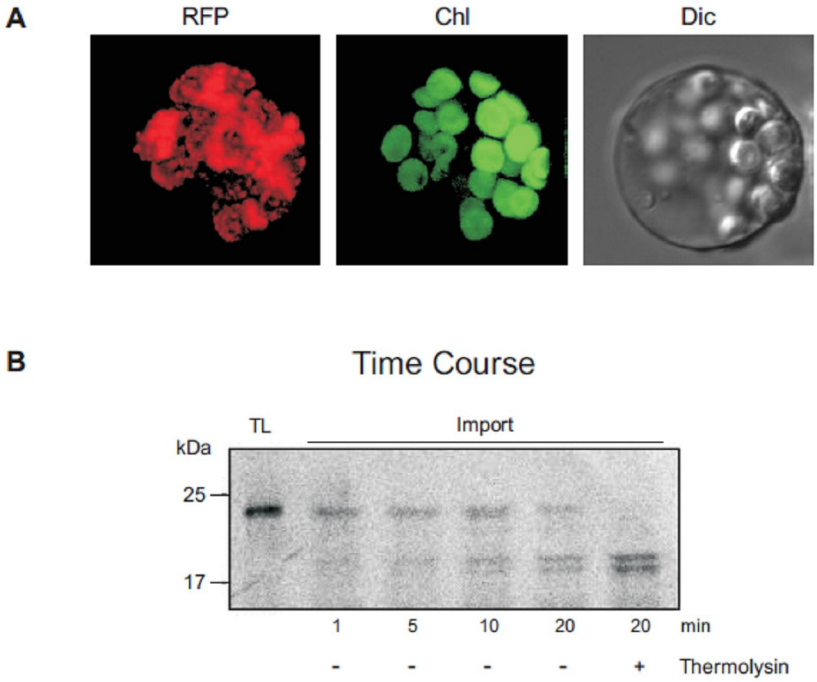

Fig. 3.9: Localisation of PAM68.

A) Fluorescence micrographs of *A. thaliana* protoplasts transfected with a C-terminal fusion of dsRED to the complete PAM68 protein. The pictures are presented in false colour with RFP fluorescence (RFP) shown in red and chlorophyll autofluorescence (Chl) in green; Dic = differential interference contrast microscopy. **B)** Import of PAM68 in pea chloroplasts. After import chloroplasts were treated with thermolysin for 20 min. TL = translation product.

3.4) Expression Analyses of *PAM68* and *PAM68HL*

3.4.1) Expression Profile of *PAM68* is Comparable to *psbA*

Expression analyses of *PAM68* and *PAM68HL* with Genevestigator (www.genevestigator.com; Zimmermann *et al.*, 2004) showed that the genes are expressed in every green tissue at every developmental stage of the plant (data not shown). The Gene Chronologer tool of Genevestigator was used to compare the transcription of both genes at different growth stages with the expression pattern of photosynthetic genes like *psbA* or *psbD* (Fig.3.10). The *PAM68* expression profile shows nearly the same cycle during development as the *psbA* gene with the highest expression after 28 days of germination, suggesting a possible co-regulation with photosynthetic components. The transcription rate of PAM68HL on the other side is kept quite constant during development.

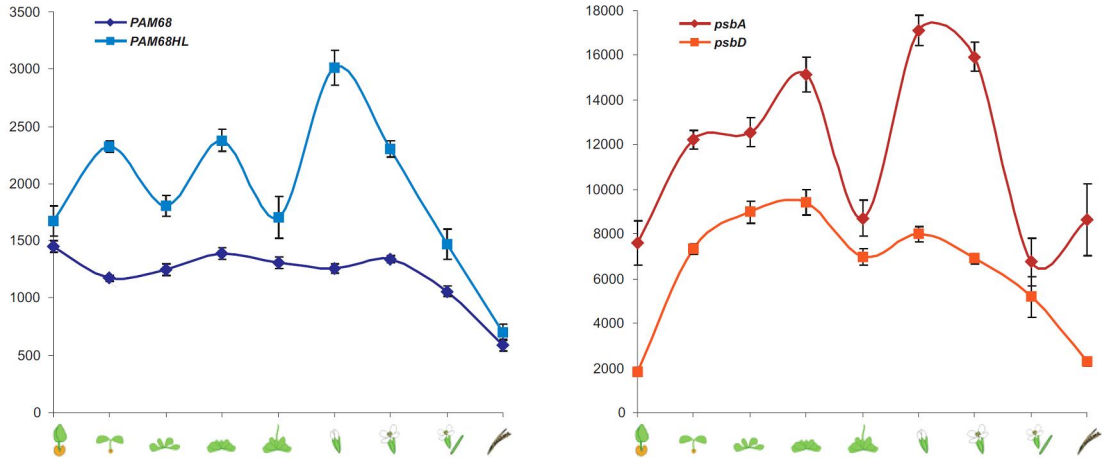

Abb. 3.10: Gene expression during development of the plant.

Expression analysis of *PAM68, PAM68HL, psbA,* and *psbD* with the Gene Chronologer tool of Genevestigator (www.genevestigator.com) during the development of *Arabidopsis* plants. The age of the plants at the different time points is 5, 13, 17, 20, 24, 28, 35, 44, and 50 days, respectively.

3.4.2) *PAM68* and *PAM68HL* are Co-Expressed With Photosynthetic Genes

Genes involved in related biological pathways are often expressed cooperatively, and thus information on their co-expression is useful for the understanding of biological systems. The freely available program ATTED-II provides co-regulated gene relationships in *Arabidopsis thaliana* for functional identification or for studies of regulatory relationships (http://atted.jp; Obayashi *et al.*, 2009). This tool was used to get further insight into the function of PAM68 and PAM68HL. Interestingly, both are co-expressed with genes known to be involved in PSII biogenesis (Fig. 3.11): the Deg-proteases cleave the D1 protein after damage, LPA1, LPA2 and CYP38 are important for the assembly of PSII, and the STN8 kinase phosphorylates PSII core proteins. Both showed also co-expression with proteins localised in the thylakoid lumen and with proteins that are either part of the NAD(P)H dehydrogenase (NDH) complex (CRR7; Kamruzzaman *et al.*, 2006) or are important for its activity (CRR1; Shimizu and Shikanai, 2007), expression (SIG4; Favory *et al.*, 2005) or assembly (CRR6; Munshi *et al.*, 2006). Altogether, the results of this co-expression analysis support the idea of an involvement of PAM68 and PAM68HL in photosynthetic processes.

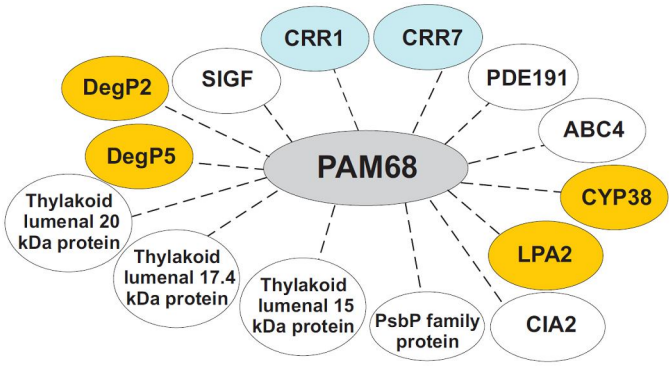

COR	name
0.81	SIGF (RNA polymerase sigma-70 factor)
0.81	PDE191 (piment defective 191)
0.79	ABC4 (aberrant chloroplast development 4)
0.78	LPA2 (low PSII accumulation 2)
0.78	Thylakoid lumenal 15 kDa protein
0.77	Thylakoid lumenal 17.4 kDa protein
0.77	DegP5 (DEG5/DEGP5/HHOA (DEGP protease 5))
0.77	CRR1 (chlororespiratory reduction 1)
0.76	CRR7 (chlororespiratory reduction 7)
0.75	CYP38 (cyclophilin 38)
0.75	Thylakoid lumenal 20 kDa protein
0.73	DegP2 (DegP protease 2)
0.71	PS II reaction center PsbP family protein
0.67	CIA2 (chloroplast import apparatus 2)

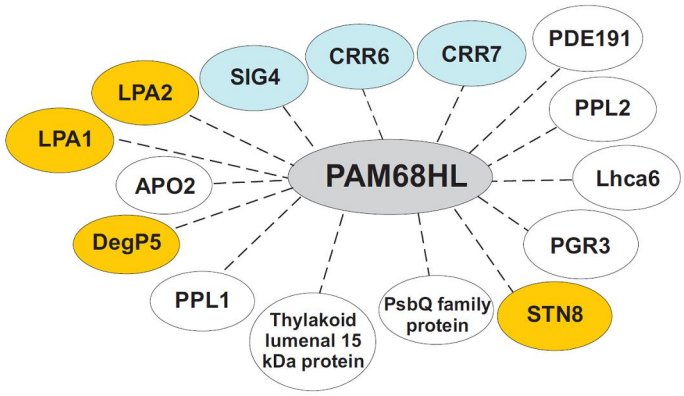

COR	name
0.81	SIG4 (Sigma factor 4)
0.81	CRR6 (chlororespiratory reduction 6)
0.80	APO2 (accumulation of photosystem one 2)
0.79	CRR7 (chlororespiratory reduction 7)
0.78	PGR3 (proton gradient regulation 3)
0.76	Oxygen evolving enhancer 3 (PsbQ) family protein
0.76	PPL2 (PSBP-like protein 2)
0.75	LHCA6 (PS I light harvesting complex gene 6)
0.72	LPA2 (low PSII accumulation 2)
0.71	PPL1 (PSBP-like protein 1)
0.70	DegP5 (DEG5/DEGP5/HHOA (DEGP protease 5)
0.70	STN8 (state transition 8)
0.70	Thylakoid lumenal 15 kDa protein
0.68	PDE191 (piment defective 191)
0.66	LPA1 (low PSII accumulation 1)

Fig. 3.11: Co-expression analysis of *PAM68* and *PAM68HL*.

Analysis was carried out with the ATTED-II database (version 5.2). Data source: publicly available microarray data (58 experiments, 1388 slides) collected by AtGenExpress; coexpression measure: mutual rank based on weighted Pearson´s correlation coefficients. Marked in yellow are PSII biogenesis factors, marked in blue are proteins that are concerned with the NDH-complex.

3.5) Photosynthetic Parameters and Leaf Pigments of *pam68-2*

3.5.1) Spectroscopic Analyses Indicate a Defect in PSII

Chlorophyll fluorescence induction experiments were carried out *in vivo* on single leaves of 4-week-old plants using the pulse amplitude modulated fluorometer Dual-PAM 100 (measurements were done as already described for the Pulse Amplitude Modulation 101/103 by Varotto *et al.* (2000)). The chlorophyll fluorescence in the *pam68* mutants transiently was below the original F_0 levels when illuminated by actinic light (Fig. 3.12A). This suggests either that a non-photochemical quenching process would transiently develop before being dissipated within 3 to 4 min, or that the electrons leave the plastoquinone pool faster as they enter it. This could be due to problems on the donor side of the

electron transfer chain (PSII) concomitantly with no alterations on the acceptor side (PSI). For the determination of the maximum fluorescence in the dark (F_M) and after illumination (F_M'), saturating pulses of white light (5000 µmol m^{-2} s^{-1}, 800 ms) were applied. After 10 min of illumination with actinic light (53 µmol m^{-2} s^{-1}) the effective quantum yield (Yield) and the photochemical quenching parameter 1-qP could be defined.

The maximum quantum yield of PSII ($(F_M - F_0)/F_M = F_V/F_M$) can be calculated from the maximal fluorescence in the dark with all PSII reaction centres (RC) closed (F_M) and the minimal level of fluorescence of dark-adapted plants with all PSII RCs open (F_0). This parameter was remarkable decreased in both *pam68*-mutant alleles (0.33 in the mutants vs. 0.82 in the wild-type; Fig. 3.12A and B). Also the effective quantum yield of PSII (Yield; $F_{M'}$-F_S/ $F_{M'}$) showed a strong reduction in the mutants (0.13 and 0.12 vs 0.61). The parameter 1-qP, which reflects the redox state of the Q_A electron acceptor of PSII, was higher in both mutant alleles (0.55 and 0.56 for the mutants, 0.21 for WT). This result indicates a more reduced plastoquinone pool in the mutant, a response likely due to a deficiency of photosynthetic electron transport. The electron transfer rate (ETR; calculated from the yield) confirmed this assumption, as it was strongly reduced in the mutants. The coefficient for non-photochemical quenching NPQ, a reflection of the plant's ability to dissipate excess light energy as heat, was found to be similar in mutant and wild-type plants. Taken together, the chlorophyll fluorescence analyses suggest that the deletion of PAM68 affects PSII function. The homologue of PAM68 however, which has no growth phenotype, behaved as wild-type in all measurements.

To further investigate the effect of the *pam68* mutant background on photosynthetic parameters, we additionally measured complemented plants of *pam68-2* (*35S::PAM68*) and double mutants generated by crossing of *pam68-2* and *pam68hl* (*pam68-2*/*pam68hl*). As shown in Figure 3.12 the overexpressor of PAM68 behaved like wild-type, whereas the double mutants showed exactly the same phenotype as the single mutants *pam68-1* and *pam68-2*. These results together with the growth phenotype led us analysing the *pam68-2* mutant in more detail concerning the apparent PSII-phenotype.

A

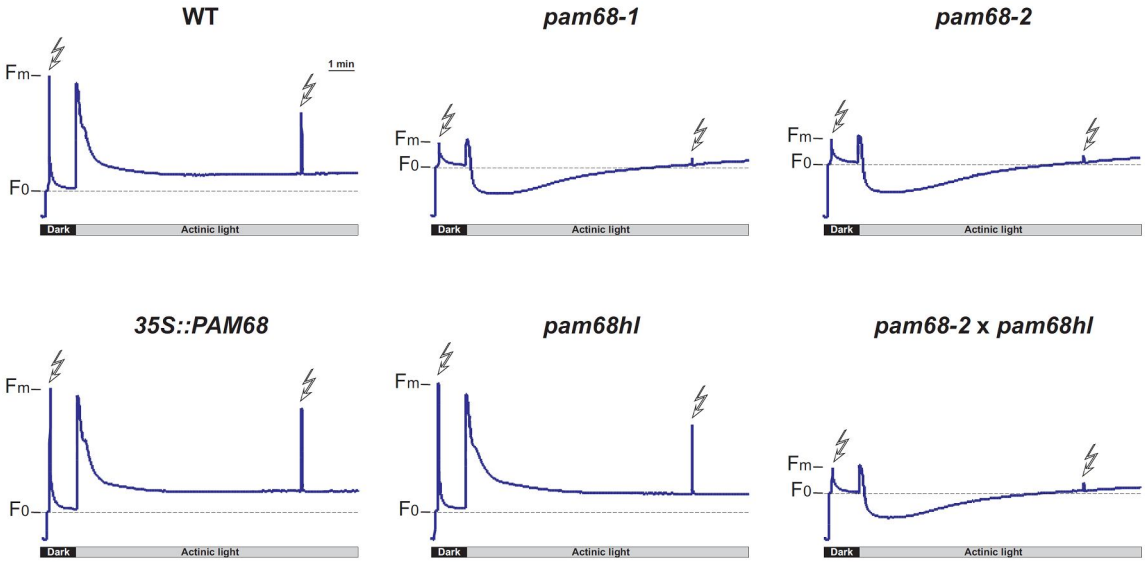

B

	F_V/F_M	Yield	ETR	NPQ	1-qP
WT	0.82 ± 0.00	0.61 ± 0.03	13.93 ± 0.62	0.28 ± 0.08	0.21 ± 0.02
pam68-1	0.33 ± 0.02	0.13 ± 0.01	2.88 ± 0.28	0.26 ± 0.08	0.55 ± 0.03
pam68-2	0.33 ± 0.02	0.12 ± 0.01	2.80 ± 0.22	0.27 ± 0.10	0.56 ± 0.03
pam68hl	0.82 ± 0.01	0.62 ± 0.02	13.93 ± 0.47	0.36 ± 0.10	0.21 ± 0.01
pam68-2 x pam68hl	0.37 ± 0.01	0.15 ± 0.01	3.38 ± 0.22	0.26 ± 0.07	0.52 ± 0.03
35S::PAM68	0.83 ± 0.01	0.64 ± 0.02	14.53 ± 0.48	0.17 ± 0.03	0.20 ± 0.02

Fig. 3.12: Fluorescence measurements with the Dual-PAM.

A) Chlorophyll fluorescence induction kinetics of WT, *pam68-1*, *pam68-2, pam68hlpam68-2/pam68hl* and *pam68-2* transformants complemented with the coding sequence of *PAM68* (35S::PAM68). Measurements were applied to 4-week-old plants using the Dual-PAM 100 after 20 min of dark-adaptation. Saturating pulses were indicated by flashes. **B)** Photosynthetic parameters F_V/F_M = (F_M - F_0) / F_M: maximum quantum efficiency of PSII photochemistry; Yield = ($F_{M'}$ – F_S) / $F_{M'}$ effective quantum yield of PSII; ETR = Yield * PPFD: electron transport rate; qP = (F_M – $F_{M'}$) / (F_M – $F_{0'}$); 1-qP = coefficient of photochemical quenching; NPQ = (F_M - $F_{M'}$) / $F_{M'}$: non-photochemical quenching. PPFD: photosynthetic photon flux density.

3.5.2) Pigment Measurements Suggest Reduction of Reaction Centres

Because of the pale green leaves of the *pam68-2* mutant plants, a quantitative analysis of leaf pigments was carried out by HPLC (see chapter 2.2.5). As expected, the mutant contained only 65% of wild-type chlorophyll (Chl *a*+*b*) level (Fig. 3.13). This reduction was not the same for both chlorophylls, as the ratio of Chl *a*/*b* was altered for the benefit of Chl *b*. This indicates a reduction in the Chl *a* binding reaction centres.

Pigment/Protein	WT	*pam68-2*	Relative Level in *pam68-2* (%)[a]
Chlorophyll a/b	3.1 ± 0.0	2.7 ± 0.0	87
Chlorophyll a+b	2060 ± 182	1339 ± 123	65
Neoxanthin	76 ± 8	59 ± 5	78
Violaxanthin	53 ± 5	56 ± 5	105
Antheraxanthin	3 ± 1	10 ± 3	370
Lutein	289 ± 39	198 ± 17	69
ß-Carotene	177 ± 15	87 ± 6	49

Fig. 3.13: Leaf pigment level of light-adapted WT and mutant plants.

Leaf pigments extracted from *pam68-2* and wild-type plants were determined by HPLC and reported in nmol/g leaf fresh weight. Mean values ± SD are shown. [a] Relative values for the mutant genotype are percentages based on leaf fresh weight.

In addition to the chlorophylls, various carotenoids are distributed among the photosynthetic complexes. They are involved in light harvesting, maintaining of the structure, and functionality of the photosynthetic complexes, as they quench Chl triplet states, scavenge ROS, and dissipate excess energy (Demmig-Adams *et al.*, 1996; Niyogi *et al.,* 1998). Lutein and ß-carotene are carotenoids that can be found in the inner and outer antenna, the LHC-complexes and in the reaction centres of the two photosystems. Both were below wild-type level, with the stronger reduction in ß-carotene (69% and 49%, respectively). This result, together with the reduction in the Chl *a* level, is in line with the observation of defects in PSII, as the proteins D1, D2, CP47 and CP43 bind the photosynthetic pigments Chl *a* and ß-carotene.

The increased contents of the carotenoid pigments violaxanthin and antheraxanthin, which are involved in the photoprotecting xanthophyll cycle (Niyogi, 1999), lead to the assumption that mutant plants suffer from light stress.

This is due to the conversion of violaxanthin to zeaxanthin via the intermediate antheraxanthin during light stress conditions (Jahns *et al.*, 2009).

3.6) RNA and Protein Composition in *pam68-2*

3.6.1) PSII Proteins are Diminished

To investigate structural changes of thylakoid proteins from WT and mutant (*pam68-2*; this allele will be used in all following experiments), photosynthetic complexes were solubilised using dodecyl-ß-D-maltopyranoside (ß-DM) and separated by blue native (BN) PAGE. First-dimensional separation led to six major bands (Fig. 3.14A), representing PSII-supercomplexes (band I), dimeric PSII (II), monomeric PSII (III), monomeric PSII minus CP43 (IV), trimeric LHCII (V) and monomeric LHCII (VI). Here, first differences became apparent, as there was a reduction of all visible complexes except LHCII in the mutant. The supercomplexes of PSII were even not detectable. A second-dimensional SDS-PAGE gel following the BN gel revealed more details in individual protein components of the PSII-complexes of WT and mutant. In general, all complexes of PSII were reduced. An overlay of Coomassie-stained second dimensions of WT (shown in blue) and mutant thylakoid proteins (shown in red) showed that LHCII and ATP-synthase (ATPase) were not altered in *pam68-2* (Fig. 3.14B). By contrast, the PSII dimer fraction was strongly reduced in the mutant (D1/D2, CP47, and CP43). To investigate the steady-state levels of PSII subunits affected by the mutation, total proteins of wild-type and *pam68-2* plants of equal protein-concentrations were isolated and analysed by immunoblotting using a collection of antisera raised against individual PSII polypeptides and representative proteins of other photosynthetic membrane complexes. Our results showed that the PSII polypeptides were strongly reduced, whereas other complexes were only slightly affected or remained present in WT amounts. In more detail, levels of the plastid-encoded PSII core subunits D1, D2, CP47 and CP43 were reduced to ~12, 15, 24, and 14% of wild-type levels, respectively (Fig. 3.14C). The nuclear-encoded PsbO protein, which is a subunit of the OEC, and the LHCII complex were slightly decreased (~90% and 87%, respectively). Subunits of the PSI and Cyt b_6f complex accumulated at similar levels of around 80% (PSI-F

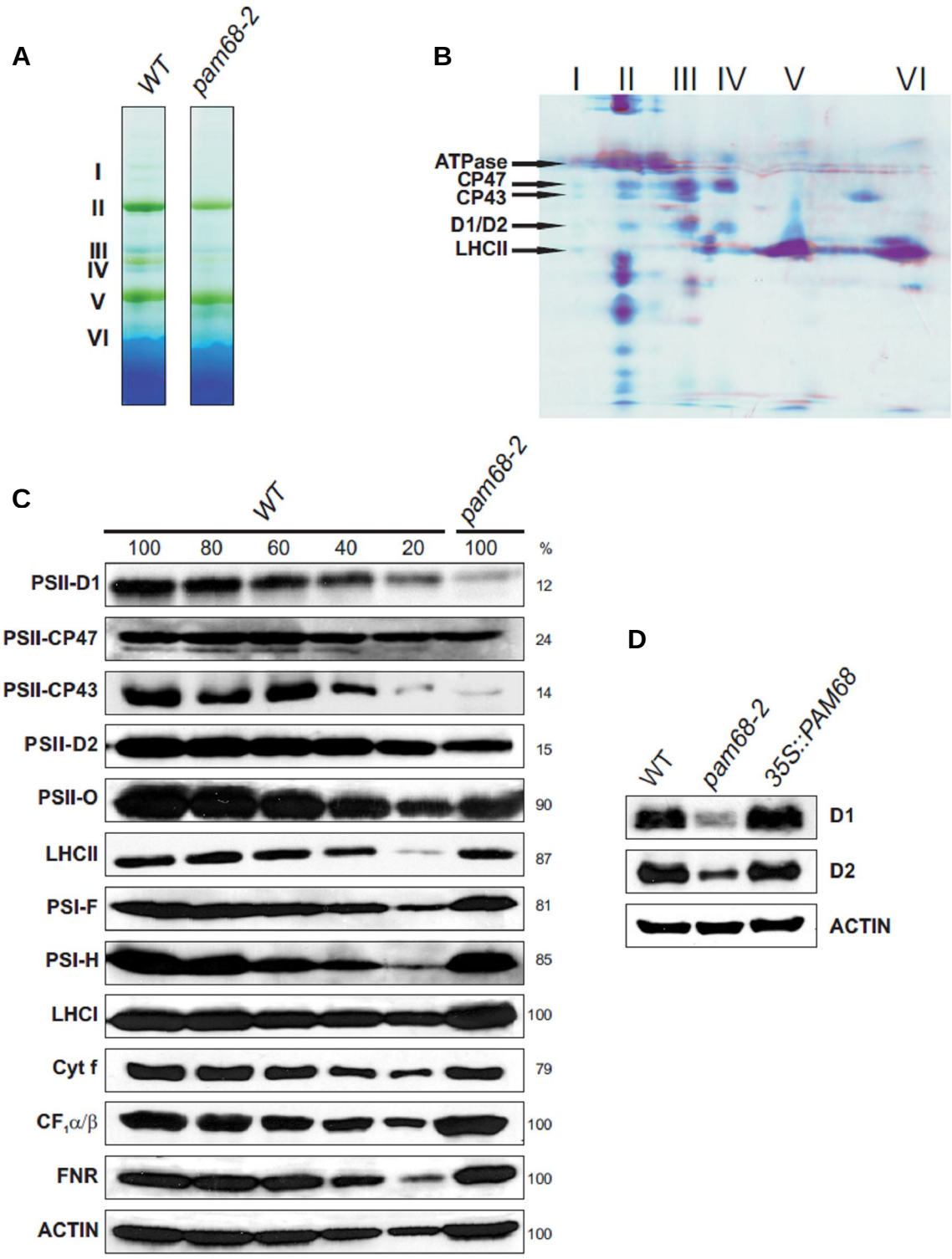

Fig. 3.14: Protein composition of thylakoid membranes.

Total protein obtained from identical amounts (fresh weight) of light-adapted wild-type (Col-0) and *pam68-2* leaves were separated by BN-PAGE (A) followed by a 2D SDS-PAGE (B) or directly by SDS-PAGE (C). **A)** BN gel analysis. I = PSII-supercomplex, II = PSII-dimer/PSI-monomer, III = PSII-monomer (with CP43), IV = PSII-monomer (without CP43), V = LHCII-trimer, VI = LHCII-monomer. **B)** Overlay of second dimension stained with Coomassie G250 of wildtype (blue) and mutant (red). **C)** Decreasing levels of wild-type proteins were loaded as indicated (100 = 100% etc.). The numbers on the right side of the panels shows the relative amount of protein in the mutant compared with the wild-type and normalised against ACTIN. **D)** Immunoblot-analyses of thylakoid proteins from WT, mutant and complemented plants with antibodies against the PSII-core proteins D1 and D2; ACTIN served as loading control.

81%, PSI-H 85%, Cyt *f* 79%). For LHCI, ATP-synthase (CF_1-α/β) and FNR (ferredoxin-$NADP^+$-oxidoreductase) no alterations on protein-level could be detected. The complementation of *pam68-2* was able to rescue the PSII-phenotype on protein level (Fig. 3.14D). The transgenic plants accumulated wild-type levels of the PSII core proteins D1 and D2.

To confirm and quantify differences in the composition of PSII complexes, immunoblot analyses were applied to examine the specific components (Fig. 3.15). The distribution of the PSII core proteins D1 and CP43 showed lack of PSII supercomplexes. However, both proteins accumulated in the PSII monomer fraction and in the dimer fraction. Hence, PSII monomers and dimers seem to be assembled in the mutant but in less extent. The distribution of PSI (PSI-L), ATP-synthase (CF_1-α/ß) and LHCII (Lhcb2) appeared as in wild-type. These results provide additional evidence that the mutant has a defect in PSII.

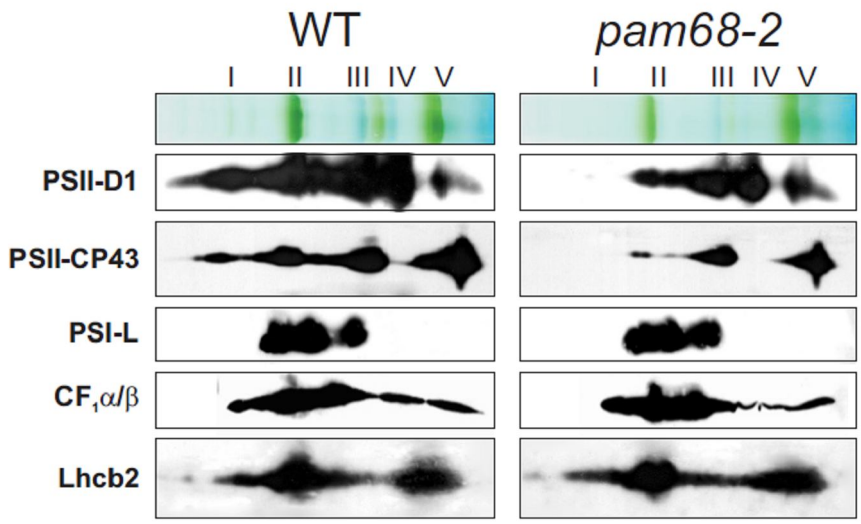

Fig. 3.15: Immunodetection of thylakoid proteins separated by 2D gel electrophoresis.
Second dimensions from Fig. 3.14 were subjected to immunoblot analysis. Bands I to V are corresponding to Fig. 3.7A.

3.6.2) Transcription of Plastid-Encoded Genes is Not Altered

The levels and patterns of the plastome-encoded PSII transcripts were investigated by RNA gel blot hybridisation (*psbA*, *psbB*, and *psbD*). Representative nuclear-encoded genes for components of other thylakoid membrane complexes were included in this analysis (*LHCB3* for LHCII, *ATPD* for ATP-synthase, *rbcL* = large subunit of Rubisco). The experiments revealed that

both, the amount and the sizes of all analysed transcripts, were not significantly altered in the mutant (Fig. 3.16A). Only *psbB* transcripts seemed to accumulate in higher amounts compared to wild-type. The reduced accumulation of PSII subunits is therefore not caused by an impaired or decreased transcription rate or by missing processing of a transcript encoding one of these structural PSII proteins, but must be due to a translational or posttranslational defect. Also the association of *psbA* mRNA with polysomes showed the same pattern in mutant and WT (Fig. 3.16B).

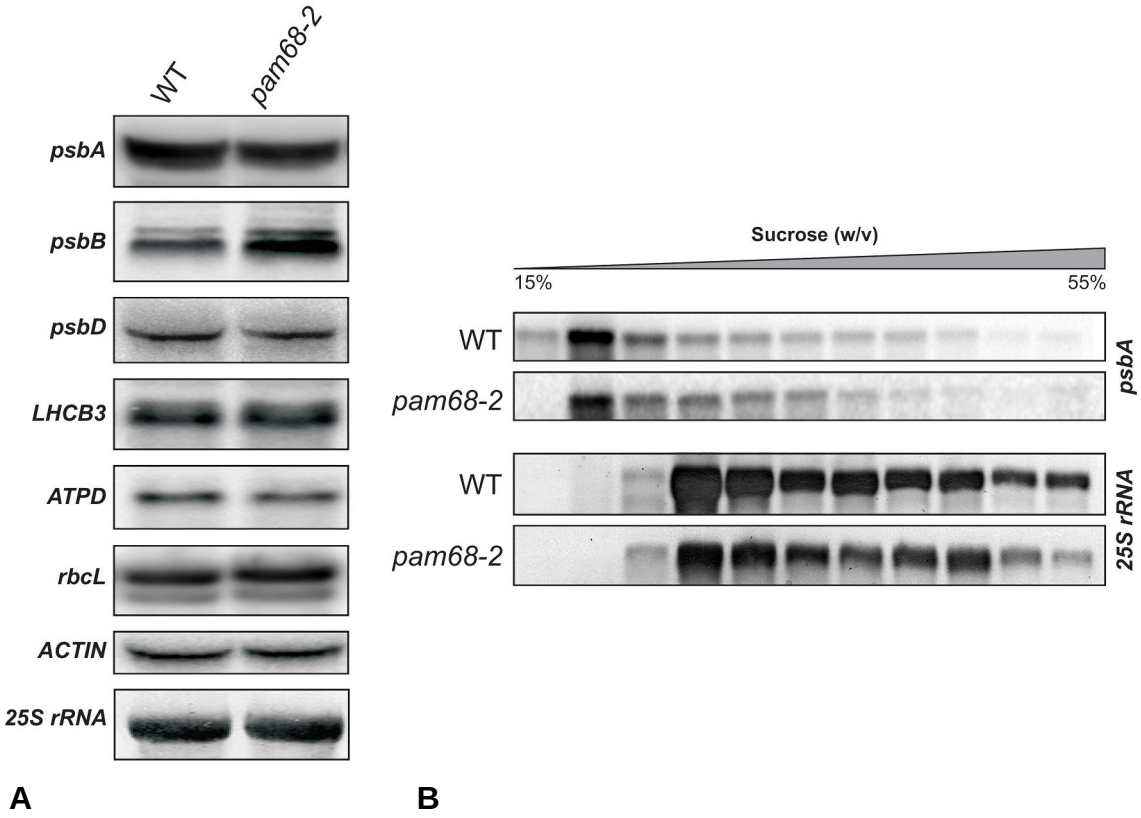

Fig. 3.16: Steady state mRNA levels and association with polysomes.

A) RNA gel blot hybridisation with total RNA from leaves of 4-week-old wild-type and *pam68-2* plants. 25S rRNA was detected by ethidium bromide (EtBr) staining. **B)** Association of the *psbA* transcript with polysomes in the *pam68-2* mutant. Whole-cell extracts were fractionated in linear 15 to 55% sucrose gradients by ultracentrifugation. Gradients were divided into 11 fractions, and equal proportions of each fraction were analysed. Upper panels: RNA gel blots of polysome gradient fractions were hybridised with a probe that detects *psbA*. Lower panels: Staining of the RNA gel blots with methylene blue to visualise distribution of 25S rRNAs.

3.7) Synthesis and Stability of Thylakoid Proteins in *pam68-2*

3.7.1) The Stability of PSII Proteins is Barely Affected

To monitor the stability of assembled photosynthetic proteins, the synthesis of plastid-encoded proteins was blocked with lincomycin under growing light conditions and protein signals were quantified by immunoblot-analyses. The PSII core proteins CP47 and PSII-E (α-subunit of cyt *b*559), together with the tested proteins from other photosynthetic complexes, showed no differences in their stability in all genotypes tested over a time period of 8 hours (Fig. 3.17). By contrast, the PSII core proteins D1, D2, and CP43 displayed increased degradation rates in *pam68-2* (71%, 75%, and 51%, respectively) and *lpa1* (82%,

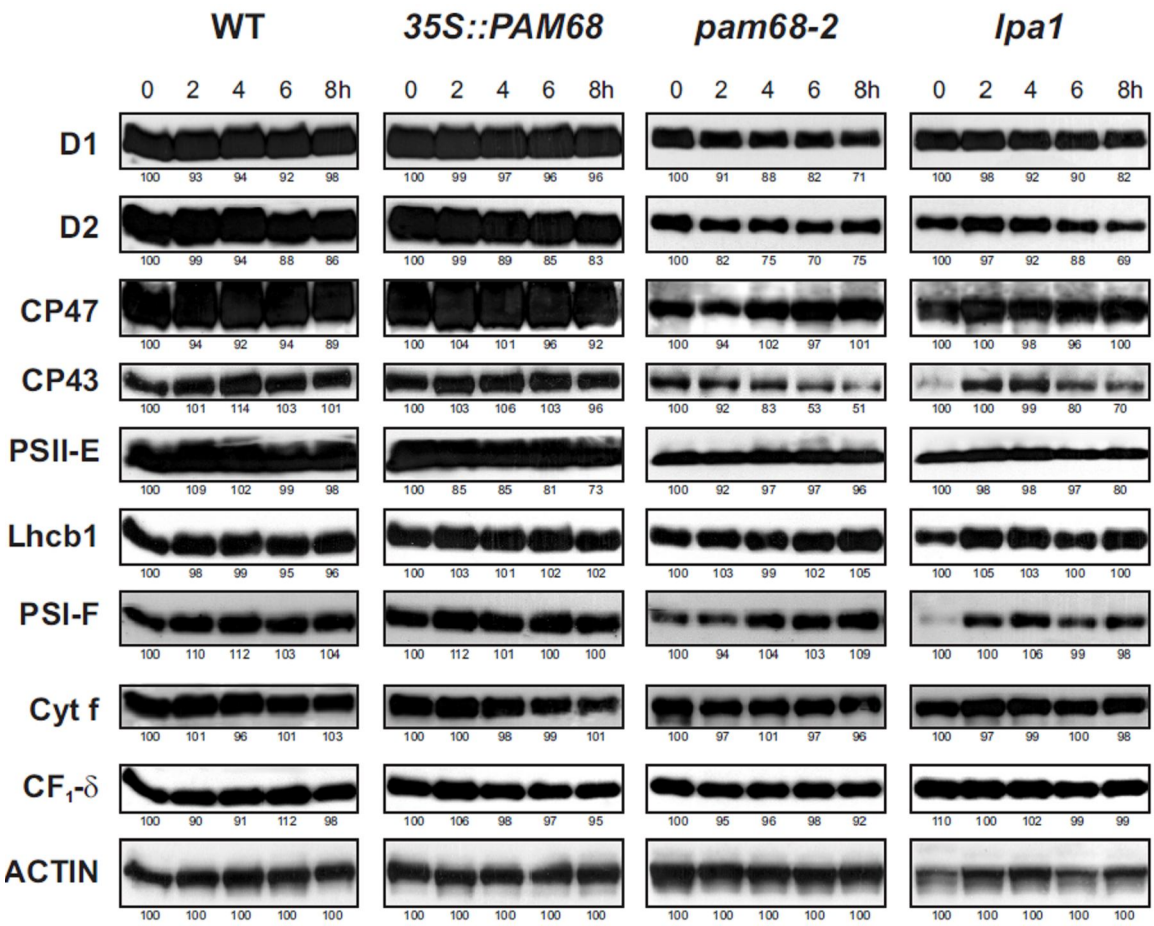

Fig. 3.17: Stability of photosynthetic proteins.

Intact leaves were incubated with lincomycin under growing light for 8 h. Every two hours, samples were assayed by immunoblot-analyses of total protein extracts. The percentages of protein levels are shown below the respective panels. They were calculated by comparison with amounts found in corresponding samples taken at time 0 and normalised against ACTIN.

69%, and 70%, respectively) compared with wild-type (98%, 86%, and 101%, respectively) and overexpressor of PAM68 (96%, 83%, and 96%, respectively). But the degradation rate after 8 h of lincomycin treatment was only 10-25% higher as in the wild-type control, suggesting that the proteins are quite stable once they have been assembled into complexes. For more detailed analysis however, this experiment has to be repeated with leaves incubated in lincomycin and DCMU (3-(3,4-dichlorophenyl)-1,1-dimethylurea) as DCMU blocks the electron transfer from Q_A to Q_B, thus leading to a net oxidation of the PQ pool.

3.7.2) Synthesis of PSII Core Proteins is Diminished

The *de novo* synthesis and assembly of thylakoid membrane protein complexes was investigated in intact mutant and wild-type leaves by pulse-labelling experiments with [^{35}S]methionine/cysteine. To monitor synthesis of the plastid encoded PSII core proteins, cytosolic translation was blocked with cycloheximide. Under the used conditions (1 h, 60 µmol photons m^{-2} s^{-1}), the most prominent

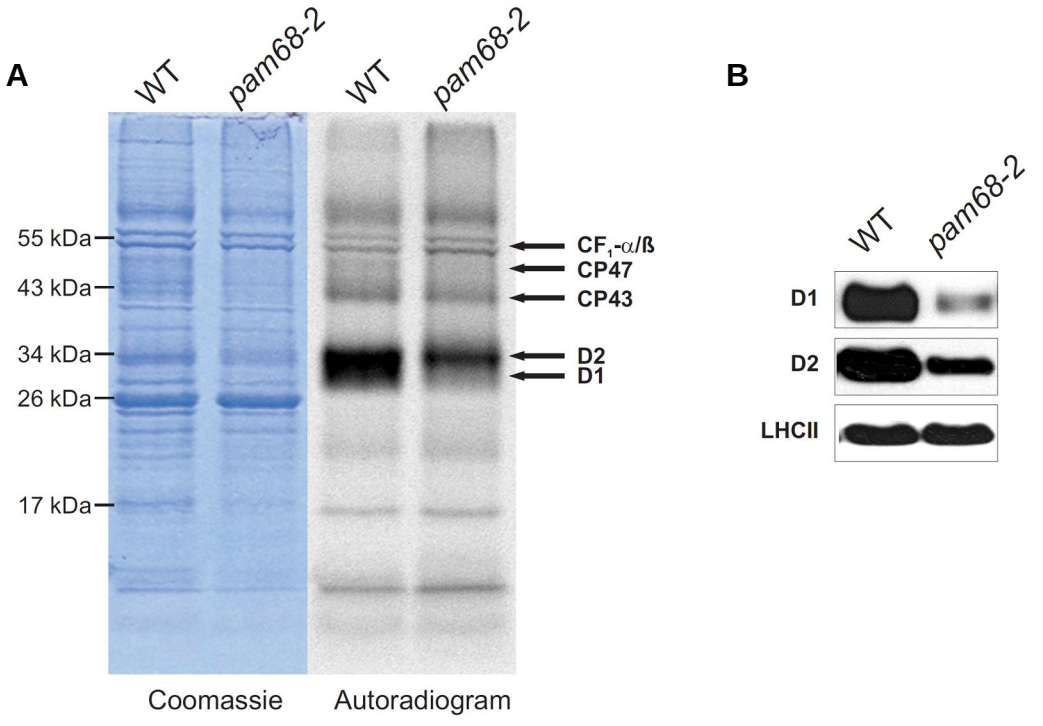

Fig. 3.18: Synthesis of PSII-D1 and D2.

WT and mutant plants were grown on MS-media supplemented with 1,5% sucrose under growing light conditions. Radioactive [^{35}S]-methione/cysteine was incorporated into intact leaves for 1 h at a light intensity of 60 µmol photons $m^{-2}s^{-1}$. Afterwards thylakoid proteins were isolated and loaded on a SDS-gel. **A)** Coomassie stain and autoradiogram of the SDS-gel. CF_1-α/ß = subunit α and ß of thylakoid ATP-synthase **B)** Immunoblot-analyses with the isolated thylakoid proteins. Same amounts were loaded on a second SDS-gel and subjected to semi-dry blot analysis.

bands on the autoradiogram were the D1 and D2 protein of PSII (Fig. 3.18A). For both a weaker incorporation of radioactivity could be detected with a stronger reduction for the D1 protein. The rates of synthesis of the PSII RC subunits CP43 and CP47, and the chloroplast ATP-synthase (CF_1-α/ß) remained unchanged in the mutant. For comparison of the synthesis rate with steady-state levels of PSII-proteins, the samples were subjected to immunoblot-analyses (Fig. 3.18B) with antibodies against D1, D2 and LHCII. Here it became evident that while steady-state levels were 10% in the mutant, newly synthesised protein was about 25%.
To investigate the possibility that PAM68 is involved in the assembly of PSII-complexes, we performed a two-dimensional BN/SDS-PAGE with radiolabelled

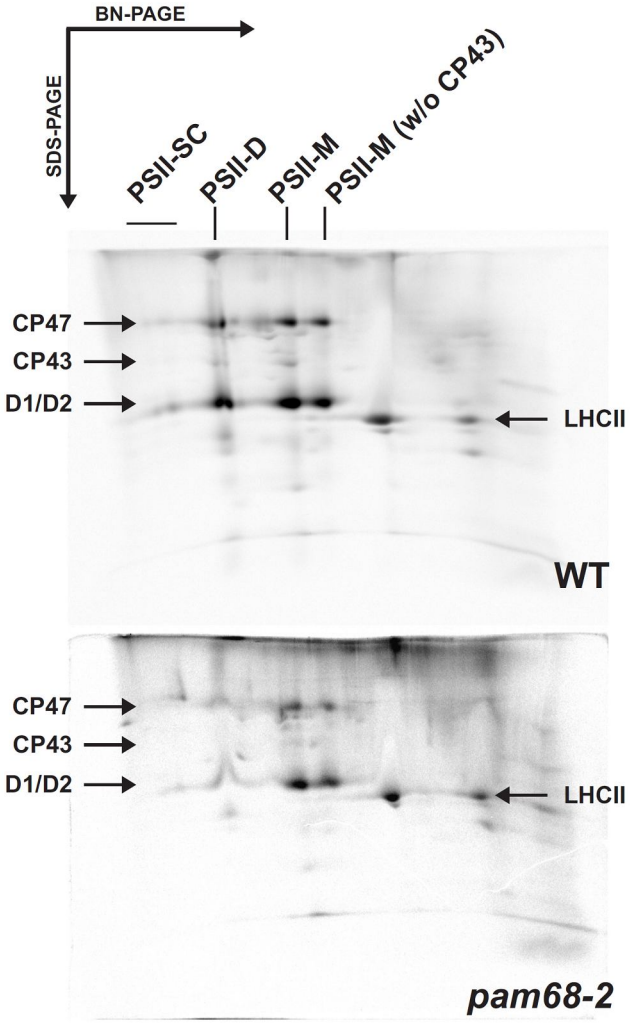

Fig. 3.19: Synthesis of PSII-complexes.

Autoradiograms after *in vivo* [^{35}S]methionine pulse labelling of wild-type (upper panel) and *pam68-2* (lower panel) thylakoid proteins for 1.5 h followed by a 2D BN/SDS-PAGE. PSII-SC = PSII-supercomplexes, PSII-D = PSII-dimers, PSII-M = PSII-monomers with CP43, PSII-M (w/o CP43) = PSII-monomers without CP43.

thylakoid proteins. For LPA1, known to be involved in the assembly of PSII, Peng *et al.* (2006) could show, that a great amount of the *de novo* synthesised thylakoid proteins was not assembled into higher molecular complexes in the respective mutant. Therefore they concluded that the assembly of the PSII-complexes is disturbed in the mutant. In contrast to *lpa1*, *pam68-2* did not show accumulation of free proteins (Fig. 3.19). The PSII RC proteins D1, D2, CP47, and CP43 were only present in PSII monomers in the mutant. PSII dimers or supercomplexes were not detectable. These results suggest that the assembly of PSII monomers is not disturbed in *pam68-2*, as there is no accumulation of unassembled proteins. But the dimerisation of PSII-monomers is diminished.

To further elucidate the question, whether PAM68 is a PSII assembly factor or exhibits a function in upstream processes, *in vivo* pulse labelling experiments were repeated with *lpa1* as control. To ensure that the newly synthesised PSII-proteins, especially the D1-protein, were not degraded in the mutants during the experiment, the pulse-labelling was performed under very low light conditions of 20 µmol photons m^{-2} s^{-1} for 20 min. The most prominent band consisted of PSII RC proteins D1 and D2. These two proteins were strongly reduced in both

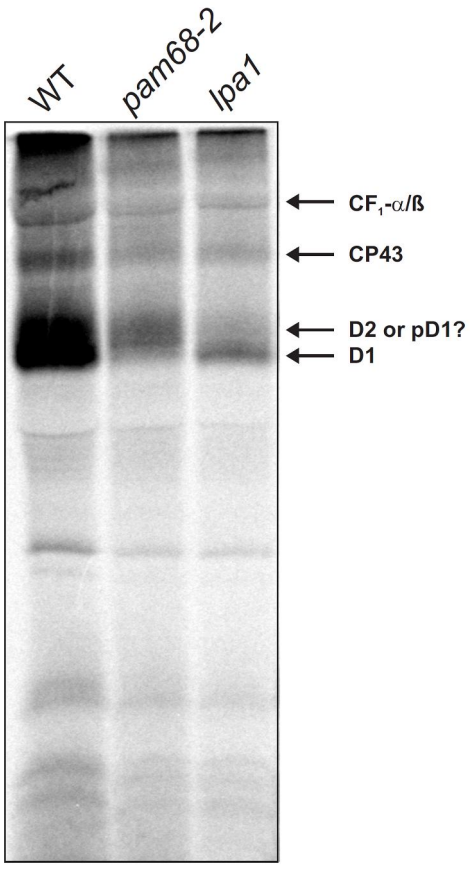

Fig. 3.20: Pulse labelling of *lpa1* and *pam68-2*.

Intact leaves were pulse-labelled with [^{35}S]methionine/cysteine for 20 min with light intensities of 20 µmol photons m^{-2} s^{-1}. Synthesis of nucleus-encoded proteins was blocked by addition of cycloheximide. Thylakoid proteins were isolated and subjected to SDS-PAGE analysis. pD1 = precursor of D1.

mutants. Still, concerning D1 and D2 synthesis, *lpa1* and *pam68-2* clearly differed. While *lpa1* showed a pattern similar to WT except for a strong decrease in D1 synthesis (as reported earlier by Peng *et al.*, 2006), newly synthesised D1/D2 migrated higher in *pam68-2* background. This can be interpreted in two ways: (i) accumulation of pD1 occurs, or (ii) only synthesis of D1 but not of D2 is decreased.

3.8) PAM68 Interacts With PSII Core Proteins *in vitro*

For a function in PSII assembly, PAM68 needs to interact with one of the hydrophobic core subunits of PSII. To test this possibility, the interaction of PAM68 with the subunits of the PSII core *in vivo* in yeast using a split-ubiquitin system designed to assess interactions of membrane proteins was examined (Pasch *et al.*, 2005). The system is based on the possibility to divide ubiquitin into two parts, an N-terminal half (*Nub*I) and a C-terminal half (Cub). When allowed to interact, the two parts spontaneously reassemble to reconstitute ubiquitin. For the interaction assay, the wild-type *Nub*I was mutated (creating *Nub*G), which shows a lower affinity to Cub. Thus, the two parts have to be brought into close proximity by two interacting test proteins to assemble ubiquitin.

A prey construct plasmid, in which the Cub moiety was fused to the C-terminus of PAM68 was prepared and co-transformed into yeast with the respective fusion protein NubG-X. The resulting transformants were analysed for growth on plates

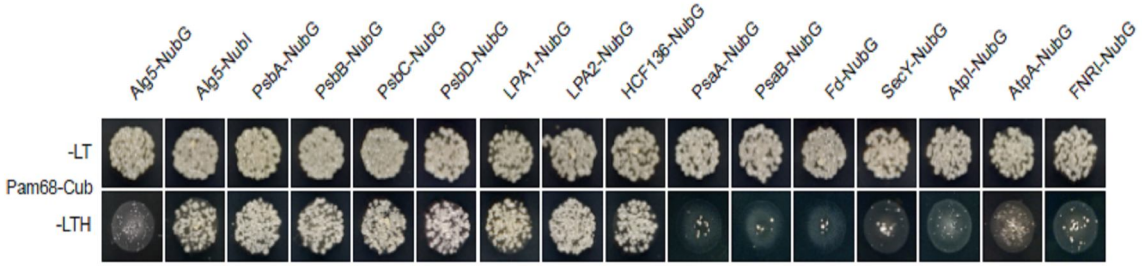

Fig. 3.21: Interaction partners of PAM68.

Growth of yeast cells expressing PAM68-Cub-TF with different *Nub*G-fusion proteins. Yeast cells containing the indicated combinations of PAM68 and the prey proteins were spotted onto medium lacking Leu and Trp (-LT) or onto medium lacking also His (-LTH) and grown for three days at 30°C). Positive control: Alg5-NubI construct (fusion of the yeast ER protein Alg5 with wild-type Nub); negative control: Alg5-NubG construct (fusion of Alg5 with the mutated Nub). Nub = N-terminal half of ubiquitin, Cub = C-terminal half of ubiquitin. Danja Schünemann, Bochum

lacking leucine and tryptophane (-LT) or leucine, tryptophane and histidine (-LTH). As shown in Figure 3.21, coexpression of PAM68 with the core proteins of PSII (D1, D2, CP47 and CP43) resulted in growth on (-LTH)-plates. With the tested subunits of other photosynthetic complexes like the PSI core proteins PsaA and PsaB, the ATP-synthase subunits AtpA and AtpI, the ferredoxin-$NADP^+$-oxidoreductase (FNR) or ferredoxin (Fd), no interaction could be observed. Interestingly, also for the PSII assembly factors LPA1, LPA2 and HCF136 a positive result appeared, suggesting that PAM68 may be involved in the biogenesis of PSII, probably acting in one cascade with these three proteins. LPA1 was supposed to be involved in the assembly of D1 into the PSII precomplex. When PAM68 also binds to this protein *in planta*, it is possibly part of the integration machinery. However, an interaction with SecY, the translocase of this pathway, was not detectable. For the homologue of PAM68, PAM68HL, no interactions partners came up in this experiment (data not shown).

3.9) Growth Phenotype of *pam68-2* is Due to Oxidative Stress

The *pam68-2* mutant showed severe defects in accumulating components of PSII accompanied by lower photosynthetic activity. Thus, the stunted phenotype of mutant plants could be due to secondary effects of the mutation resulting from insufficient energy needed for normal nutrition. To distinguish between primary defects due to lack of PAM68 and secondary effects caused by a deficiency in the products of photosynthesis, wild-type and mutant plants were supplied with 0.5 % sucrose as a carbon source to support normal growth development. The PSII assembly mutant *lpa1* showed a comparable growth phenotype on soil (Fig. 3.22A) and served as a control. For the *lpa1* mutant, ecotype Landsberg *erecta* (Ler) was used as wild-type control, which is the background of the mutation. Figure 3.22B displays the phenotype of mutant and wild-type plants grown for 25 days on MS-media (supplemented with 0.5% sucrose) under long day conditions (LD; 16 h light / 8 h dark, GL). Under the different light intensities tested the mutant plants exhibited always stunted growth and pale green leaves on both MS media and soil. But the difference between WT and mutant concerning the size of the leaves varied. Under low light (20 µmol photons m^{-2} s^{-1}) the leaf area of *pam68-2* was ~50% of WT (Col-0), whereas under light conditions of 150 µmol photons m^{-2} s^{-1} this value was about 30%. The same was true for *lpa1* in

comparison to its WT background (Ler). These results suggest oxidative stress for both mutant plants already under growing light conditions, as the decrease in size could also be observed under 110 µmol photons m^{-2} s^{-1}. However, with a higher concentration of sucrose in the media, it may be possible to rescue the phenotype completely, at least under low light.

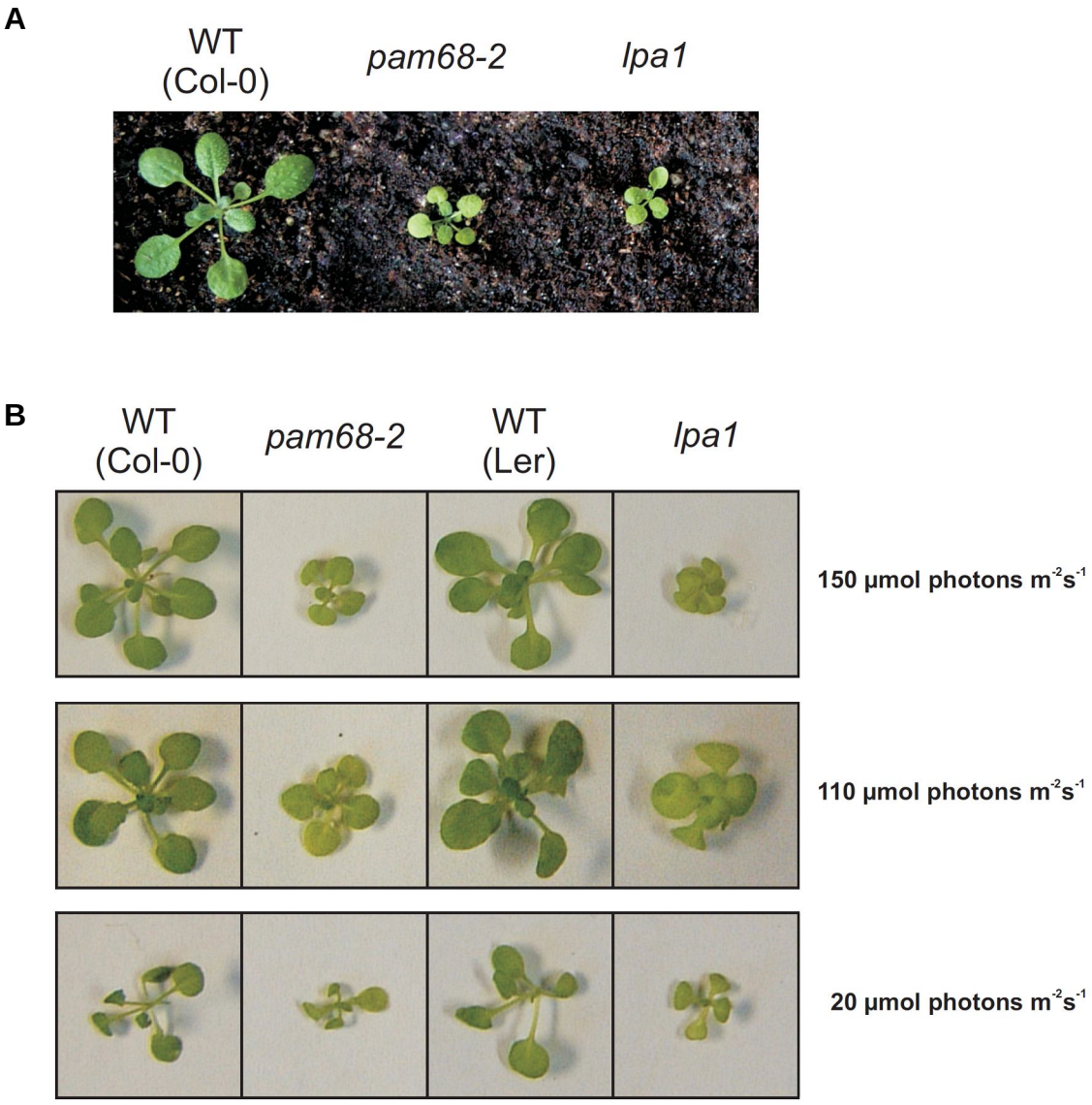

Fig. 3.22: Effect of sucrose treatment on wild-type, *pam68-2* and *lpa1* plants.

A) Wild-type (Col-0) and mutant plants germinated directly on soil and grown for 1 month under a 16 h photoperiod (LD) and 120 µmol photons m^{-2} s^{-1}. **B)** 25-day-old plants germinated and grown under LD conditions on MS media containing 0.5 % sucrose under different light intensities. Col-0 = ecotype Columbia-0, background of *pam68-2*; Ler = ecotype Landsberg *erecta*, background of *lpa1*.

4) Discussion

4.1) PAM68/PAM68HL: Two *Arabidopsis* Proteins of Cyanobacterial Origin

The biogenesis and assembly of the photosynthetic complexes is a multistep process. It has to be strongly coordinated, as both nucleus- and chloroplast-encoded proteins have to be synthesised and assembled into functional complexes in the right stoichiometry. Additionally, ligation of various cofactors occurs at different steps of the assembly process. Thus, this process is likely to require auxiliary and regulatory factors. Since the discovery of the first nucleus-encoded auxiliary factor for PSII biogenesis, HCF136 (Meurer *et al.,* 1998), much effort was made to identify more components. As the coding capacity of the chloroplast genome is limited, it was suggested that the biogenesis and assembly of PSII is mainly regulated by nucleus-encoded proteins (Goldschmidt-Clermont, 1998; Barkan and Goldschmidt-Clermont, 2000; Rochaix, 2001; Leister, 2003). The identification of these factors will undoubtedly improve our understanding of the assembly of photosynthetic complexes and how their functionality is maintained. Here, we report the isolation and characterisation of the PAM68 protein and its homologue, PAM68HL, in *Arabidopsis thaliana*. All available evidence indicates that PAM68 behaves as a PSII-specific assembly factor, whereas PAM68HL seems to be important for the activity of the NDH-complex (NAD(P)H-dehydrogenase).

4.2) Both Proteins Are Localised in the Chloroplast

The prediction of a chloroplast transit peptide for the homologous proteins in all photosynthetic organisms (sequenced to date) indicated that the PAM68 and PAM68HL proteins are localised in the chloroplast. The localisation was confirmed by immunoblot-analyses with a peptide-antibody raised against an epitope of *Arabidopsis* PAM68 and PAM68HL, respectively. With these antibodies, the proteins could be detected in both, total protein extracts and isolated thylakoid membranes of WT but not of the respective mutant (pers. comm. Renate Kreller). Also in an overexpression line of PAM68 in the mutant-

background of *pam68-2*, the protein appeared at the same size as in WT but in higher amounts. Additionally, *in vitro* import of PAM68 into intact chloroplasts and translocation of a PAM68::RFP construct into *Arabidopsis* protoplasts was carried out (Fig. 3.3). In both experiments, the protein was transported into the chloroplast. These results together with a prediction for two transmembrane domains in the C-terminal part of PAM68 and PAM68HL, strongly suggest a localisation in the thylakoid membrane. Interestingly, for all orthologues two transmembrane domains in the C-terminal part of the protein were predicted as well. However, an additional hint for thylakoid localisation was given by recent proteomic approaches, where PAM68 and PAM68HL were found in thylakoid membrane preparations (Zybailov *et al.*, 2008; Peltier *et al.*, 2004). The co-expression data also substantiate this assumption.

4.3) PAM68 Has a Function in PSII Biogenesis

4.3.1) PSII Function Is Diminished

PSII function is easily monitored by fluorescence measurements with the Dual-PAM fluorometer. Here, *pam68-2* plants show a typical photosynthesis affected phenotype (Fig. 3.12). F_0, the minimal level of fluorescence of dark-adapted plants, was higher in the mutant, indicating photoinhibition on the acceptor side. Simultaneously, the maximal fluorescence in the dark was decreased resulting in a strongly reduced F_V/F_M-ratio, which represents the maximal quantum yield of PSII. Such a strong reduction of this parameter as in *pam68-2* points to a decrease in accumulation or function of PSII. Another hint for defects in photosynthesis was given by the parameter for photochemical quenching, 1-qP. It was remarkably increased, which means that the PQ pool is more reduced. This suggests an intact electron transfer downstream of the PQ pool. In summary, all these spectroscopic data propose a PSII-phenotype for *pam68-2*.

The composition of the leaf pigments nicely fits into this assumption, as the mutant exhibits reduced levels of lutein, ß-carotene and chlorophyll, especially Chl *a*, which are found in PSII reaction centres. Furthermore, the contents of xanthophylls point to oxidative stress in the mutant plant.

4.3.2) PSII RC Proteins Accumulate to Less Extent

The spectroscopic measurements, suggesting a reduction in PSII performance, were supported by the analyses of protein levels of PSII reaction centre components. Here it became evident that PSII complexes were severely decreased in the mutant. D1, D2, CP47 and CP43 are reduced to less than 25% of wild-type level (Fig. 3.14). Because of CES mechanisms, it is difficult to distinguish whether there is a defect in the accumulation of all four PSII core proteins or if only synthesis of the dominant subunit D2 is diminished, resulting additionally in reduced protein levels of D1, CP47, and CP43.

However, in the *lpa1* mutant, all four PSII core proteins were reduced with the strongest reduction in D1 protein level and CP43, as it is the case for *pam68-2*. Because of the interaction of PAM68 with D1 in the split-ubiquitin system as well as equally reduced amounts of the PSII core proteins in both mutants, it is likely that defects in *pam68-2* are due to inefficient biogenesis of D1. The mutation of *PAM68* does not affect the accumulation of the chloroplast ATP synthase and the light-harvesting complex of PSI. In the protein level of the LHCII, the OEC, the cytochrome b_6f complex, and the PSI complex only a slight decrease is visible. However, it is often observed within PSII mutants that their PSI content is also affected, indicating that the reduced PSI and Cyt b_6f levels in PSII mutants are due to secondary effects of the mutation (Meurer *et al.*, 1998; Plücken *et al.*, 2002). In the case of *pam68-2* this view is supported by analyses of structural changes within the thylakoid complexes. No alterations could be observed for all complexes excepting PSII, as no PSII-supercomplexes and only small amounts of dimers and monomers were detectable. Therefore, a direct effect of the *pam68* mutation on PSI appears to be unlikely but cannot be excluded at the current stage of investigation.

To unravel the reason for less accumulating PSII proteins, transcription of the respective genes was analysed. No alterations in the abundance or patterns of PSII, LHCII, and ATP-synthase gene transcripts were detected in the *pam68* mutant. These results demonstrate that the reduced PSII contents are not due to the absence of transcripts encoding one of these structural PSII proteins but may be due to impaired translation or, alternatively, accelerated degradation of the PSII subunits once they have been synthesised. Beside the protein and transcript level of photosynthetic proteins, also the abundance of *PAM68* mRNA and

protein was controlled. Both accumulated at very low levels, suggesting that the PAM68 protein is not a stoichiometric component of the mature PSII complex.

4.3.3) *pam68-2* Shows No Accelerated Degradation of Proteins

To give further insight into the function of PAM68, *in vivo* pulse experiments were carried out (Figures 3.18, 3.19, and 3.20). In contrast to the steady-state level of the PSII core proteins D1, D2, CP47 and CP43, the amount of *de novo* synthesised proteins was quite different. D1 and D2 synthesis is decreased in PAM68-deficient plants, whereas the synthesis rate of CP47 and CP43 was comparable to wild-type. Diminished synthesis of D1 and D2 could be due to an accelerated degradation of these proteins maybe because of defects in the repair cycle of PSII, as these two proteins are the main targets for light-induced damage. To clarify this, we analysed the turnover rate and degradation of D1 and D2. In pulse-chase experiments, no significant difference between WT and mutant was detectable (data not shown). Also BN/SDS-PAGE of labelled thylakoid proteins and immunoblot-analyses of the second dimension argue against a defect in the degradation of PSII proteins during the repair cycle as no accumulation of degradation products was visible. Testing the growth of mutant plants under different conditions, however, could not rule out defects in the repair process (Fig. 3.22). The phenotype of *pam68-2* was the same for plants grown directly on soil or grown on medium supplemented with 0.5% sucrose under growing light conditions. But under lower light the plants grew better, suggesting oxidative stress in mutant plants.

Comparison with the recently discovered TLP18.3 protein, which was assumed to be involved in the repair cycle of PSII in *Arabidopsis* (Sirpiö *et al.*, 2007), demonstrates clear differences. Plants lacking the TLP18.3 protein did not reveal any visible phenotype under standard growth conditions. Also the amount of photosynthetic proteins in immunoblot analyses was not affected, but the degradation of newly synthesised D1 after high-light treatment was significantly decreased. All together we can conclude that PAM68 is not a component of the degradation machinery of PSII proteins during the repair cycle. But we can not exclude the possibility of an involvement in *de novo* synthesis or integration of damaged proteins.

4.3.4) Is PAM68 an Assembly or Stability Factor of PSII?

PSII specific stability and assembly factors are becoming increasingly uncovered in cyanobacteria, green algae and flowering plants. Mutation of one of these components in *Arabidopsis* leads generally to a visible growth phenotype and defects in photosynthesis. Most of these described proteins are involved in the biogenesis of the PSII reaction centre protein D1 (CtpA, HCF136, HCF173, LPA1, and CYP38) and mutants exhibit a typical “PSII-phenotype”. As this is also the case for *pam68-2*, we tested it for deficiencies in the assembly and/or stabilisation of PSII proteins and compared the results with the recently described PSII assembly factor LPA1 (Peng *et al.*, 2006). Blue native PAGE with labelled thylakoid proteins from *lpa1* showed an accumulation of free proteins, which were not assembled in photosynthetic complexes. Also, the incorporation of [^{35}S]Met/Cys into D1 and D2 was significantly reduced. This is also true for *pam68-2*. However, BN/SDS PAGE of labelled thylakoid proteins showed that most of the radioactivity was found to be associated with the PSII complexes in both mutant and wild-type. Unassembled proteins were barely detectable, indicating sufficient assembly of PSII complexes in *pam68-2* although no dimers could be observed in the experiment (Fig. 3.18). But this is probably due to reduced levels of dimers, which were not detectable under these conditions, as immunoblot-analyses of photosynthetic complexes could show assembly of D1 and CP43 into PSII-dimers (Fig. 3.15). These results indicate that PAM68 is not directly involved in the assembly of PSII complexes, since the absence of free proteins can also result from a decreased stability or accelerated degradation of the newly synthesised proteins. In this work no accumulation of degradation products could be observed. In immunoblot-analyses of lincomycin-treated thylakoid proteins the stability of the investigated proteins showed no big differences between WT and mutant. So it seems unlikely that PAM68 is important for the stability of thylakoid proteins. It might be that the degradation of proteins is too fast to be detected in the experiments we carried out until now. However, it is remarkable that all the tested conditions provided no indication of an increase of degradation products. Another possibility is of course an involvement of PAM68 in the dimerisation. In the mutant the reduction of PSII dimers seems to be higher than the reduction of monomers (Figures 3.14, 3.15, 3.19). But this would also be the case, if one of the PSII core proteins is not

accurately synthesised or folded into the thylakoid membrane leading to a decreased stability of the complex. Also instability of the monomer itself is possible. For clarification of an involvement in assembly or stabilisation of PSII complexes, it is important to investigate a possible comigration of PAM68 with these complexes. An interaction of PAM68 with core proteins of PSII, namely D1, D2, CP47, and CP43, could already be observed in a split-ubiquitin assay. The translocase cpSecY, which integrates at least D1 into the thylakoid membrane, did not interact with PAM68 substantiating the suspicion that PAM68 is not part of the assembly process.

4.3.5) Possible Involvement of PAM68 in Synthesis of D1

Conversely, synthesis of thylakoid proteins might be defective in *pam68-2*. *In vivo* labelling experiments revealed decreased synthesis of D1. This is also the case for plants lacking the D1 translation factor HCF173 (Schult *at al.*, 2007). In this mutant the synthesis and the steady-state level of the corresponding *psbA* mRNA is significantly reduced. Polysome association experiments suggested that this is primarily caused by reduced translation initiation of *psbA* mRNA. Previous results with *pam68-2* on the other hand suggested no alterations in the distribution pattern compared to WT (Fig. 3.16B). Also the steady-state level of the *psbA* mRNA is not affected. Thus, PAM68 is not important for the translation initiation of D1. Further support is provided by the differences in accumulation of thylakoid proteins. The OEC components PsbO and PsbP are less abundant in *hcf173* (≤ 25%) than in *pam68-2* (~ 90%). The more drastic phenotype of *hcf173* is also visible in the stronger reduction of the maximum quantum yield of PSII, F_V/F_M (0.15 vs. 0.33 in *pam68-2*). If PAM68 is involved in synthesis of D1, it is probably acting downstream of HCF173, as the effect of a mutation is less vigorous. One possibility is a stabilising role during the elongation of the D1 protein. It might also be that the binding of cpSRP54 to the D1 nascent chain and the translocation to the thylakoid membrane is dependent on the function of PAM68. Clarification could be achieved by testing the interaction of more constructs like cpSRP54 with PAM68 in yeast or biochemically with co-immunoprecipitation experiments. For HCF136 and LPA1, an interaction with PAM68 in yeast could already be shown, suggesting that PAM68 might be part of the same biological pathway. However,

as PAM68 also interacts with four PSII core proteins (D1, D2, CP47, and CP43) the function might be more general.

In vivo labelling of thylakoid proteins revealed a reduction in the *de novo* synthesis of two bands running at a size of ~ 34 kDa (Fig. 3.18 and 3.20). The lower band represents mature D1, whereas the upper band can either display the synthesis of D2 or of pD1. A hint for pD1 is the unchanged synthesis rate of CP47 and CP43. This observation speaks against a defect in D2-synthesis, as CP47 (and probably also CP43) is a CES-subunit of D2 and thus the translation of the two chlorophyll binding proteins should also be down-regulated in the mutant. However, the steady-state protein level of both is strongly reduced, suggesting an increased degradation. A less available amount of D1 protein for the biogenesis of the PSII complex would consequentially lead to the degradation of dispensable proteins like CP43 or CP47.

4.4) PAM68HL is Not Involved in the Same Processes as PAM68

Co-expression analyses of PAM68 and PAM68HL suggested an involvement in photosynthetic processes for both proteins (Fig. 3.11). Different PSII biogenesis factors like LPA2, DegP5, thylakoid lumen proteins or components of the oxygen-evolving complex are co-expressed with both proteins. But in general there are some differences, as PAM68 seems to be more co-expressed with PSII biogenesis factors, whereas PAM68HL shows co-expression with many proteins important for the activity of the NDH complex. Also the phenotype of deletion mutants suggests an involvement in PSII biogenesis rather for PAM68 than for its homologue, as PAM68HL-deficient plants exhibit no growth phenotype (Fig. 3.8). This is not surprising as the NDH complex is involved in electron pathways around PSI and plays not a major role during photosynthesis (Rumeau *et al.*, 2007). Thus, a depletion of the NDH complex is not resulting in a strong phenotype (Sirpiö *et al*., 2009). NDH is not ubiquitous among oxygenic photosynthetic organisms, being absent from many green algae like *Chlamydomonas* but present in cyanobacteria and a lot of plant species (Rumeau *et al.*, 2007). As already mentioned (see section 3.2), PAM68HL seems to be the result of a duplication event. The duplication most likely occurred after endosymbiosis, probably after the splitting of green algae and flowering plants as there is only one homologue in green algae. PAM68 is more closely related to

green algae as PAM68HL. Preliminary experiments with a deletion mutant of PAM68HL revealed that the PSI/NDH supercomplex is absent. This was further confirmed by spectroscopic measurements of the functional status of the NDH complex. *Pam68hl* exhibited a typical NDH-defective phenotype in this experiment. However, the involvement of PAM68HL in the activity of the NDH complex has to be analysed in more detail. Anyway, deletion of both proteins in one plant did not result in an additional growth phenotype (Fig. 3.8), giving further support to the assumption that PAM68 and PAM68HL are not acting in the same process.

4.5) Evolution of Auxiliary Factors

Eukaryotes co-opted photosynthesis from prokaryotes by engulfing and stably integrating a photoautotrophic prokaryote in a process known as primary endosymbiosis (reviewed in Gould *et al.,* 2008). During evolution, this endosymbiont was more and more integrated into its host organism. The main part of its genome was either lost or transferred into the nucleus of the host cell (Martin *et al.*, 1998). This made photosynthesis quite complicated, as biogenesis of photosynthetic complexes includes now on the one hand translation of proteins directly in the chloroplast, and on the other hand synthesis of nucleus-encoded proteins in the cytosol, followed by translocation into the chloroplast across its two envelope membranes (Reumann *et al.*, 2005). Hence, new proteins and protein complexes evolved to assist this multistep formation of photosynthetically active thylakoid membranes. Dependent on the function of these biogenesis factors, they emerged at different time points during evolution. Proteins that are important for the translocation of nucleus-encoded components into the chloroplast probably evolved early on in the conversion of the endosymbiont into an organelle (Gould *et al.,* 2008). The evolution of factors directly involved in the biogenesis of photosynthetic complexes, especially of PSII, is depicted in Figure 4.1. The Oxa1/Alb3/YidC family of membrane insertases is highly conserved. All members seem to play an important role in the membrane protein biogenesis of respiratory and energy transduction proteins and exist in mitochondria, chloroplasts and bacteria (Yi and Dalbey, 2005). A second protein family which originated quite early in evolution is the tellurite resistance C (TerC) family. For a knock-out line of the homologue in *Arabidopsis* it was recently shown that it is

involved in thylakoid membrane biogenesis in early chloroplast development (Kwon and Cho, 2008). Orthologues of AtTerC are present in a variety of bacteria, archaea, algae and other plant species.

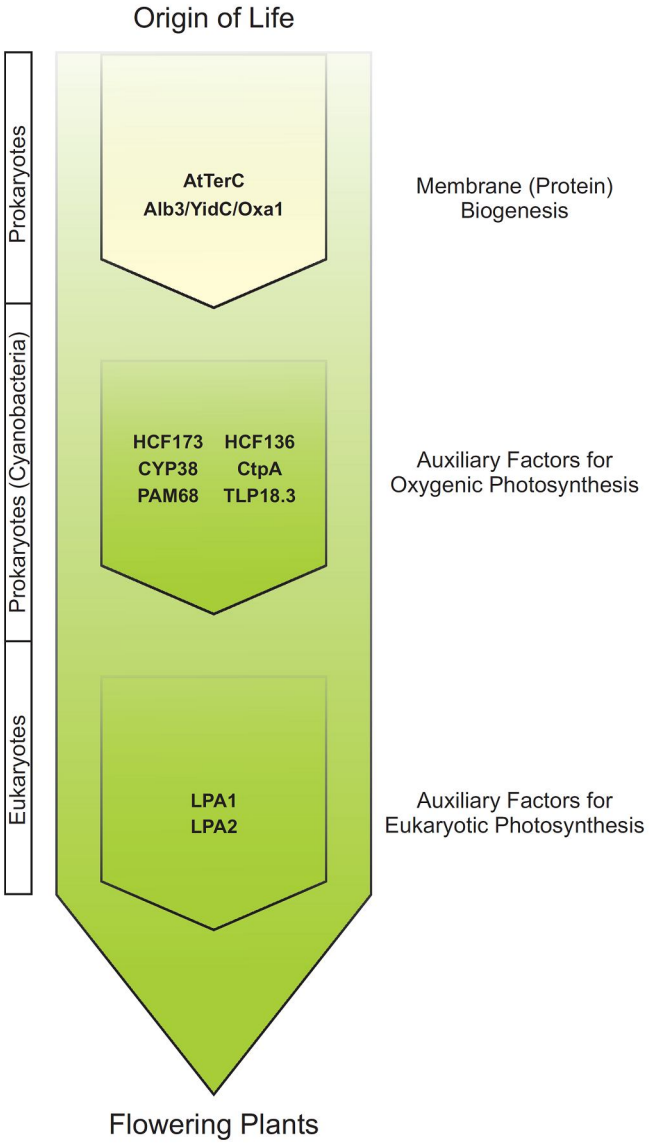

Fig. 4.1: Evolution of auxiliary proteins.

LPA1 (Peng *et al.*, 2006), LPA2 (Ma *et al.*, 2007), AtTerC (Kwon and Cho, 2008), TLP18.3 (Sirpiö *et al.*, 2007), HCF173 (Schult *et al.*, 2007), HCF136 (Meurer *et al.*, 1998; Plücken *et al.*, 2002), CYP38 (Sirpiö *et al.*, 2008), CtpA (Bowyer *et al.*, 1992; Merchant and Dreyfuss, 1998), Alb3 (Sundberg *et al.*, 1997).

Beside these two proteins that evolved before separation of the cyanobacteria, several more PSII biogenesis factors occurred after this splitting event. HCF173, HCF136, CYP38, and CtpA play a role in translation, chlorophyll-binding, folding and processing of D1, respectively (Schult *et al.*, 2007; Plücken *et al.*, 2002; Sirpiö *et al.*, 2008; Merchant and Dreyfuss, 1998). TLP18.3 facilitates degradation

of D1 after photo-damage (Sirpiö *et al.*, 2007). However, until now there are two auxiliary factors for PSII biogenesis known that emerged after the engulfment of a cyanobacterium, LPA1 and LPA2 (Peng *et al.*, 2006; Ma *et al.*, 2007). Both have orthologues only in eukaryotic organisms that perform photosynthesis, namely green algae and plants. LPA2 is thereby the "younger" protein as there exists only one orthologue in green algae (*Ostreococcus*). Mutants of these two proteins show a much weaker phenotype compared with many of the more conserved biogenesis factors like Alb3, HCF173 or HCF136.

The new PSII biogenesis factor PAM68, described in this work, emerged early during evolution of photosynthetic organisms as it is present in all cyanobacterial groups. After endosymbiosis, a duplication event led to the appearance of PAM68HL, which has orthologues in the same plant species (sequenced until now) as PAM68. The orthologues in the green algae *Chlamydomonas reinhardtii* and *Ostreococcus lucimarinus*, however, seem to originate from PAM68 and not from PAM68HL (see phylogram, Fig. 3.2). This would fit into the assumption that PAM68HL is somehow involved in the activity of NDH, as this complex is not present in green algae.

4.6) Conclusion

The biological function of PAM68 and PAM68HL is still not completely resolved, even though the point of action for PAM68 is quite constricted. Comparison of *pam68-2* with *hcf173* and *lpa1* suggested that PAM68 probably acts downstream of HCF173 and upstream of LPA1. HCF173 was supposed to ensure initiation of *psbA* mRNA translation as component of a high-molecular weight complex that contains *psbA* RNA (Schult *et al.*, 2007). LPA1 on the other hand is thought to act as a chaperone, assisting the proper folding and integration of D1 into the thylakoid membrane and promoting the subsequent interaction between D1 and D2 (Peng *et al.*, 2006). The role of PAM68 might be stabilisation of the whole *psbA* mRNA/polysome complex (Fig. 4.2A) or of the D1 nascent chain during transition to (Fig. 4.2B) or integration into the thylakoid membrane (Fig. 4.2C). The latter possibility is supported by the observed interaction of PAM68 with LPA1 and HCF136 in yeast. However, for further elucidation, a possible binding

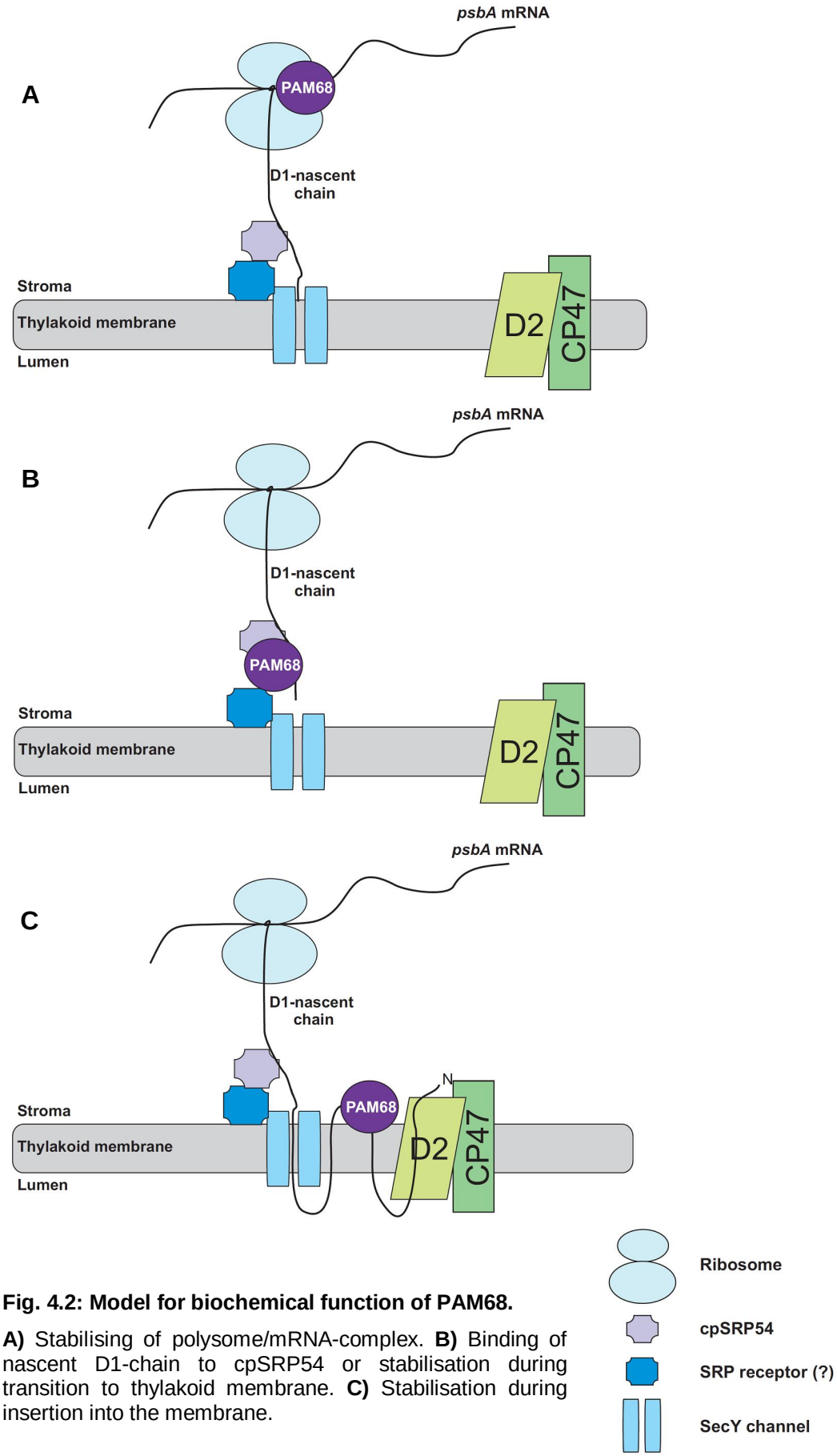

Fig. 4.2: Model for biochemical function of PAM68.

A) Stabilising of polysome/mRNA-complex. **B)** Binding of nascent D1-chain to cpSRP54 or stabilisation during transition to thylakoid membrane. **C)** Stabilisation during insertion into the membrane.

of PAM68 to proteins of the transition/integration machinery, like cpSRP54 or Alb3, has to be tested biochemically (co-immunoprecipitation experiments). Analysis of ancestor proteins might also be important. Deletion of the orthologue in *Synechocystis* does not result in such a strong effect, but experiments with this mutant suggested also a slight PSII phenotype (Prof. Nickelsen; pers. comm.). As the duplication of PAM68 occurred after the engulfment of the chloroplastid precursor, it would additionally be interesting to test whether the ancestral protein combined the function of both, PAM68 and PAM68HL.

5) References

A

Alonso, J.M., Stepanova, A.N., Leisse, T.J., Kim, C.J., Chen, H., Shinn, P., Stevenson, D.K., Zimmerman, J., Barajas, P., Cheuk, R., Gadrinab, C., Heller, C., Jeske, A., Koesema, E., Meyers C.C., Parker, H., Prednis, L., Ansari, Y., Choy, N., Deen, H., Geralt, M., Hazari, N., Hom, E., Karnes, M., Mulholland, C., Ndubaku, R., Schmidt, I., Guzman, P., Aguilar-Henonin, L., Schmid, M., Weigel, D., Carter, D.E., Marchand, T., Risseeuw, E., Brogden, D., Zeko, A., Crosb, W.L., Berry, C.C., and Ecker, J.R. (2003) Genome-wide insertional mutagenesis of Arabidopsis thaliana. *Science* **301**, pp. 653-657.

Amunts, A., Drory, O., and Nelson, N. (2007) The structure of a plant photosystem I supercomplex at 3.4 A resolution. *Nature* **447**, pp. 58-63.

Anderson, J.M. (2006) The grana margins of plant thylakoid membranes. *Physiol. Plantarum* **76**(2), pp. 243-248.

Aro, E.M., Virgin, I. and Andersson, B. (1993) Photoinhibition of photosystem II. Inactivation, protein damage and turnover. *Biochim. Biophys. Acta* **1143**, pp. 113-134.

B

Baena-González, E., and Aro, E.M. (2002) Biogenesis, assembly and turnover of photosystem II units. *Phil. Trans. R. Soc. London* B **357**, pp. 1451-1460.

Bannai, H., Tamada, Y., Maruyama, O., Nakai, K., and Miyano, S. (2002) Extensive feature detection of N-terminal protein sorting signals. *Bioinformatics* **18**(2), pp. 298-305.

Barber, J. and Andersson, B. (1992) Too much of a good thing: light can be bad for photosynthesis. *Trends Biochem. Sci.* **17**, pp. 61-66.

Barkan, A. (1988) Proteins encoded by a complex chloroplast transcription unit are each translated from both monocistronic and polycistronic mRNAs. *EMBO J.* **7**(9), pp. 2637-2644.

Barkan, A., and Goldschmidt-Clermont, M. (2000) Participation of nuclear genes in chloroplast gene expression. *Biochimie* **82**, pp. 559-572.

Bassi, R., dal Belin Peruffo, A., Barbato, R., and Ghisi, R. (1985) Differences in chlorophyllprotein complexes and composition of polypeptides between thylakoids from bundle sheaths and mesophyll cells in maize. *Eur. J. Biochem.* **146**, pp. 589-595.

Bowyer, J.R., Packer, J.C.L., McCormack, B.A., Whitelegge, J.P., Robinson, C., and Taylor, M. (1992) Carboxyl-terminal processing of the D1 protein and photoactivation of water splitting in photosystem II. *J. Biol. Chem.* **267**, pp. 5424–5433.

C

Choquet, Y., Stern, D.B., Wostrikoff, K., Kuras, R., Girard-Bascou, J., and Wollman, F.A. (1998) Translation of cytochrome *f* is autoregulated through the 5´ untranslated region of *petA* mRNA in *Chlamydomonas* chloroplasts. *Proc. Natl. Acad. Sci.* USA **95**, pp. 4380–4385.

Choquet, Y., and Vallon, Q. (2000) Synthesis, assembly and degradation of thylakoid membrane proteins. *Biochimie* **82**(6-7), pp. 615-634.

Choquet, Y., Wostrikoff, K., Rimbault, B., Zito, F., Girard-Bascou, J., Drapier, D., and Wollman, F.A. (2001) Assembly-controlled regulation of chloroplast gene translation. *Biochem. Soc. Trans.* **29**, pp. 421–426.

Claros, M.G., and Vincens, P. (1996) Computational method to predict mitochondrially imported proteins and their targeting sequences. *Eur. J. Biochem.* **241**, pp. 779-786.

Clough, S.J., and Bent, A.F. (1998) Floral dip: a simplified method for *Agrobacterium*-mediated transformation of *Arabidopsis thaliana*. *Plant J.* **16**, pp. 735-743.

D

Dekker, J.P., and Boekema, E.J. (2005) Supramolecular organization of thylakoid membrane proteins in green plants. *Biochim. Biophys. Acta* **1706**, pp. 12-39.

Demmig-Adams, B., Gilmore, A.M., and Adams III, W.W. (1996) Carotenoids 3: in vivo function of carotenoids in higher plants. *FASEB J.* **10**(4), pp. 403-412.

de Vitry, C., Olive, J., Drapier, D., Recouvreur, M., and Wollman, F.A. (1989) Posttranslational events leading to the assembly of photosystem II protein complex: A study using photosynthesis mutants from *Chlamydomonas reinhardtii*. *J. Cell Biol.* **109**, pp. 991-1006.

de Vitry, C., and Vallon, O. (1999) Mutants of *Chlamydomonas*: tools to study thylakoid membrane structure, function and biogenesis. *Biochimie* **81**, pp. 631–643.

Dovzhenko, A., Dal Bosco, C., Meurer, J., and Koop, H.U. (2003) Efficient regeneration from cotyledon protoplasts in *Arabidopsis thaliana*. *Protoplasma* **222**(1-2), pp. 107-111.

E

Eichacker, L.A., Soll, J., Lauterbach, P., Rüdiger, W., Klein, R.R., and Mullet, J.E. (1990) *In vitro* synthesis of chlorophyll *a* in the dark triggers accumulation of chlorophyll *a* apoproteins in barley etioplasts. *J. Biol. Chem.* **265**, pp. 13566–13571.

Emanuelsson, O., Nielsen, H., and von Heijne, G. (1999) ChloroP, a neural network-based method for predicting chloroplast transit peptides and their cleavage sites. *Protein Sci.* **8**, pp. 978-984.

Emanuelsson, O., Nielsen, H., Brunak, S., and von Heijne, G. (2000) Predicting subcellular localization of proteins based on their N-terminal amino acid sequence. *J. Mol. Biol.* **300**, pp. 1005-1016.

Erickson, J. M., Rahire, M., Malnoe, P., Girard-Bascou, J., Pierre, Y., Bennoun, P., and Rochaix, J.D. (1986) Lack of the D2 protein in a *Chlamydomonas reinhardtii psbD* mutant affects photosystem II stability and D1 expression. *EMBO J.* **5**, pp. 1745–1754.

F

Färber, A., Young, A.J., Ruban, A.V., Horton, P., and Jahns, P. (1997). Dynamics of Xanthophyll-Cycle Activity in Different Antenna Subcomplexes in the Photosynthetic Membranes of Higher Plants (The Relationship between Zeaxanthin Conversion and Nonphotochemical Fluorescence Quenching). *Plant Physiol.* **115**, pp. 1609-1618.

Favory, J.J., Kobayshi, M., Tanaka, K., Peltier, G., Kreis, M., Valay, J.G., and Lerbs-Mache, S. (2005) Specific function of a plastid sigma factor for ndhF gene transcription. *Nucleic Acids Res.* **33**(18), pp. 5991-5999.

G

Gamble, P.E., and Mullet, J.E. (1989) Translation and stability of proteins encoded by the plastid *psbA* and *psbB* genes are regulated by a nuclear gene during light-induced chloroplast development in barley. *J. Biol. Chem.* **264**, pp. 7236–7243.

Golden, S.S., Brusslan, J., and Haselkorn, R. (1986) Expression of a family of *psbA* genes encoding a photosystem II polypeptide in the cyanobacterium *Anacystis nidulans* R2. *EMBO J.* **5**, pp. 2789-2798.

Goldschmidt-Clermont, M. (1998) Coordination of nuclear and chloroplast gene expression in plant cells. *Int. Rev. Cytol.* **177**, pp. 115-180.

Gould, S.B., Waller, R.F., and McFadden, G.I. (2008) Plastid evolution. *Ann. Rev. Plant Biol.* **59**, pp. 491-517.

Greenberg, B.M., Gaba, V., Mattoo, K. and Edelman, M. (1987) Identification of a primary in vivo degradation product of the rapidly turning-over 32 kD protein of photosystem II. *EMBO J.* **6**, pp. 2865-2869.

H

Hager, M., Hermann, M., Biehler, K., Krieger-Liszkay, A., and Bock, R. (2002) Lack of the small plastid-encoded PsbJ polypeptide results in a defective water-splitting apparatus of photosystem II, reduced photosystem I levels and hypersensitivity to light. *J. Biol. Chem.* **277**, pp. 14031-14039.

Haußühl, K., Andersson, B., and Adamska, I. (2001) A chloroplast DegP2 protease performs the primary cleavage of the photodamaged D1 protein in plant photosystem II. *EMBO J.* **20**(4), pp. 713-722.

Hird, S.M., Webber, A.N., Wilson, R.J., Dyer, T.A., and Gray, J.C. (1991) Differential expression of the *psbB* and *psbH* genes encoding the 47 kDa chlorophyll *a*-protein and the 10 kDa phosphoprotein of photosystem II during chloroplast development in wheat. *Curr. Genet.* **19**, pp. 199–206.

Horton, P., Park, K.J., Obayashi, T., Fujita, N., Harada, H., Adams- Collier, C.J., and Nakai, K. (2007) WoLF PSORT: protein localization predictor. *Nucleic Acids Res.* **35**, pp. W585-587.

J

Jach, G., Binot, E., Frings, S., Luxa, K., and Schell, J. (2001) Use of red fluorescent protein from *Discosoma* sp. (dsRED) as a reporter for plant gene expression. *Plant J.* **28**, pp. 483-491.

Jackson, A.O., and Larkins, B.A. (1976) Influence of Ionic Strength, pH, and Chelation of Divalent Metals on Isolation of Polyribosomes from Tobacco Leaves. *Plant Physiol.* **57**(1), pp. 5-10.

Jahns, P., Latowski, D., and Strzalka, K. (2009) Mechanism and regulation of the violaxanthin cycle: The role of antenna proteins and membrane lipids. *Biochim. Biophys. Acta* **1787**, pp. 3-14.

Jarvis, P., and Robinson, C. (2004) Mechanisms of protein import and routing in chloroplasts. *Curr. Biol.* **14**, R1064-R1077.

Jensen, K.H., Herrin, D.L., Plumley, F.G., and Schmidt, G.W. (1986) Biogenesis of photosystem II complexes: Transcriptional, translational and posttranslational regulation. *J. Cell Biol*. **103**, pp. 1315-1325.

K

Kamiya, N., and Shen, J.R. (2003) Crystal structure of oxygen-evolving photosystem II from *Thermosynechococcus vulcanus* at 3.7-A resolution. *Proc. Natl. Acad. Sci.* USA **100**, pp. 98-103.

Kamruzzaman , M., Kobayashi, Y., and Shikanai, T. (2005) Identification of a novel protein, CRR7, required for the stabilization of the chloroplast NAD(P)H dehydrogenase complex in *Arabidopsis*. *Plant J.* **44**, pp. 1036-1044.

Kapri-Pardes, E., Naveh, L., and Adam, Z. (2007) The thylakoid lumen protease Deg1 is involved in the repair of photosystem II from photoinhibition in *Arabidopsis. Plant Cell* **19**, pp. 1039-1047.

Karimi, M., Inze, D., and Depicker, A., (2002) Gateway vectors for Agrobacterium-mediated plant transformation. *Trends Plant Sci.* **7**(5), pp. 193-195.

Kim, J., Klein, P.G., and Mullet, J.E. (1991) Ribosomes pause at specific sites during synthesis of membrane-bound chloroplast reaction centre protein D1. *J. Biol. Chem.* **266**, pp. 14931–14938.

Kim, J., Eichacker, L.A., Rüdiger, W., and Mullet, J.E. (1994) Chlorophyll regulates accumulation of the plastid-encoded chlorophyll-proteins P700 and D1 by increasing apoprotein stability. *Plant Physiol.* **104**, pp. 907–916.

Klein, R.R., and Mullet, J.E. (1987) Control of gene expression during higher plant chloroplast biogenesis. Protein synthesis and transcript levels of *psbA*, *psaA–psaB*, and *rbcL* in darkgrown and illuminated barley seedlings. *J. Biol. Chem.* **262**, pp. 4341–4348.

Klein, R.R., Mason, H.S., and Mullet, J.E. (1988) Light-regulated translation of chloroplast proteins. I. Transcripts of psaA-psaB, and rbcL are associated with polysomes in dark-grown and illuminated barley seedlings. *J. Cell Biol.* **106,** pp. 289–301.

Kleine, T., Maier, U.G., and Leister, D. (2009) DNA transfer from organelles to the nucleus: the idiosyncratic genetics of endosymbiosis. *Ann. Rev. Plant Biol.* **60**, pp. 115-138.

Klimmek, F., Sjodin, A., Noutsos, C., Leister, D., and Jansson, S. (2006) Abundantly and rarely expressed Lhc protein genes exhibit distinct regulation patterns in plants. *Plant Physiol.* **140**, pp. 793-804.

Koncz, C., Mayerhofer, R., Koncz-Kalman, Z., Nawrath, C., Reiss, B., Redei, G.P., and Schell, J. (1990) Isolation of a gene encoding a novel chloroplast protein by T-DNA tagging in *Arabidopsis thaliana*. *Embo J*. **9**, pp. 1337-1346.

Koop, H.U., Steinmüller, K., Wagner, H., Rossler, C., Eibl, C., and Sacher, L. (1996) Integration of foreign sequences into the tobacco plastome via polyethylene glycol-mediated protoplast transformation. *Planta* **199**, pp. 193-201.

Krause, G.H. and Weis, E. (1991) Chlorophyll fluorescence and photosynthesis: The basics. *Annu. Rev. Plant Physiol. Plant Mol. Biol.*, **42**, pp. 313–349.

Kuroda, M., Kobashi, K., Kaseyama, H., and Satoh, K. (1996) Possible involvement of a low redox potential component(s) downstream of photosystem I in the translational regulation of the D1 subunit of the photosystem II reaction centre in isolated pea chloroplasts. *Plant Cell Physiol.* **37**, pp. 754–761.

Kwon, K.C., and Cho, M.H. (2008) Deletion of the chloroplast-localized *AtTerC* gene product in *Arabidopsis thaliana* leads to loss of the thylakoid membrane and to seedling lethality. *The Plant J.* **55**, pp. 428-442.

L

Larkin, M.A., Blackshields, G., Brown, N.P., Chenna, R., McGettigan, P.A., McWilliam, H., Valentin, F., Wallace, I.M., Wilm, A., Lopez, R., Thompson, J.D., Gibson, T.J. and Higgins, D.G. (2007) ClustalW and ClustalX version 2. *Bioinformatics* **23**(1), pp. 2947-2948.

Leister, D. (2003) Chloroplast research in the genomic age. *Trends Genet.* **19**, pp. 47-56.

Li, Y., Rosso, M.G., Strizhov, N., Viehoever, P., and Weisshaar, B. (2003) GABI-Kat SimpleSearch: a flanking sequence tag (FST) database for the identification of T-DNA insertion mutants in *Arabidopsis thaliana*. *Bioinformatics* **19**, pp. 1441-1442.

Lindahl, M., Spetea, C., Hundal, T., Oppenheim, A., Adam, Z. and Andersson, B. (2000) The thylakoid FtsH protease plays a role in the light-induced turnover of the photosystem II D1 protein. *Plant Cell* **12**, pp. 419-431.

Loll, B., Kern, J., Saeger, W., Zouni, A., and Biesiadka, J. (2005) Towards complete cofactor arrangement in the 3.0 Â resolution structure of photosystem II. *Nature* **438**, pp. 1040–1044.

M

Ma, J., Peng, L., Guo, J., Lu, Q., Lu, C., and Zhang, L. (2007) LPA2 is required for efficient assembly of photosystem II in *Arabidopsis thaliana*. *The Plant Cell* **19**, pp. 1980-1993.

Margulis, L. (1971) Symbiosis and evolution. *Sci. Am.* **225**, pp. 48–57.

Martienssen R. (1998) Functional genomics: probing plant gene function and expression with transposons. *Proc. Natl. Acad. Sci*. **95**, pp. 2021-2026.

Martin, W., Stoebe, B., Goremykin, V., Hansmann, S., Hasegawa, M., Kowallik, M., and Kowallik, K. (1998) Gene transfer to the nucleus and the evolution of chloroplasts. *Nature* **393**, pp. 162-165.

Mattoo, A.K., Hoffman-Falk, H., Marder, J.B., and Edelman, M. (1984) Regulation of protein metabolism: coupling of photosynthetic electron transport to *in vivo* degradation of the rapidly metabolized 32-kilodalton protein of the chloroplast membranes*. Proc. Natl. Acad. Sci., USA* **81**, pp. 1380–1384.

Maxwell, K., and Johnson, G.N. (2000) Chlorophyll fluorescence – a practical guide. *J. of Exp. Botany* **51**(345), pp. 659-668.

Merchant, S., and Dreyfuss, B.W. (1998) Posttranslational assembly of photosynthetic metalloproteins. *Ann. Rev. Plant Physiol. And Plant Mol. Biol.* **49**, pp. 25-51.

Meurer, J., Plücken, H., Kowallik, K.V., and Westhoff, P. (1998) A nuclear-encoded protein of prokaryotic origin is essential for the stability of photosystem II in *Arabidopsis thaliana*. *EMBO J.* **17**, pp. 5286-5297.

Mohamed, A., and Jansson, C. (1989) Influence of light on accumulation of photosynthesis-related transcripts in the cyanobacterium *Synechocystis* 6803. *Plant Mol. Biol.* **13**, pp. 693-700.

Morais, F., Barber, J., and Nixon, P.J. (1998) The chloroplast-encoded alpha subunit of cytochrome *b*-559 is required for assembly of the photosystem two complex in both the light and the dark in *Chlamydomonas reinhardtii*. *J. Biol. Chem.* **273**, pp. 29315–29320.

Mühlbauer, S.K., and Eichacker, L.A. (1998) Light-dependent formation of the photosynthetic proton gradient regulates translation elongation in chloroplasts. *J. Biol. Chem.* **273**, pp. 20935–20940.

Mulo, P., Sirpiö, S., and Aro, E.M. (2008) Auxiliary proteins involved in the assembly and sustenance of photosystem II. *Photosynth. Research* **98**, pp. 489-501.

Müller, B., and Eichacker, L.A. (1999) Assembly of the D1 precursor in monomeric photosystem II reaction center precomplexes precedes chlorophyll *a*-triggered accumulation of reaction center II in barley etioplasts. *Plant Cell* **11**, pp. 2365-2377.

Mullet, J.E., and Klein, R.R. (1987) Transcription and mRNA stability are important determinants of higher plants chloroplast RNA levels. *EMBO J.* **6**, pp. 1571–1579.

Mullet, J.E., Klein, P.G., and Klein, R.R. (1990) *Proc. Natl. Acad. Sci.* USA **87**, pp. 4038-4042.

Mullineaux, C.W. (2005) Function and evolution of grana. *Trends in Plant Science* **10**(11), pp. 521-525.

Munshi, M.K., Kobayashi, Y., and Shikanai, T. (2006) Chlororespiratory reduction 6 is a novel factor required for accumulation of the chloroplast NAD(P)H dehydrogenase complex in *Arabidopsis. Plant Physiol.* **141**(2), pp. 737-744.

N

Nada, A., and Soll, J. (2004) Inner envelope protein 32 is imported into chloroplasts by a novel pathway. *J. Cell Sci.* **117**(Pt17), pp. 3975-3982.

Nanba, O., and Satoh, K. (1987) Isolation of a photosystem II reaction center consisting of D-1 and D-2 polypeptides and cytochrome b-559. *Proc. Natl. Acad. Sci. USA* **84**, pp. 109-112.

Nelson, N., and Yocum, C.F. (2006) Structure and function of photosystem I and II. *Annu. Rev. Plant Biol*. **57**, pp. 521–565.

Nilsson, F., Andersson, B., and Jansson, C. (1990) Photosystem II characteristics of a constructed *Synechocystis* 6803 mutant lacking synthesis of the D1 polypeptide. *Plant Mol. Biol.* **14**, pp. 1051–1054.

Nilsson, R., Brunner, J., Hoffman, N.E., and van Wijk, K.J. (1999) Interactions of ribosome nascent chain complexes of the chloroplast-encoded D1 thylakoid membrane protein with cpSRP54. *EMBO J.* **18**, pp. 733–742.

Nilsson, R., and van Wijk, K.J. (2002) Transient interaction of cpSRP54 with elongation nascent chains of the chloroplast-encoded D1 protein: 'cpSRP54 caught in the act'. *FEBS Lett.* **524**(1-3), pp. 127-133.

Nishiyama, Y., Allakhverdiev, S.I., and Murata, N. (2006) A new paradigm for the action of reactive oxygen species in the photoinhibition of photosystem II. *Biochim. Biophys. Acta* **1757**, pp. 742-749.

Niyogi, K.K., Grossman, A.R., and Björkman, O. (1998) *Arabidopsis* mutants define a central role for the xanthophyll cycle in the regulation of photosynthetic energy conversion. *Plant Cell* **10**, pp. 1121-1134.

Niyogi, K.K. (1999) Photoprotection revisited: Genetic and molecular approaches. *Ann. Rev. Plant Physiol. Plant Mol. Biol.* **50**, pp. 333-359.

Nowaczyk, M.M., Hebeler, R., Schlodder, E., Meyer, H.E., Warscheid, B., and Rogner, M. (2006) Psb27, a cyanobacterial lipoprotein, is involved in the repair cycle of photosystem II. *Plant Cell* **18**, pp. 3121-3131.

O

Obayashi, T., Hayashi, S., Saeki, M., Ohta, H., and Kinoshita, K. (2009) ATTED-II provides coexpressed gene networks for *Arabidopsis*. *Nucleic Acids Res.* **37**, pp. 987-91.

Oelmüller, R., Herrmann, R.G., and Pakrasi, H.B. (1996) Molecular studies of CtpA, the carboxyl-terminal processing protease for the D1 protein of the photosystem II reaction center in higher plants. *J. Biol. Chem.* **271**(36), pp. 21848-21852.

Ohashi, K., Murakami, A., Tanaka, A., Tsuji, H., and Fujita, Y. (1992) Developmental changes in amounts of Thylakoid components in plastids of barley leaves. *Plant Cell Physiol.* **33**, pp. 371–377.

Ohnishi, N., and Takahashi, Y. (2001) PsbT polypeptide is required for efficient repair of photodamaged photosystem II reaction centre. *J. Biol. Chem.* **276**, pp. 33 798–33 804.

Ossenbühl, F., Göhre, V., Meurer, J., Krieger-Liszkay, A., Rochaix, J.D., and Eichacker, L.A. (2004) Efficient assembly of photosystem II in *Chlamydomonas reinhardtii* requires Alb3.1p, a homolog of *Arabidopsis* ALBINO3. *Plant Cell* **16**, pp. 1790-1800.

P

Pakrasi, H.B., Nyhus, K.J., and Granok, H. (1990) Targeted deletion mutagenesis of the beta subunit of cytochrome *b*559 protein destabilizes the reaction centre of photosystem II. *Z. Naturforsch.* **45**, pp. 423–429.

Pasch, J.C., Nickelsen, J., and Schünemann, D. (2005) The yeast split-ubiquitin system to study chloroplast membrane protein interactions. *Appl. Microbiol. Biotechnol.* **69**, pp. 440–447.

Peltier, J.B., Ytterberg, A.J., Sun, Q., van Wijk, K.J. (2004) New functions of the thylakoid membrane proteome of Arabidopsis thaliana revealed by a simple, fast, and versatile fractionation strategy. *J. Biol. Chem.* **279**(47), pp. 49367-83.

Peng, L.W., Ma, J.F., Chi, W., Guo, J.K., Zhu, S.Y., Lu, Q.T., Lu, C.M., and Zhang, L.X. (2006) Low PSII accumulation1 is involved in the efficient assembly of photosystem II in *Arabidopsis thaliana*. *Plant Cell* **18**, pp. 955–969.

Pesaresi, P., Varotto, C., Meurer, J., Jahns, P., Salamini, F., and Leister, D. (2001) Knock-out of the plastid ribosomal protein L11 in *Arabidopsis*: effects on mRNA translation and photosynthesis. *Plant J.* **27**, pp. 179-189.

Pierleoni, A., Martelli, P.L., Fariselli, P., and Casadio, R. (2006) BaCelLo: a Balanced subCellular Localization predictor. *Bioinformatics* **22**(14), pp. 408-416.

Plücken, H., Müller, B., Grohmann, D., Westhoff, P., and Eichacker, L.A. (2002) The HCF136 protein is essential for assembly of the photosystem II reaction center in *Arabidopsis thaliana*. *FEBS Lett.* **532**, pp. 85–90.

Porra, R.J. (2002) The chequered history of the development and use of simultaneous equations for the accurate determination of chlorophylls *a* and *b*. *Photosynth. Res.* **73**, pp. 149-156.

Prasil, O., Adir, N. and Ohad, I. (1992) Dynamics of photosystem II: mechanism of photoinhibition and recovery processes. In *Barber,J. (ed.), Topics in Photosynthesis* **11**. Elsevier, Amsterdam, The Netherlands, pp. 295-348.

R

Reumann, S., Inoue, K., and Keegstra, K. (2005) Evolution of the general import pathway of plastids. *Mol. Memb. Biol.* **22**(1-2), pp. 73-86.

Rochaix, J.D. (2001) Assembly, function, and dynamics of the photosynthetic machinery in *Chlamydomonas reinhardtii*. *Plant Physiol.* **127**, pp. 1394-1398.

Rokka, A., Suora, M., Saleem, A., Battchikova, N., and Aro, E.M. (2005) Synthesis and assembly of thylakoid protein complexes: Multiple assembly steps of photosystem II. *Biochem. J.* **388**, pp. 159-168.

Rosso, M.G., Li, Y., Strizhov, N., Reiss, B., Dekker, K,. Weisshaar, B. (2003) An *Arabidopsis thaliana* T-DNA mutagenized population (GABI-Kat) for flanking sequence tag-based reverse genetics. *Plant Mol. Biol.* **53**(1-2), pp. 247-59.

Rumeau, D., Peltier, G., and Cournac, L. (2007) Chlororespiration and cyclic electron flow around PSI during photosynthesis and plant stress response. *Plant Cell Environ.* **30**(9), pp. 1041-1051.

S

Sambrook, J., Fritsch, E.F., and Maniatis, T. (1989) Molecular Cloning. (New York: Cold Spring Harbor Laboratory Press).

Schägger, H., and von Jagow, G. (1987) Tricine-sodium dodecyl sulfate-polyacrylamide gel electrophoresis for the separation of proteins in the range from 1 to 100 kDa. *Anal. Biochem.* **166**, pp. 368-379.

Schägger, H., and von Jagow, G. (1991) Blue native electrophoresis for isolation of membrane protein complexes in enzymatically active form. *Anal. Biochem.* **199**, pp. 223-231.

Schein, A.I., Kissinger, J.C., and Ungar, L.H. (2001) Chloroplast transit peptide prediction: a peek inside the black box. *Nucleic Acids Res.* **29**, E82.

Schreiber, U., Schliewa, U., and Bilger, W. (1986) Continuous recording of photochemical and non-photochemical chlorophyll fluorescence quenching with a new type of modulation fluorometer. *Photosynth. Res.* **10**, pp. 51-62.

Schult, K., Meierhoff, K., Paradies, S., Tölle, T., Wolff, P., and Westhoff, P. (2007) The nuclear-encoded factor HCF173 is involved in the initiation of translation of the *psbA* mRNA in *Arabidopsis thaliana*. *The Plant Cell* Preview, doi/10.1105/tpc.106.042895.

Schünemann, D., Gupta, S., Persello-Cartieaux, F., Klimyuk, V.I., Jones, J.D.G., Nussaume, L., and Hoffman, N.E. (1998) A novel signal recognition particle targets light-harvesting proteins to the thylakoid membranes. *Proc. Natl. Acad. Sci.* USA **95**, pp. 10312–10316.

Schünemann, D. (2004) Structure and function of the chloroplast signal recognition particle. *Curr. Genet.* **44**, pp. 295–304.

Schünemann, D. (2007) Mechanisms of protein import into thylakoids of chloroplasts. *Biol. Chem.* **388**, pp. 907-915.

Shi, L.X., and Schröder, W.P. (2004) The low molecular mass subunits of the photosynthetic supracomplex, photosystem II. *Biochim. Biophys. Acta* **1608**(2-3), pp. 75-96.

Shimizu, H., and Shikanai, T. (2007) Dihydrodipicolinate reductase-like protein, CRR1, is essential for chloroplast NAD(P)H dehydrogenase in *Arabidopsis. Plant J.* **52**(3), pp. 539-547.

Sirpiö, S., Allahverdiyeva, Y., Suorsa, M., Paakkarinen, V., Vainonen, J., Battchikova, N., and Aro, E.M. (2007) TLP18.3, a novel thylakoid lumen protein regulating photosystem II repair cycle. *Biochem. J.* **406**, pp. 415-425.

Sirpiö, S., Khrouchtchova, A., Allahverdiyeva, Y., Hansson, M., Fristedt, R., Vener, A.V., Scheller, H.V., Jensen, P.E., Haldrup, A., und Aro, E.M. (2008) AtCYP38 ensures early bioenesis, correct assembly and sustenance of photosystem II. *Plant J.* **55**(4), pp. 639-651.

Sirpiö, S., Allahverdiyeva, Y., Holmström, M., Khrouchtchova, A., Haldrup, A., Battchikova, N., and Aro, E.M. (2009) Novel nuclear-encoded subunits of the chloroplast NAD(P)H dehygrogenase complex. *J. Biol. Chem.* **284**(2), pp. 905-912.

Small, I., Peeters, N., Legeai, F., and Lurin, C. (2004) Predotar: A tool for rapidly screening proteomes for N-terminal targeting sequences. *Proteomics* **4**, pp. 1581-1590.

Soll, J., and Schleiff, E. (2004) Protein import into chloroplasts. *Nat. Rev. Mol. Cell Biol.* **5**, pp. 198-208.

Stroebel, D., Choquet, Y., Popot, J.L., and Picot, D. (2003) An atypical haem in the cytochrome b(6)f complex. *Nature* **426**, pp. 413-418.

Sundberg, E., Slagter, J.G., Fridborg, I., Cleary, S.P., Robinson, C., and Coupland, G. (1997). ALBINO3, an *Arabidopsis* nuclear gene essential for chloroplast differentiation, encodes a chloroplast protein that shows homology to proteins present in bacterial membranes and yeast mitochondria. *Plant Cell* **9**, pp. 717–730.

Suorsa, M., Zhang, L., Paakkarinen, V., Regel, R., Herrmann, R., and Aro, E.M. (2001) Role of PsbE, F, L and J in the assembly of photosystem II. In *PS2001 Proc. 12th Int. Congr. on Photosynthesis,* 18–24 August 2001, Brisbane, Australia: CSIRO.

Suorsa, M., Regel, R.E., Paakkarinen, V., Battchikova, N., Herrmann, R.G., and Aro, E.M. (2004) Protein assembly of photosystem II and accumulation of subcomplexes in the absence of low molecular mass subunits PsbL and PsbJ. *Eur. J. Biochem.* **271**, pp. 96-107.

T

Tatusova, T.A., and Madden, T.L. (1999) BLAST 2 Sequences, a new tool for comparing protein and nucleotide sequences. *FEMS Microbiol. Lett.* **174**, pp. 247-250.

Taylor, R.G., Walker, D.C., and McInnes, R.R. (1993) *E.coli* host strains significantly affect the quality of small scale plasmid DNA preparations used for sequencing. *Nucleic Acids Research* **21**(7), pp. 1677-1678.

Tikkanen, M., Nurmi, M., Kangsjärvi, S., Aro, E.M. (2008) Core protein phosphorylation facilitates the repair of photodamaged photosystem II at high light. *Biochim. Biophys. Acta*, doi: 10.1016/j.bbabio.2008.08.004.

Towbin, H., Staehelin, T., and Gordon, J. (1979) Electrophoretic transfer of proteins from polyacrylamide gels to nitrocellulose sheets: procedure and some applications. *Proc. Natl. Acad. Sci.* USA **76**, pp. 4350-4354.

Tzvetkova-Chevolleau, T., Hutin, C., Noël, L..D., Goforth, R., Carde, J.P., Caffarri, S., Sinning, I., Groves, M., Teulon, J.M., Hoffman, N.E., Henry, R., Havaux, M., and Nussaume, L. (2007) Canonical signal recognition particle components can be bypassed for posttranslational protein targeting in chloroplasts. *Plant Cell* **19**(5), pp. 1635-1648.

V

Varotto, C., Pesaresi, P., Maiwald, D., Kurth, J., Salamini, F., and Leister, D. (2000). Identification of photosynthetic mutants of *Arabidopsis* by automatic screening for altered effective quantum yield of photosystem 2. *Photosynthetica* **38**, pp. 497–504.

Vermaas, W. (1988) Protein composition of the photosystem II core complex in genetically engineered mutants of the cyanobacterium *Synechocystis* sp. PCC 6803. *Photosynth. Res.* **17**, pp. 97–113.

Vermaas, W. (1993) Molecular-biological approaches to analyse photosystem II structure and function. *A. Rev. Plant Physiol. Plant. Mol. Biol.* **44**, pp. 457–481.

von Wettstein, D., Gough, S., and Kannangara, C.G. (1995) Chlorophyll synthesis. *Plant Cell* **7**, pp. 1039–1057.

W

Waegemann, K., and Soll, J. (1991) Characterization of the protein import apparatus in isolated outer envelopes of chloroplasts. *Plant J.* **1**, pp. 149-158.

Wollman, F.A., Minai, L., and Nechushtai, R. (1999). The biogenesis and assembly of photosynthetic proteins in thylakoid membranes. *Biochim. Biophys. Acta* **1141**, pp. 21–85.

Y

Yi, L., and Dalbey, R.E. (2005) Oxa1/Alb3/YidC system for insertion of membrane proteins in mitochondria, chloroplasts and bacteria (Review). *Mol. Memb. Biol.* **22**(1-2), pp. 101-111.

Yu, J., and Vermaas, W. (1990) Transcript levels and synthesis of photosystem II components in cyanobacterial mutants with inactivated photosystem II genes. *Plant Cell* **2**, pp. 315-322.

Z

Zhang, L.X., Paakkarinen, V. van Wijk, K.J., and Aro, E.M. (1999) Co-translational assembly of the D1 protein into photosystem II. *J. Biol. Chem.* **274**, pp. 16062-16067.

Zhang, L.X., Paakkarinen, V. van Wijk, K.J., and Aro, E.M. (2000) Biogenesis of the chloroplast-encoded D1 protein: Regulation of translation elongation, insertion, and assembly into photosystem II. *Plant Cell* **12**, pp. 1769-1781.

Zhang, L., Paakkarinen, V., Suorsa, M., Aro, E.M. (2001) A SecY homologue is involved in chloroplast-encoded D1 protein biogenesis. *J. Biol. Chem.* **276**, pp. 37809-37814.

Zhang, L.X., and Aro, E.M. (2002) Synthesis, membrane insertion and assembly of the chloroplast-encoded D1 protein into photosystem II. *FEBS Letters* **512**, pp. 13-18.

Zimmermann, P., Hirsch-Hoffmann, M., Hennig, L., and Gruissem, W. (2004) GENEVESTIGATOR: Arabidopsis microarray database and analysis toolbox. *Plant Physiology* **136**(1), pp. 2621-2632.

Zouni, A., Witt, H.T., Kern, J., Fromme, P., Krauss, N., Saenger, W., and Orth, P. (2001) Crystal structure of photosystem II from *Synechococcus elongatus* at 3.8 Â resolution. *Nature* **409**, pp. 739–743.

Zybailov, B., Rutschow, H., Friso, G., Rudella, A., Emanuelsson, O., Sun, Q., van Wijk, K.J. (2008) Sorting signals, N-terminal modifications and abundance of the chloroplast proteome. *PLoS ONE* **3**(4), e1994.

6) Supplementary Data

6.1) Vector Maps

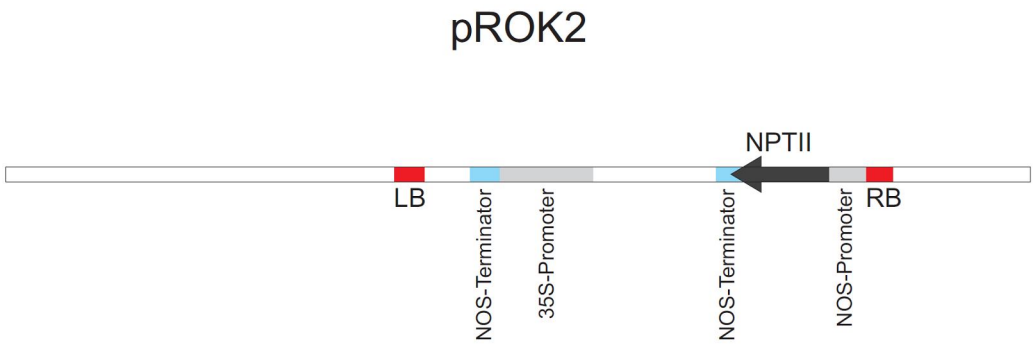

Fig. 6.1: T-DNA transformation vector pROK2 (SALK-collection).

Binary cloning vector used for insertional mutagenesis of an *Arabidopsis* population (Alonso *et al.*, 2003). LB = left border, RB = right border of T-DNA; NPTII = neomycin phosphotransferase II; NOS-Promoter = Nopaline Synthase Promoter; NOS-Terminator = Nopaline Synthase Terminator; 35S = Cauliflower Mosaic Virus Promoter.

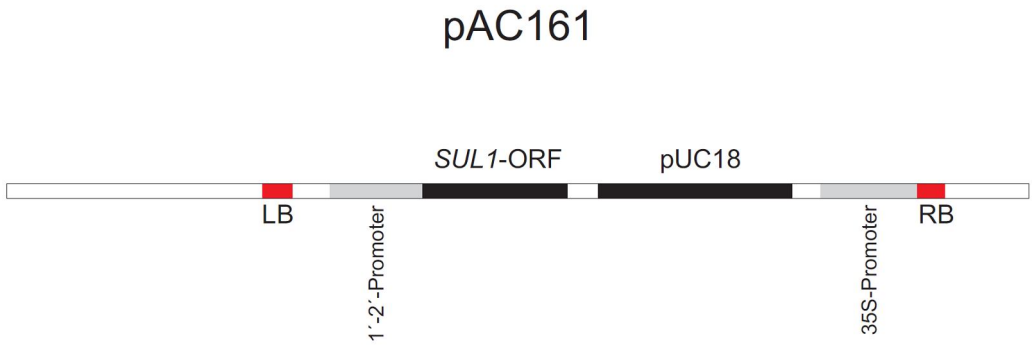

Fig. 6.2: T-DNA transformation vector pAC161 (GABI-collection).

Binary cloning vector used for insertional mutagenesis of an *Arabidopsis* population (Rosso *et al.*, 2003). LB = left border, RB = right border of T-DNA; SUL1-ORF = gene for resistance against the herbizide sulfadiazine; 1´-2´-promoter = drives expression of the SUL1 ORF; 35S = Cauliflower Mosaic Virus Promoter.

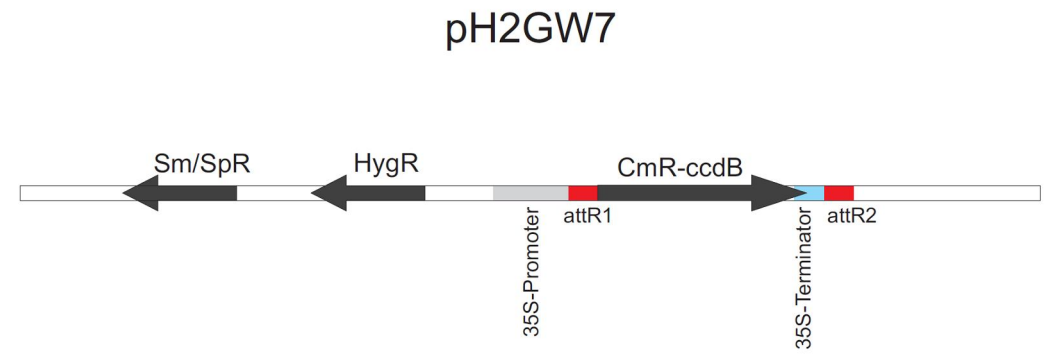

Fig. 6.3: Binary vector for Agrobacterium-mediated plant transformation.

The pH2GW7 gateway vector (Karimi *et al.* (2002) was used for complementation of pam68-2 plants with a pH2GW7/PAM68 construct including full-length coding sequence of *PAM68*. Sm/SpR = resistance against streptomycin and spectinomycin (for selection of positive clones); HygR = resistance against hygromycin (for selection of plant transformants); attR1/attR2 = attachment sites: DNA recombination sites; CmR = chloramphenicol resistance gene; ccdB = cytotoxic protein, used for negative selection.

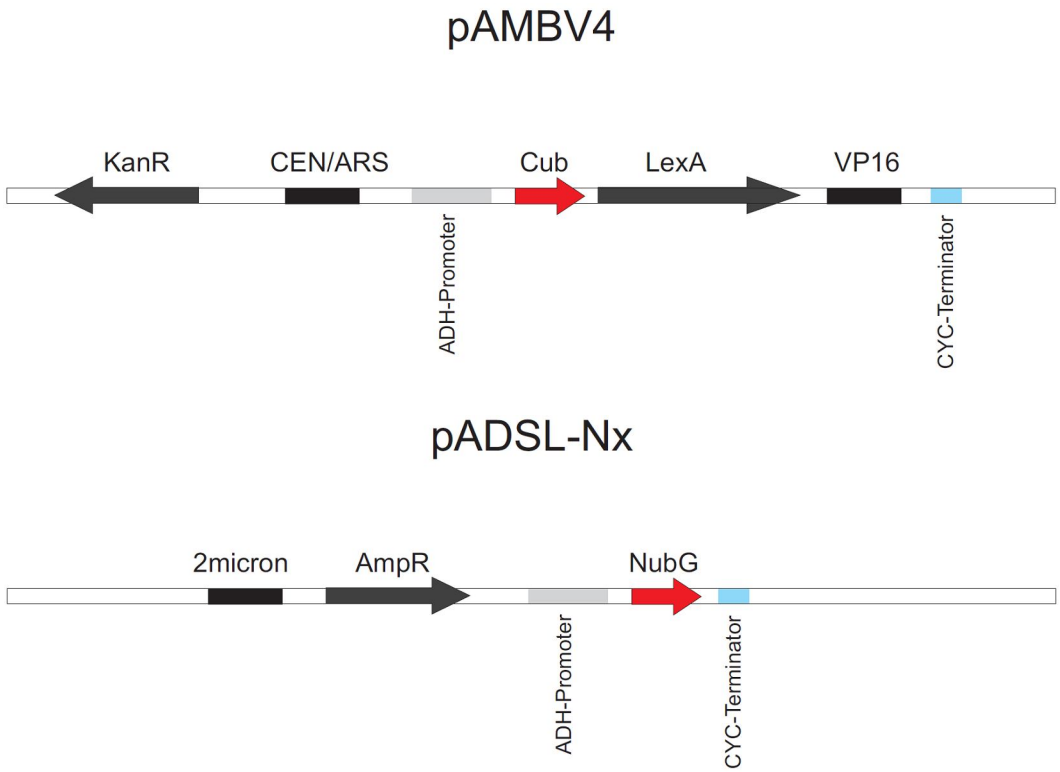

Fig. 6.4: Yeast split-ubiquitin vectors.

A) pAMBV4. ADH-promoter = Saccharomyces cerevisiae ADH1 promoter; Cub = amino acids 34-76 of yeast ubiquitin; LexA = amino acids 1-200 of LexA; VP16 = Herpes simplex VP16 transactivator; CYC-terminator = S.cerevisiae CYC1 terminator; CEN/ARS = origin of replication (allows propagation of plasmids in yeast at low copy numbers); KanR = kanamycine resistance gene. **B)** pADSL-Nx. NubG = amino acids 1-38 of yeast ubiquitin; 2micron = origin of replication (allows propagation of plasmids in yeast at low copy numbers); AmpR = ampicillin resistance gene.

Acknowledgements

First of all, I would like to thank Prof. Dr. Dario Leister, who gave me the opportunity to carry out my PhD research under his supervision.

Additionally, I would like to thank Prof. Dr. Jörg Nickelsen for taking over the “Zweitgutachten”.

Moreover, I would like to thank everyone, who contributed to the experimental outcome of this work: Prof. Dr. Peter Jahns for the pigment analyses, Prof. Dr. Danja Schünemann for the split-ubiquitin assay, Dr. Elena Aseeva for the import, Renate Kreller for assistance on biochemical experiments.

Special thanks to Dr. Ute Armbruster for excellent supervision during the third year of my PhD. Thanks also for the correction of my thesis.

Many thanks to Angie, the kind soul of our group, for always be willing to listen to everybody’s problems.

Additionally, I would like to thank Dr. Cordelia Bolle and Christian for reading and correcting my thesis.

I am thankful for all the nice colleagues I met in this lab, especially for my office-flatmates, who made the last years quite enjoyable. A special thank to Henning, who always took care of the coffee preparation.

Finally, I am grateful to my mother, who kept me alive the last years with her cuisine. Thanks to Jürgen and all my friends, who took care of me, particularly in the last months of confusion.

Curriculum vitae

Personal Data

Date of birth: 14 August 1980
Place of birth: Munich, Germany
Nationality: German

Research Experiences

03/2006 – 11/2009	Ludwig-Maximilians-Universität München; Department Biology I, Botany PhD in "PAM68: A New Component of the PSII Biogenesis Machinery" Supervisor: Prof. Dr. Dario Leister
01/2005 – 11/2005	Ludwig-Maximilians-Universität München; Department Biology I, Botany Diploma thesis in "Vorbereitungen zur Plastidentransformation von *Physcomitrella patens*" Supervisor: Prof. Dr. Hans-Ulrich Koop (Grade 1.0)
05/2003 – 02/2006	Ludwig-Maximilians-Universität München; Department Biology I, Botany Student assistant in different researcher groups (Prof. Dr. J. Soll, Prof. Dr. R. Herrmann, Prof. Dr. D. Leister)

Education

10/2000 – 12/2005	Ludwig-Maximilians-Universität München; Department Biology I, Botany Diploma studies in Biology (Grade 1.1)
09/1991 – 06/2000	Ruperti-Gymnasium Mühldorf Abitur (Grade 2.5)

Publications

Schliebner, I., Pribil, M., Zühlke, J., Dietzmann, A., and Leister, D. (2008) A survey of chloroplast protein kinases and phosphatases in *Arabidopsis thaliana*. *Current Genomics* **9**(3), pp. 184-190.

Armbruster, U., Hertle, A., Makarenko, E., Zühlke, J., Pribil, M., Dietzmann, A., Schliebner, I., Aseeva, E., Fenino, E., Scharfenberg, M., Voigt, C., and Leister, D. (2009) Chloroplast proteins without cleavable transit peptides: rare exceptions or a major constituent of the chloroplast proteome? *Molecular Plant*, published September 30.

Posters

Zühlke, J., Armbruster, U., and Leister, D.: PAM68 – Ein neuer PSII-Biogenese-Faktor. 22. Tagung Molekularbiologie der Pflanzen, Dabringhausen 2009.

Scholarships

12/2006 – 11/2009 Scholarship of the „Bayerische Elite-Universität“

Languages

German - mother tongue
English - fluent

Ehrenwörtliche Versicherung

Hiermit versichere ich, dass ich die vorliegende Arbeit selbständig und nur unter Verwendung der angegebenen Hilfsmittel und Quellen angefertigt habe. Die Autorin hat zuvor nicht versucht, anderweitig eine Dissertation einzureichen oder sich einer Doktorprüfung zu unterziehen. Die Dissertation wurde keiner weiteren Prüfungskommission weder in Teilen noch als Ganzes vorgelegt.

München, November 2009

Jessica Zühlke